

November 2023

Novel Systems Engineering Framework Analysis of Photovoltaic Models and Equations

Peter R. Michael
University of South Florida

Follow this and additional works at: <https://digitalcommons.usf.edu/etd>



Part of the [Electrical and Computer Engineering Commons](#)

Scholar Commons Citation

Michael, Peter R., "Novel Systems Engineering Framework Analysis of Photovoltaic Models and Equations" (2023). *USF Tampa Graduate Theses and Dissertations*.
<https://digitalcommons.usf.edu/etd/10067>

This Dissertation is brought to you for free and open access by the USF Graduate Theses and Dissertations at Digital Commons @ University of South Florida. It has been accepted for inclusion in USF Tampa Graduate Theses and Dissertations by an authorized administrator of Digital Commons @ University of South Florida. For more information, please contact digitalcommons@usf.edu.

Novel Systems Engineering Framework Analysis of Photovoltaic Models and Equations

by

Peter R. Michael

A dissertation submitted in partial fulfillment
of the requirements for the degree of
Doctor of Philosophy
Department of Electrical Engineering
College of Engineering
University of South Florida

Major Professor: Wilfrido A. Moreno, Ph.D.
Chung Seop Jeong, Ph.D.
Fernando Falquez, Ph.D.
D. Yogi Goswami, Ph.D.
Danvers E. Johnston, Ph.D.

Date of Approval:
October 26, 2023

Keywords: PV Statistical Equation Simplification, PV 5 Parameter Verification, 6 Parameter PV Model, Transcendental Equation Free PV I-V Plot

Copyright © 2023, Peter R. Michael

Dedication

This dissertation is dedicated to my father, a great Civil Engineer, and my grandfather, an incredible Electrical Engineer.

Acknowledgments

I thank the numerous engineers and technicians who advised and guided me in my long career. My father, who, due to World War II pressures, obtained a Civil Engineering degree in 2.5 years and thus was sympathetic in allowing me extra time to complete my bachelor's degree. To my grandfather, who engrained the principle of treating all coworkers, high and low, fairly and kindly. This lesson was displayed when the most junior engineer who worked for my grandfather later became the head of Grand Coulee Dam and enabled a personal tour of the facility. To Tom Bamberg, a US Navy technician extraordinaire who opened my eyes to the value of constructability, testing, and verification. To Professor Jackson Fuller, my advisor at the University of Colorado, a practical engineer who greatly helped me. Another of Professor Jackson's students, University of South Florida Professor Dr. Fehr, helped me with early concepts of direct current power practical applications and encouraged me in my Ph.D. Dr. Moreno who picked up the full burden as my advisor after the passing of Dr. Fehr. My Master's education at Arizona State University which taught me the intricacies of systems engineering and deconfounding multivariable measurements. And finally, to my mother, who taught me to adapt, keep working, and when life delivers lemons, make lemonade, and sometimes, color should be spelled colour.

Table of Contents

List of Tables	v
List of Figures	vii
List of Terms and Abbreviations	x
Abstract	xii
Chapter 1: Introduction	1
1.1 Statement of Problem.....	2
1.1.1 Complex PV Equations.....	2
1.1.2 New Verification Method for Solved PV Parameters.....	2
1.1.3 Transcendental Equation for the Graphing of I-V Curves.....	3
1.2 Research Questions	3
1.3 Methods and Contributions of Solutions	3
1.3.1 PV Equation Simplification Verification.....	3
1.3.2 Verification of Solved PV Parameters.....	3
1.3.3 Six Parameter Model and Simplified Method to Graph PV I-V Curves	4
Chapter 2: Existing State of Photovoltaic Systems.....	5
Chapter 3: A Brief Photovoltaic History	7
3.1 Early Years.....	7
3.2 Scientific Understanding.....	9
3.3 Photoelectric and Photovoltaic Effects	9
3.4 Photoelectric to Semiconductor Photovoltaic Systems.....	11
3.5 Alternative PV Materials	12
Chapter 4: Existing PV Equations and Models.....	13
4.1 Background.....	13
4.1.1 P-N Junction Diode.....	13
4.1.2 Early PV Cell Model.....	14
4.1.3 Early PV Cell Equations	15
4.2 Modern PV Cell Models and Equations	15
4.2.1 The Five Parameter Model.....	15
4.2.2 Equations for Five Parameter Model	16
4.2.3 Alternative Seven and Nine Parameter Models.....	17
4.3 Modification of PV Cell Equations and Model for PV Modules.....	18
4.3.1 PV Module Description	18

4.3.2 PV Cell to Module Equivalent Model	21
4.3.3 PV Cell to Module Equations	23
4.4 PV Module Test Conditions and Characteristics	23
4.4.1 Test Conditions	23
4.4.2 Test Results	24
4.4.3 Parameter Data	25
4.4.4 Short, Open, and Maximum Power Condition Equations.....	26
4.4.5 Graphing the I-V and Power Curves.....	28
4.4.6 Temperature Considerations	29
Chapter 5: Statistical Verification of the Simplification of the PV Equation.....	30
5.1 Abstract	30
5.2 Introduction.....	30
5.3 Measurement.....	31
5.4 Primary Conditions	32
5.5 Circuit Conditions.....	32
5.6 Data Sources for Analysis.....	33
5.7 BP-MSX120 Reference PV Module.....	34
5.8 PV Equations at Primary Conditions	35
5.9 Simplification Method Data Analysis and Results	36
5.9.1 Comparison Analysis	36
5.9.2 Short Circuit Condition.....	37
5.9.3 Open Circuit Condition.....	38
5.9.4 Maximum Power Condition.....	39
5.10 Discussion and Explanation of Results.....	40
5.11 Conclusion	40
5.12 Additional Simplifications	41
5.12.1 R_s to R_p Ratio	41
5.12.2 R_p versus $R_s + R_p$	41
5.12.3 Simplification of V_{oc}	41
Chapter 6: Solving for the Parameters in the Five Parameter Model	43
6.1 Module Characteristics and Parameters.....	43
6.2 Solution Analysis	43
6.3 Equations for I_L and I_o	44
6.4 Three Additional Equations for η , R_s , and R_p	45
6.4.1 First Equation.....	45
6.4.2 Conditions for Additional Equations	46
6.4.3 Second Equation	47
6.4.4 Third Equation	49
6.5 Transcendental Numerical Solutions	50
6.6 Equations to Solve	52
6.7 Transcendental Equation Solution Process Flow.....	52
6.8 TK Solver Equation Solutions	54
6.8.1 Equation Set Up	54
6.8.2 TK Solver Inputs.....	55

6.8.3 Seed Value Inputs and Convergence	57
6.8.4 TK Solver Example.....	59
Chapter 7: Systems Engineering Methodology for Verification of PV Module Parameter	
Solutions	63
7.1 Background.....	63
7.2 Abstract.....	63
7.3 Introduction.....	64
7.4 PV Module Conditions	65
7.5 Solution Equations for Five PV Parameters	66
7.6 Solving for Five PV Parameters	67
7.6.1 Datasheet Values.....	67
7.6.2 Solution Methods and Sources.....	68
7.6.3 Solution Parameter Sets	69
7.6.4 Reported Solution Errors	69
7.7 Solution Verification.....	70
7.7.1 Physical Parameter Verifications.....	71
7.7.1.1 Diode Ideality Factor	71
7.7.1.2 Series Resistance.....	71
7.7.1.3 Parallel Resistance	72
7.7.2 RMS 5 Error Equation Verification.....	72
7.8 Discussion of Errors.....	74
7.8.1 Current Check at Short Circuit	74
7.8.2 Current Check at Open Circuit	74
7.8.3 Current Check at Maximum Power	75
7.8.4 Voltage Check at Open Circuit.....	75
7.8.5 Voltage Check at Maximum Power.....	75
7.8.6 Overall RMS 5 Error.....	75
7.9 Analysis of Error Sensitivity.....	76
7.10 Recommendations.....	77
7.11 Conclusion	78
Chapter 8: Six Parameter PV Model and I-V Graphing	79
8.1 Introduction.....	79
8.2 Existing PV Equation.....	79
8.3 Six Parameter Model.....	80
8.4 Six Parameter Equations.....	81
8.5 Voltage and Current Bounds.....	81
8.6 Calculations of V_e for the Six Parameter Model.....	82
8.7 Spreadsheet Implementation.....	84
8.8 LabVIEW Configuration	85
8.9 Implementation in LabVIEW	88
8.10 LabVIEW Virtual Instrument	90
Chapter 9: Conclusion.....	91

References.....	92
Appendix A: Copyright Permissions	97
Appendix B: 5.94 kW PV System	100
Appendix C: Thermal Voltage.....	101
Appendix D: PV Terminology Selection Criteria.....	103
Appendix E: Sinton FMT-500 PV Testing and the Two Diode Model.....	104
E.1 Summary.....	104
E.2 Support Documentation and Equipment	104
E.3 Safety	105
E.4 PV Module Stand Setup and Test Cart Connections.....	105
E.5 Dark Room Setup	106
E.6 PV Module Mounting.....	108
E.7 PV Module Testing.....	109
E.8 Comparison of Two Diode Currents	111
Appendix F: MATLAB Code to Solve Equation (23).....	113
Appendix G: Systems Engineering Selection of Solver	115
About the Author	End Page

List of Tables

Table 4.1	PV Connection Topology Loss Comparison	21
Table 4.2	Newpowa NPA50-12 PV Module Data	26
Table 4.3	Primary Circuit Conditions	26
Table 4.4	Mitsubishi PV-UD185MF5 Temperature Sensitivity	29
Table 5.1	BP-MSX120 Performance Characteristic Data	34
Table 5.2	Solver Parameter Values for a BP-MSX120 PV Module	35
Table 5.3	Short Circuit Factors for a BP-MSX120 PV Module	37
Table 5.4	Short Circuit Values for 385 PV Modules	38
Table 5.5	Open Circuit Factors for a BP-MSX120 PV Module	39
Table 5.6	Open Circuit Values for 385 PV Modules	39
Table 5.7	Maximum Power Factors for a BP-MSX120 PV Module	39
Table 5.8	Maximum Power Values for 385 PV Modules	40
Table 6.1	Sample Sources for Numerical Solutions	51
Table 6.2	PV Characteristic Inputs to Solve Five Parameters	51
Table 7.1	KG200GT Datasheet Characteristics	68
Table 7.2	Solution Set Methods and Sources	68
Table 7.3	Parameter Solutions	69
Table 7.4	Solution Set Error Reporting	70
Table 7.5	RMS 5 Error Analysis Results	73
Table 7.6	Error Analysis with Fewer Digits	76

Table 7.7	Source, RMS 3 Error, and RMS 5 Error.....	77
Table 8.1	Range of Parameters	82
Table 8.2	I-V Graph Input Data for KC200GT	88
Table E.1	Comparison of Diode 1 to Diode 2.....	112
Table G.1	Solver Evaluation Matrix.....	115

List of Figures

Figure 1.1	Pearl Street Power Station 1882	1
Figure 2.1	5.94 kW PV System.....	5
Figure 2.2	FGCU Solar Field	6
Figure 3.1	Alexandre Edmond Becquerel	7
Figure 3.2	Mr. Cove and His Sun Electric Generator 1884	8
Figure 3.3	Photoelectric Effect.....	10
Figure 3.4	Photovoltaic Effect.....	10
Figure 3.5	Patent 2,402,662 Fig. 3 P-N Junction	11
Figure 3.6	Patent 2,780,765 Fig. 1 Sunlight and Fig. 2 PV Module	12
Figure 4.1	A Four Parameter PV Model from 1955.....	14
Figure 4.2	The Five Parameter PV Model	15
Figure 4.3	The Seven Parameter PV Model.....	17
Figure 4.4	The Nine Parameter PV Model.....	18
Figure 4.5	PV Cell Example.....	18
Figure 4.6	FGCU Solar Field PV Module Example	19
Figure 4.7	Newpowa 50-watt PV Module.....	19
Figure 4.8	Cell Connection Topologies Newpowa Module.....	20
Figure 4.9	PV Module Model with Five Parameter Cells	22
Figure 4.10	AM1.5 Global Solar Irradiance Data	24
Figure 4.11	Newpowa PV Module Performance Label	25

Figure 4.12	Five Parameter Model at Short, Open, and Maximum Power Conditions	27
Figure 4.13	I-V and Power Graphs Newpowa PV Module.....	28
Figure 5.1	Sample Selection Process Flow	34
Figure 5.2	PV I-V and Power Graphs for BP-MSX120 Module	36
Figure 6.1	Slopes at I_{sc} and P_{mp}	46
Figure 6.2	Equation Solution Process Flow	53
Figure 6.3	TK Solver Equations and Formula for $Y (U_p)$	56
Figure 6.4	TK Solver Formula Equations	56
Figure 6.5	Constants and PV Module Characteristic Data Inputs.....	57
Figure 6.6	Notional Ranges of R_s and R_p	59
Figure 6.7	Inputs of PV Characteristic Data	60
Figure 6.8	Input of Seed Values	60
Figure 6.9	Solutions for Newpowa 50W PV Module	61
Figure 6.10	Newpowa 50W PV Module Five Parameter Model	61
Figure 6.11	Solution Error Example	62
Figure 7.1	Five Parameter PV Model.....	64
Figure 7.2	PV I-V and Power Graphs for KG200GT PV Module.....	65
Figure 8.1	Six Parameter PV Model	80
Figure 8.2	Six Parameter I-V Data Process Flow	84
Figure 8.3	Spreadsheet Implementation of KC200GT PV Module.....	85
Figure 8.4	I_L and I_o Calculation Block Diagram	86
Figure 8.5	LabVIEW I_L and I_o Calculation Block Diagram	87
Figure 8.6	LabVIEW I_L and I_o Calculation Front Panel	88

Figure 8.7	LabVIEW I-V and Power Graph Block Diagram.....	89
Figure 8.8	LabVIEW I-V and Power Graph Front Panel.....	90
Figure B.1	5.94 kW PV System One Line Diagram.....	100
Figure E.1	Sinton Test System	105
Figure E.2	Test Box Connections	106
Figure E.3	PV Module and Stand	107
Figure E.4	Clamps and Light Source.....	107
Figure E.5	Completed Test Dark Room	108
Figure E.6	PV Module and Light Source	109
Figure E.7	Hidden C-Clamps and Light Sensor	109
Figure E.8	Example Test Results.....	110
Figure E.9	Error Message	111
Figure E.10	Diode Current Densities.....	111

List of Terms and Abbreviations

A	Amps
AM	Air Mass
C	Coulomb
CODATA	Committee on Data for Science and Technology
DC	Direct Current
E.M.F	Electro-Motive-Force, Voltage
FGCU	Florida Gulf Coast University
GW	gigawatt 10E9 watts
I	Current in Amps
I-V	Current-Voltage
I _d	Diode current
I _e	External Current of PV system
IEC	International Electrotechnical Commission
I _{mp}	Current at maximum power
I _p	Parallel path current
I _L	Photon Light Generated Current
I _o	Diode reverse or inverse saturation current
I _p	Current through a PV Parallel Resistance
I _{rs}	Current through a PV Series Resistance, same as I _e
I _{sc}	Current at Short Circuit
J	Joule
k	Boltzmann's Constant
K	Temperature in Kelvin
km	kilometer, 10E3 meters
kW	kilowatt 10E3 watts of electrical power
kWh	kilowatt-hour, a unit of electrical energy, 3,600,000 Joules
m	meter(s)
mA	milliamps 10E-3 amps
module	enclosed system including multiple PV cells, also called a PV panel
mV	millivolts 10E-3 volts
MW	Mega Watt 10E6 watts
mp	maximum power
NEC	National Electric Code
nA	nanoamps 10E-9 amps
NIST	National Institute of Standard and Technology
nm	nanometer 10E-9 meters
N _s	Number of Series connected PV cells contained in a module
N _x	Individual PV cell in a module, x is cell number
P	Power in Watts

P-N	Junction of P type and N type semiconductor material
P_{mp}	PV module maximum power
PV	Photovoltaic
q	Charge of an electron
R_e	External resistance
RMS	Root Mean Square
RMSE	Root Mean Square Error
R_p	Parallel Resistance
R_{pcell}	Parallel Resistance of individual PV cell
R_s	Series Resistance
R_{scell}	Series Resistance of individual PV cell
R_{sh}	Shunt Resistance, alternate name for Parallel Resistance R_p
STC	Standard Test Conditions
T	Temperature in Kelvin
UPS	Uninterruptible Power Supply
V	Volts
V_{cell}	PV cell voltage
V_d	Diode Voltage
VDC	Volts Direct Current
V_e	external Voltage of a PV system
VI	virtual instrument
V_j	diode junction Voltage
V_{mp}	Voltage at maximum power
V_{oc}	Voltage at Open Circuit
V_p	external PV Voltage, same as V_e
v_t	Thermal voltage of a diode
W	Watt
η	Eta diode ideality factor, unitless
μ	micro 10E-6
Ω	Ohms unit of electrical resistance
Υ	Upsilon PV module thermal voltage = $\eta v_t N_s$

Abstract

This dissertation analyzes Photovoltaic PV equations and models for silicon based systems from a Systems Engineering framework. Background information includes an introduction, a summary of the state of PV use, a brief history of photovoltaics, and the detailed derivation of equations that enable the finding of the PV parameters contained in the PV models.

The novel inquiry, leveraging systems engineering frameworks, includes three areas useful in analyzing PV equations and models. The first is a statistical verification of common simplifications of PV equations at the primary conditions of short circuit, open circuit, and maximum power. Additional analysis shows other simplifications that should and should not be utilized. The second is a novel systems engineering methodology to verify parameter solutions found when solving the equations derived from the Five Parameter PV Model. Once the five parameters were determined and verified, existing methods to plot a PV current-voltage I-V curve require solving the transcendental PV equation for each data point. The third novel idea presents a Six Parameter Model, which enables graphing the PV I-V curve without solving the PV five parameter transcendental equation.

Chapter 1: Introduction

Our industrial society depends on electrical power. From the electricity operating this computer, as these words were typed, the air conditioning systems that keep us comfortable, the lights in an operating room that help save our lives, to the factory that builds more solar photovoltaic modules, our civilization requires electricity.

At the start of our electrical age in the late 19th century, electrical generation primarily utilized a form of stored solar energy as fuel. The stored energy was coal, created from photosynthesis driven plant growth, which was morphed, compressed, and converted over time to form this fossil fuel.

The first electrical generation facility in the United States was the Pearl Street Station, built in 1882 [1]. The plant operated on coal. Figure 1.1 shows the station with a wagon unloading the solar derived coal.



Figure 1.1 Pearl Street Power Station 1882. Public Domain image {1}.

Even with the addition of other fossil fuels, such as oil and gas, the existing economic view supported the continuation of this electrical generation model. As engineers expanded available technologies and widened the economic analysis of electrical generation to a systems view, humans started to understand the advantages of multiple methods of electrical generation. One of the methods devised was exploiting the photovoltaic effect and the associated no-cost fuel method of electrical power generation. This dissertation utilizes systems engineering framework concepts to introduce novel ideas to simplify, verify, and understand PV equation solutions, modeling, and graphing for silicon based systems.

1.1 Statement of Problem

1.1.1 Complex PV Equations

PV systems include semiconductor P-N junctions and the associated nonlinear diode equation. Existing methods that justify the simplifications of the PV equations include single-point examples or a notional statement on the relative size of the factors and how this relative size justifies the elimination of terms. An investigation found no method that generally verifies the commonly applied simplification of the PV equations for silicon based PV systems.

1.1.2 New Verification Method for Solved PV Parameters

The method to finding the five PV parameters, diode ideality factor η , series resistance R_s , parallel resistance R_p , photon light current I_L , and diode reverse saturation current I_o , in the Five Parameter PV Model requires numerically solving three complex concurrent transcendental equations and using the results to solve two standard equations. Numerous methods, such as Newton-Raphson, provide methods to solve and derive answers, with multiple manuscripts producing inconsistent and conflicting parameter solutions. An investigation found no sources

that applied the systems engineering verification method to check that the solved parameter results correctly fit the PV Model equation.

1.1.3 Transcendental Equation for the Graphing of I-V Curves

Once the solutions of the PV equation five parameters were solved and verified, graphing the PV I-V curve requires the solution of a transcendental equation for each data point. No method or model that enables the simplified graphing of a PV I-V curve is currently available.

1.2 Research Questions

1. For silicon based PV systems, is there a method available to verify the simplification of PV Equations at short circuit, open circuit, and maximum power?
2. Is there a method to verify the parameter solutions found for the PV equation?
3. Is a method available to graph a PV I-V curve without solving a transcendental equation for each data point?

1.3 Methods and Contributions of Solutions

1.3.1 PV Equation Simplification Verification

A systems engineering verification method involved obtaining a statistically valid sample of silicon based PV modules, calculating the five parameters solution for each sample, and showing the simplification applies to the general population. Simpler equations enable easier and less error prone solutions.

1.3.2 Verification of Solved PV Parameters

Applying Systems Engineering principles, the author developed an error determination method to verify the solutions found when solving for the PV Model five parameters, η , R_s , R_p , I_L ,

and I_0 . The method provides the means to verify and ensure reasonable and accurate parameter solution values.

1.3.3 Six Parameter Model and Simplified Method to Graph PV I-V Curves

A novel Six Parameter Model is introduced, which simplifies the analysis and graphing of the PV I-V curves. With the Six Parameter Model, the PV I-V curve can be plotted without solving a transcendental equation for each data point.

Chapter 2: Existing State of Photovoltaic Systems

The costs of Photovoltaic PV modules have dropped from over \$100 per watt in 1975 to a current price of under \$0.50 per watt [2]. For residential installations, the levelized costs of PV energy production has dropped from \$0.50 per kilowatt-hour kWh in 2010 to \$0.128 per kWh in 2020 [3]. Using the National Renewable Energy Lab, System Advisor Model [4], a techno-economic software program, the author analyzed the self-built and installed 5.94 kW home PV systems and calculated an economic break-even duration of under 13 years. The PV system's life expectancy is over 25 years. In the United States, as of 2021, there were over 3,000,000 PV installations on homes [5]. Figure 2.1, with the single-line diagram in Appendix B, shows the 5.94 kW PV system, with the eighteen 330-watt modules visible at the bottom. The five small panels at the top center of the figure are a solar thermal hot water collection system with, to the right, a tiny 10-watt PV module that powers the water circulation pump.



Figure 2.1 5.94 kW PV System.

Lower costs and the push for renewable/sustainable energy production have led to a massive worldwide expansion of PV installations. In 2008, the United States had 340 megawatts MW of PV installed, and in 2022, 97.2 gigawatts GW [6]. The 2020 World Energy Outlook projects growth from 150 GW in 2021 to 2,000 to 4,000 GW of installed capacity in 2030 [7]. The number and size of PV Plants continue to expand, with the current largest PV Power Plant, the Bhadla Solar Park in India, covering 57 km² with a planned capacity of 2.245 GW [8]. With regulatory size limits of under 75 MW, Florida Power and Light has over 25 Solar Energy Centers with a nameplate rating of 74.5 MW. Babcock Preserve covers 430 acres, has a nameplate rating of 74.5 MW, and contains 345,369 PV modules [9]. A smaller 2 MW nameplate rating plant at Florida Gulf Coast University FGCU covers 15 acres and contains 10,800 PV modules. A drone image of part of the FGCU PV Plant is shown in Figure 2.2.



Figure 2.2 FGCU Solar Field.

The existing and expanding use of PV systems merits technical investigation and additional research. This dissertation contributes to this endeavor.

Chapter 3: A Brief Photovoltaic History

3.1 Early Years

The photovoltaic effect was discovered in 1839 by Alexandre Edmond Becquerel [10]. While illuminating platinum, which was coated with silver compounds, Mr. Becquerel, shown in Figure 3.1, noted voltage generation. At one time, the photovoltaic effect was known as the Becquerel effect.



Figure 3.1 Alexandre Edmond Becquerel. Public Domain image {2}.

In 1848, Willoughby Smith, an Electrical Engineer working on underwater telegraph wires for the Gutta Percha Company, developed a process to test these cables. The method utilized selenium, and during testing, he discovered that the resistance changed when exposed to sunlight. This effect was published in 1873 in the journal Nature [11] and led to the photoelectric cell.

In 1877, William Adams and Richard Day discovered that exposing selenium to light produces electricity [12]. Experimentation showed that “it was clear that a current could be started in the selenium by the action of the light alone.” This discovery started the PV age.

Leveraging the Adams and Day discovery, Charles Fritts, in 1883, built the first working selenium cells [13]. George Cove leveraged the selenium cells to build a solar module, a panel consisting of multiple connected cells. Multiple modules created a solar array installed on a building rooftop in New York City in 1884. The array generated $\frac{1}{4}$ horsepower with 272 square feet of PV modules [14]. At one sun of irradiance, described in Chapter 4, the conversion efficiency was about 0.75%. Modern, high-quality PV modules have efficiencies of above 20%.

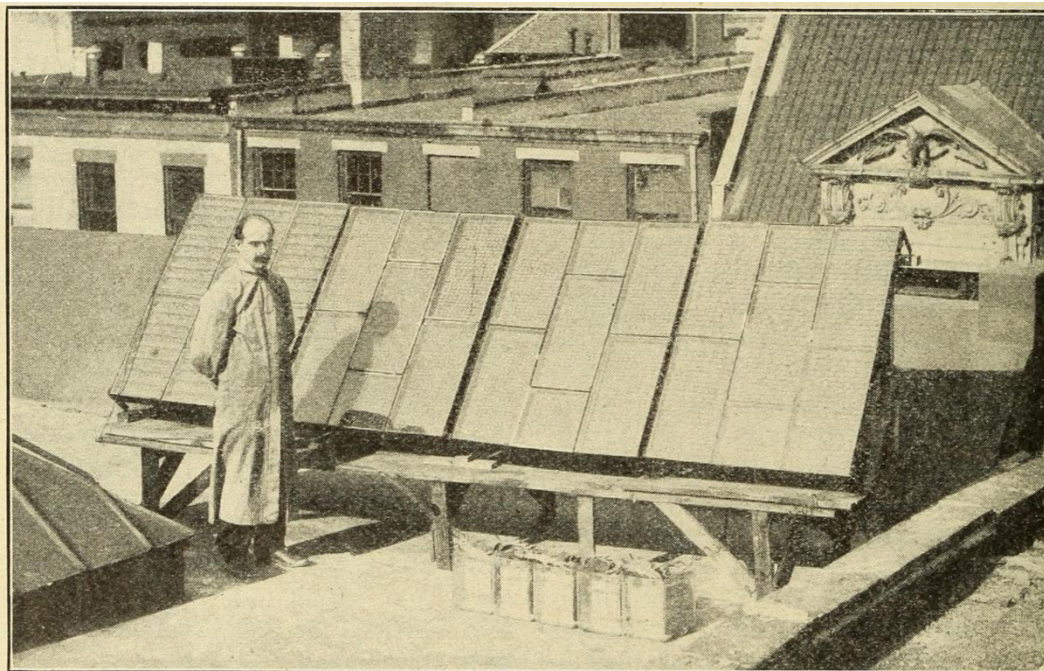


Figure 3.2 Mr. Cove and His Sun Electric Generator 1884. Public Domain image {3}.

While experimenting with radio waves to investigate Maxwell's equations, Heinrich Hertz discovered in 1887 an effect when illuminating a spark gap with ultraviolet light [15]. Hertz discovered that light exposure produced a stronger spark, a photoelectric effect.

In 1888, Aleksandr Stoletow experimented with the production of electric current with ultraviolet rays [16]. His work established Stoletow's Law, which states that photoelectric current is directly proportional to light intensity. Later, in 1900, Elster and Geitel experimentally verified the law of proportionality [17]. The law states that photon induced current is directly proportional to the light intensity. The relationship between photon input and current output is a fundamental concept used in PV analysis, where, ideally, one photon of sufficient energy generates one electron.

3.2 Scientific Understanding

In 1905, Albert Einstein published, in German, with the English title translation, "On a heuristic point of view concerning the generation and transformation of light" [18]. This publication successfully explained the scientific basis of the Photoelectric Effect and won Einstein his Nobel Prize in 1921 [19].

Robert Millikan attempted to invalidate Einstein's theory of the Photoelectric Effect. Instead, Millikan's experiment proved Einstein's theory and led to his winning the Nobel Prize in 1923. The prize was for work on the electron and Photoelectric Effect [20]. In addition to other works, Millikan determined the charge of an electron 'q,' one of the factors used in the PV equations described in Chapter 4.

3.3 Photoelectric and Photovoltaic Effects

Throughout literature, the terms Photoelectric and Photovoltaic Effects are utilized. The energy of incident photons drives both effects. The Photoelectric Effect happens when sufficiently

high energy photons cause the ejection of electrons from a material. Figure 3.3 shows the Photoelectric Effect and the resulting photoelectrons.

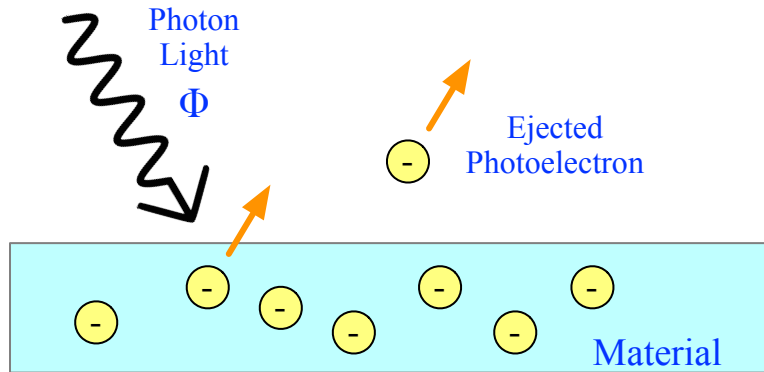


Figure 3.3 Photoelectric Effect.

The Photovoltaic Effect is the generation of voltage and current in a material when irradiated with light. The input of a sufficiently energetic photon generates a charge separation, the production of an electron-hole pair, and the movement of an electron in the n-type and a hole in the p-type materials. Photovoltaic cells are also known as solar cells. Figure 3.4 shows the Photovoltaic Effect.

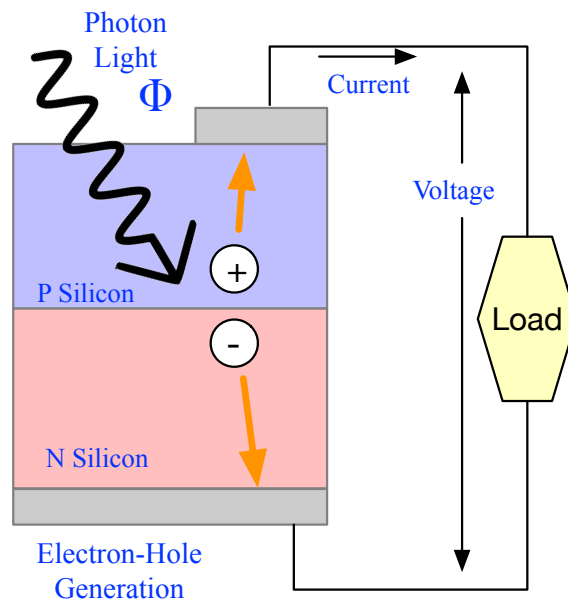


Figure 3.4 Photovoltaic Effect.

3.4 Photoelectric to Semiconductor Photovoltaic Systems

Before modern semiconductor devices, Anthotho Lamb patented a Photoelectric Device [21] in 1935. As stated in the patent, "... actinoelectric material such as cuprous oxide, selenium, tellurium, selenides ...". This device produced low voltage and low conversion efficiency systems. With advances in solid-state electronics, new semiconductor materials were developed. These new materials enabled more efficient methods to exploit the energy of photons. The semiconductor PV cell started with the United States patent 2,402,662, "Light-Sensitive Electric Device" by Russel Ohl, in June 1941 [22]. The patent states, "This invention relates to light-sensitive electric devices and more particularly to photo-E. M. F. cells comprising fused silicon of high purity." Recall that E. M. F. is electro-motive-force, another name for voltage. This invention was the photovoltaic cell. Figure 3.5 from the patent shows the "P" and "N" zones of a P-N junction semiconductor device. Ohl worked for Bell Telephone Laboratories, where the modern PV age started.

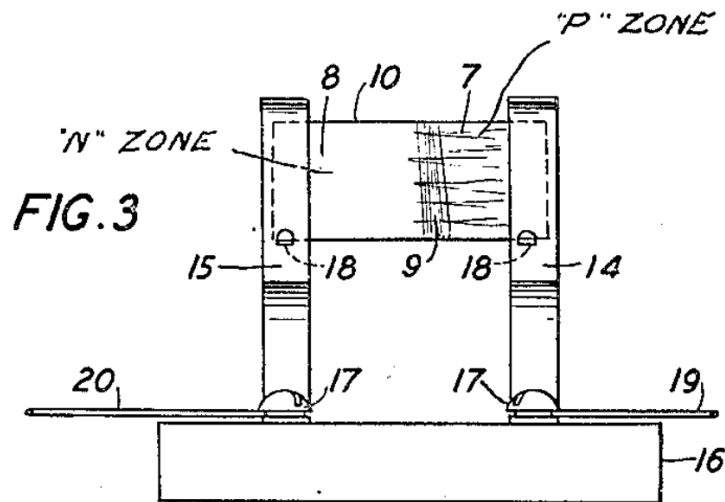


Figure 3.5 Patent 2,402,662 Fig. 3 P-N Junction. US Patent Office {4}.

In 1954, Daryl Chapin, Calvin Fuller, and GERALD Pearson, who also worked for Bell Telephone Laboratories, were granted patent 2,780,765 [23] “Solar Energy Converting Apparatus.” The apparatus was explicitly devised to convert solar irradiance to electrical energy, a first. The conversion device included a P-N junction, silicon, boron, and other modern features. Conversion efficiency was 6%, well above selenium’s $\approx 1\%$ value. Figure 3.6 shows Figure 1 from the patent and illustrates the sunlight input. Figure 2 from the patent shows the connection of multiple PV cells in series, forming a PV module, also known as a PV panel.

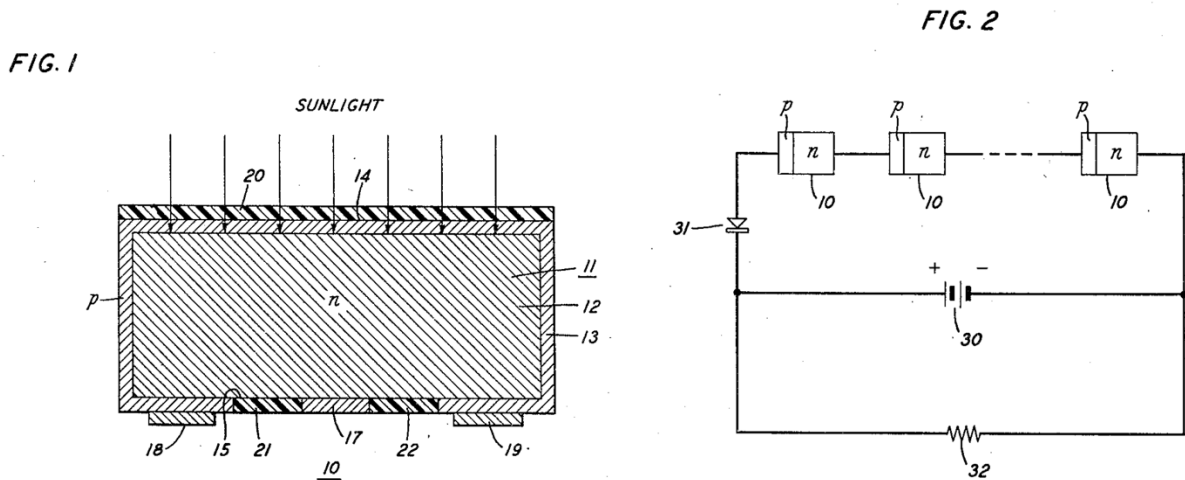


Figure 3.6 Patent 2,780,765 Fig. 1 Sunlight and Fig. 2 PV Module. US Patent Office {4}.

3.5 Alternative PV Materials

In 2021, silicon based PV systems were approximately 95% of the market share [24]. Alternative PV systems include cadmium telluride thin film, which contains toxic heavy metal, gallium arsenide, which is primarily used in space-based applications, perovskite, and organic photovoltaic materials. This dissertation focuses on silicon based PV systems.

Chapter 4: Existing PV Equations and Models

4.1 Background

4.1.1 P-N Junction Diode

As shown in Figure 3.6, the silicon based PV cell contains a P-N junction, which is a diode. In 1949, William Shockley, also from Bell Laboratories, published the theory of P-N junction diodes [25]. One of the primary accomplishments of the 1949 paper was the Shockley diode Equation (1). Note that in Equation (1), the terminology from the source was modified to match the terms used in this dissertation.

$$I_d = I_o \left(e^{\frac{V_d}{\eta v_t}} - 1 \right) \quad (1)$$

- I_d is the diode current, amps
- I_o is the diode reverse saturation current, amps
- V_d is the diode voltage, volts
- η is the diode ideality factor, no units
- v_t is the thermal voltage, volts

Embedded inside Equation (1) is the thermal voltage v_t . Equation (2) shows that the thermal voltage is a function of the variable thermal temperature T and the fundamental fixed constants k and q . Appendix C provides additional information on thermal voltage.

$$v_t = \frac{kT}{q} \quad (2)$$

- v_t is the thermal voltage, volts
- k is Boltzmann's constant, joules per Kelvin 1.380649E-23
- T is the temperature, Kelvin
- q is the charge of an electron, coulombs 1.602176634E-19

4.1.2 Early PV Cell Model

A 1955 article by U. Gianola, also from Bell Laboratories, wrote the manuscript, “Photovoltaic Noise in Silicon Broad Area p-n junctions,” and included the earliest PV cell equivalent electric circuit model found [26]. The equivalent circuit model did not include a parallel resistance, R_p , and thus is a Four Parameter Model including the series resistance R_s , photon light current I_p , the diode reverse saturation current I_o , and diode ideality factor η . The diode current I_j is controlled by the parameters I_o and η . Figure 4.1 replicates the solar cell equivalent circuit model from the 1955 source.

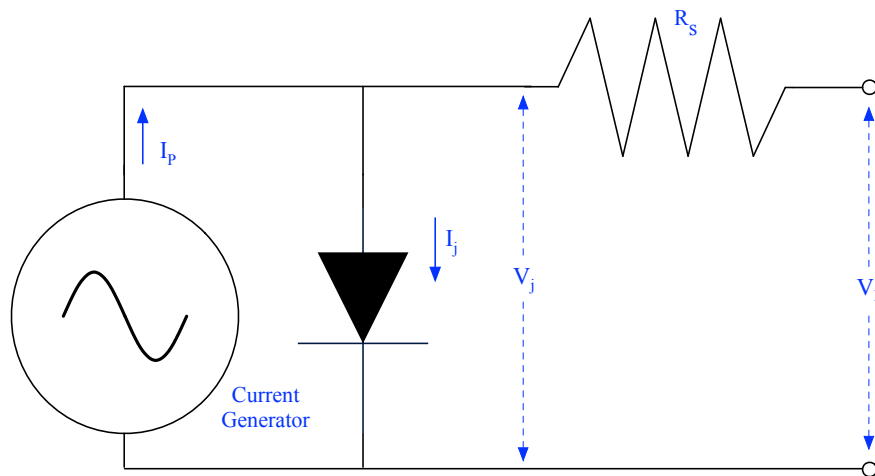


Figure 4.1 A Four Parameter PV Model from 1955.

The Four Parameter Model included the concept of a photon powered ideal current source, with an incorrect alternating current symbol since the current production is direct, a diode for the P-N junction of the solar cell, and a series resistance R_s , to account for the equivalent body resistance of the cell. The components identified in the model are listed below.

- I_p photon light generated current, I_L in this document, amps
- I_j diode junction current, I_d in this document, amps
- V_j diode voltage, V_d in this document, volts
- R_s series resistance, ohms
- V_p photovoltaic voltage, V_e for external voltage in this document, volts

4.1.3 Early PV Cell Equations

With a Model, a PV equation can be derived by applying Kirchhoff's current law and circuit analysis. Utilizing Figure 4.1 and Kirchhoff's current law, Equation (3) was obtained.

$$I_p = I_j + I_{R_s} \quad (3)$$

Inserting the Shockley diode Equation (1) for I_j derives Equation (4). For the Four Parameter Model, V_j replaced V_d in Equation (1). The external current I_c was identified as I_{R_s} , the current conducting through the series resistance.

$$I_p = I_o \left(e^{\frac{V_j}{\eta v_t}} - 1 \right) + I_{R_s} \quad (4)$$

4.2 Modern PV Cell Models and Equations

4.2.1 The Five Parameter Model

A more accurate model requires the inclusion of a parallel resistance across the diode. The parallel resistance R_p , accounts for manufacturing defects and alternate paths for current leakage. Numerous technical sources show this Five Parameter Model with a highly cited example from DeSoto [27]. The standard Five Parameter Model adds a parallel resistance R_p , sometimes called shunt resistance R_{sh} . Figure 4.2 shows the Five Parameter Model equivalent circuit.

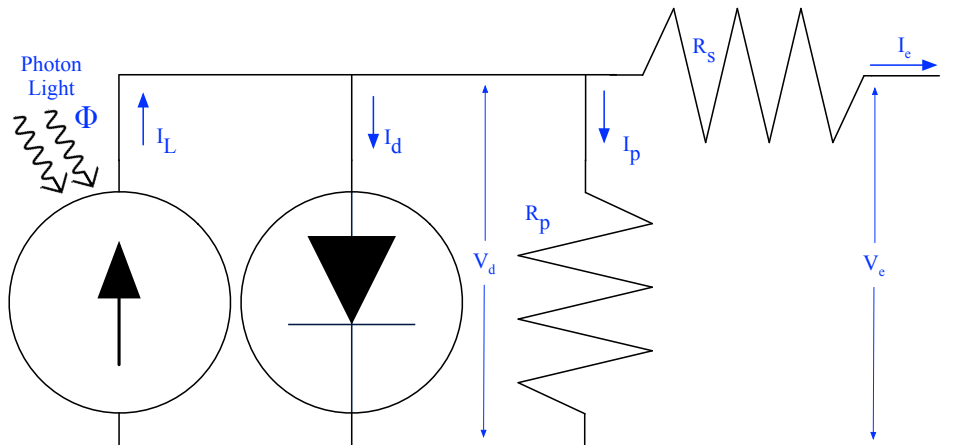


Figure 4.2 The Five Parameter PV Model.

The model shown in Figure 4.2 includes terminology utilized in the rest of this document. The five parameters of the model are η , R_s , R_p , I_L , and I_o , where η and I_o are embedded in the diode current I_d . A list of the factors in the Five Parameter Model follow. Appendix D shows the terminology selection criteria.

- Φ photon light, photons
- I_L photon light generated current, amps
- I_d diode junction current, amps
- V_d diode voltage, volts
- R_p parallel resistance, ohms
- R_s series resistance, ohms
- I_e external current, amps
- V_e external voltage, volts

4.2.2 Equations for Five Parameter Model

Referencing Figure 4.2 and applying Kirchhoff's Current Law, Equation (5) was derived. Photons with sufficient energy generate the photon light current I_L via the Photovoltaic Effect. This current was divided into diode current I_d , parallel path current I_p , and external current I_e .

$$I_L = I_d + I_p + I_e \quad (5)$$

Equation (5) can be rearranged to the more commonly used format by placing the external current I_e on the left. This change derives Equation (6).

$$I_e = I_L - I_d - I_p \quad (6)$$

Substituting the Shockley diode Equation (1) for the diode current I_d , replacing the diode voltage V_d with model parameters, and replacing the parallel current I_p with circuit parameter terms, Equation (7) was derived. This equation was the existing standard for the Five Parameter PV Cell Model.

$$I_e = I_L - I_o \left(e^{\frac{V_e + I_e R_s}{\eta v_t}} - 1 \right) - \frac{V_e + I_e R_s}{R_p} \quad (7)$$

From Equation (7), the external current I_e is the photon light current, minus current losses through the diode and the parallel resistance paths. Low diode and parallel currents are desirable because these conditions maximize the external current and the performance of the overall PV system.

4.2.3 Alternate Seven and Nine Parameter Models

In attempts to better model the P-N junction of the PV cell, alternate models include the addition of more diodes. The Seven Parameter Model adds a second diode, changes η and I_o to η_1 and I_{o1} , and adds η_2 and I_{o2} , where the ideality factor and current are embedded in the respective I_{d1} and I_{d2} currents. The first diode represents the diffusion current, while the second diode accounts for the recombination current in the depletion region [28]. Figure 4.3 shows the Seven Parameter Model, also known as the dual diode model. Calculating the values of this model requires solving for seven parameters.

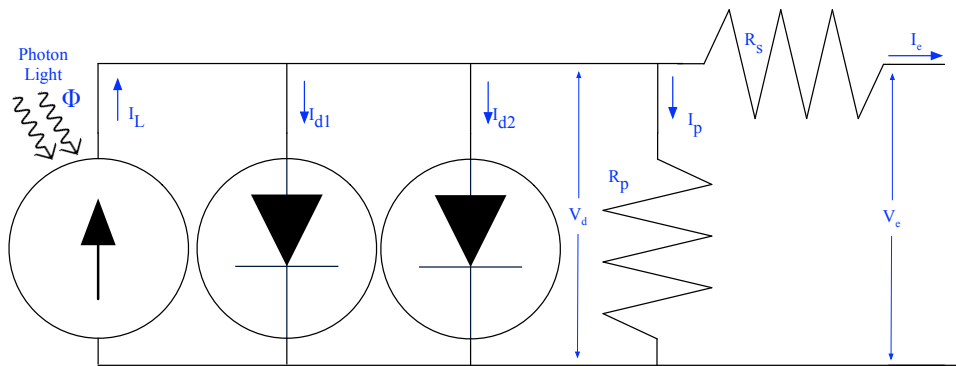


Figure 4.3 The Seven Parameter PV Model.

A more complex model adds another diode, resulting in the triple diode model. The third diode was added as a further refinement but increases the number of parameters to solve to nine. Figure 4.4 shows the Nine Parameter Model. The diode current I_d is divided between I_{d1} , I_{d2} , and I_{d3} , with embedded terms of η_1 , η_2 , η_3 , I_{o1} , I_{o2} , and I_{o3} .

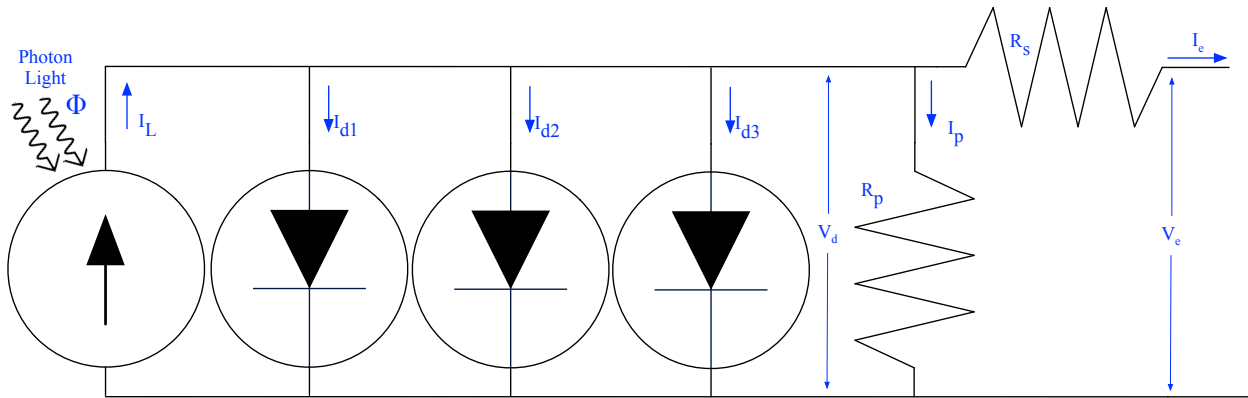


Figure 4.4 The Nine Parameter PV Model.

The question was whether the additional refinement provided by the Seven or Nine Parameter Models is worth the increased complexity. According to Tofili [29], “...the single-diode model has been proven to be precise enough...” This statement was notionally confirmed by the analysis provided in Appendix E, and for these reasons, this document utilizes the Five Parameter Model.

4.3 Modification of PV Cell Equations and Model for PV Modules

4.3.1 PV Module Description

This section derives the model and equations for a PV module, also known as a PV panel. Figure 4.2 and Equation (7) show the Five Parameter Model for a single PV cell. Figure 4.5 shows an example of a PV cell, showing the front, the back, and the edge. A PV cell consists of a single system component wafer produced via technologies leveraged from the semiconductor industry.

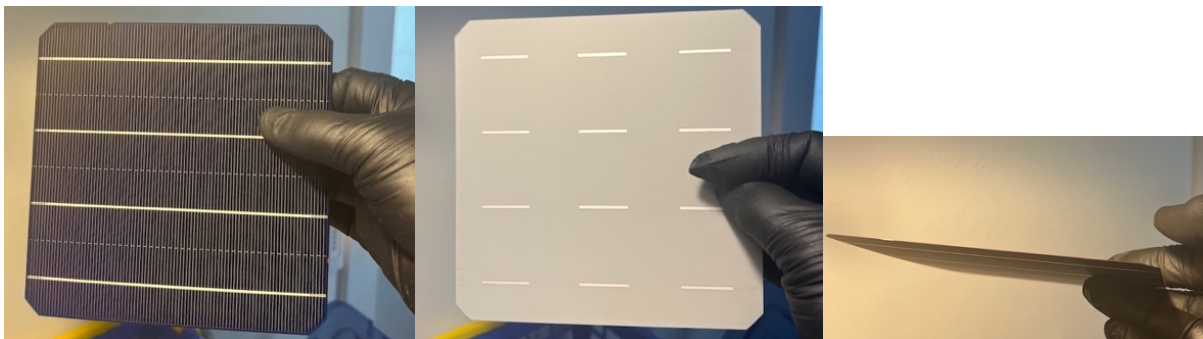


Figure 4.5 PV Cell Example.

PV modules typically include a set of series connected PV cells, which raise the approximately 600 mV open circuit voltage of a single cell to a more usable range. PV modules typically contain between 36 to 72 and more cells connected in series and provide a voltage level suitable, for example, charging storage batteries in the 36-cell case to large-scale PV power production with multiple 72-cell modules connected in series. The Kyocera KC200GT module, discussed in Chapter 7, has 54 cells in series with an open circuit voltage of 32.9 VDC. Figure 4.6 shows an example of a Mitsubishi PV-UD185MF5 module from the FGCU Solar Field, shown in Figure 2.2, and contains 50 series connected PV cells with an open circuit voltage of 30.6 VDC.



Figure 4.6 FGCU Solar Field PV Module Example.

Figure 4.7 shows a Newpowa NPA50-12, 50-watt module. This module was designed for 12 VDC battery charging and contains 36 series PV cells.



Figure 4.7 Newpowa 50-watt PV Module.

PV system designs endeavor to maximize power output, which in the case of DC systems calculates as current multiplied by voltage, as shown in Equation (8).

$$P = IV \quad (8)$$

Since power losses in a system are a function of the square of current, the optimal method to maximize power and minimize loss involves a series of connected PV cells to increase voltage and minimize current. Almost all PV modules utilized series connection topology. Figure 4.8 shows the connection topology of the Newpowa module as built with a series connection of 36 cells versus an alternate topology of two parallel sets of 18 series cells. Both topologies produce the rated 50 watts of power output but with different voltage and current levels.

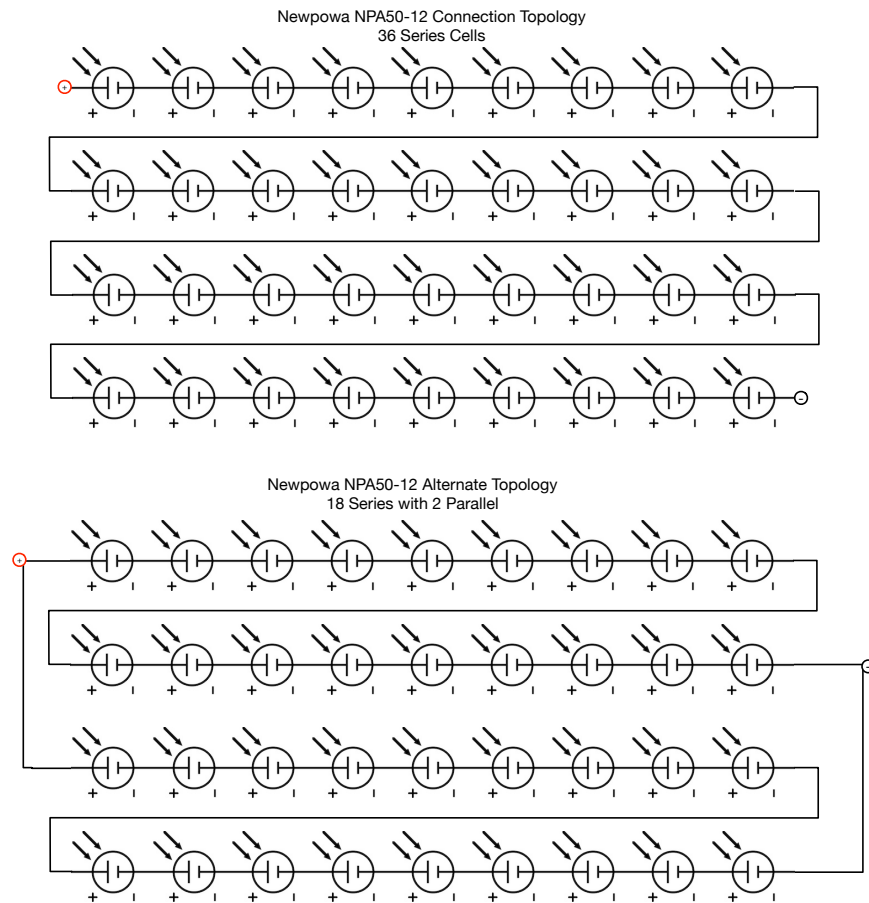


Figure 4.8 Cell Connection Topologies Newpowa Module

Table 4.1 shows losses for a circuit with a one-ohm load for the as-built series connection and two parallel connection configurations shown in Figure 4.8. This example shows why PV systems are designed with series connected cells, with designs implementing the highest allowable system voltage. The push for higher voltage has even permitted the inclusion of a provision in the National Electric Code NEC 690.7 [30] that allows the installation of 1,500-volt PV systems without following NEC Article 490, which specifies more complex and expensive requirements for voltages greater than 1,000-volt.

Table 4.1 PV Connection Topology Loss Comparison

System	Maximum Power Point Voltage	Maximum Power Point Current	System Power Output	Losses for 1 Ω Circuit
Standard	17.2 VDC	2.91 A	50.0 watts	8.47 watts
2 Parallel	8.6 VDC	5.82 A	50.0 watts	33.87 watts

4.3.2 PV Cell to Module Equivalent Model

By taking multiple copies of the Five Parameter Model shown in Figure 4.2 and connecting them in series, Figure 4.9 was derived, which shows a model of a PV module. The limitation of the model requires each cell to have the same photon light irradiance, temperature, and physical characteristics. These criteria are met since PV modules are tested under the same light and temperature conditions. In addition, when PV modules are built, the individual cells are tested, and similar cells were binned before inclusion in the same PV module.

With a series connection of identical cells irradiated with identical photon light input, the currents of I_L and I_e are the same. The term V_{cell} was utilized to identify the individual cell voltage. Cell resistances' terminologies were changed to R_{scell} for the cell series resistance and R_{pcell} for the cell parallel resistance. A specific cell was identified as N_x , where the 'x' was the cell number, and the total number of series connected PV cells was N_s . With the revised nomenclature and by

inspection, the module voltage V_e equals $V_{cell} \times N_s$, module series resistance $R_s = R_{scell} \times N_s$, and module parallel resistance $R_p = R_{pcell} \times N_s$.

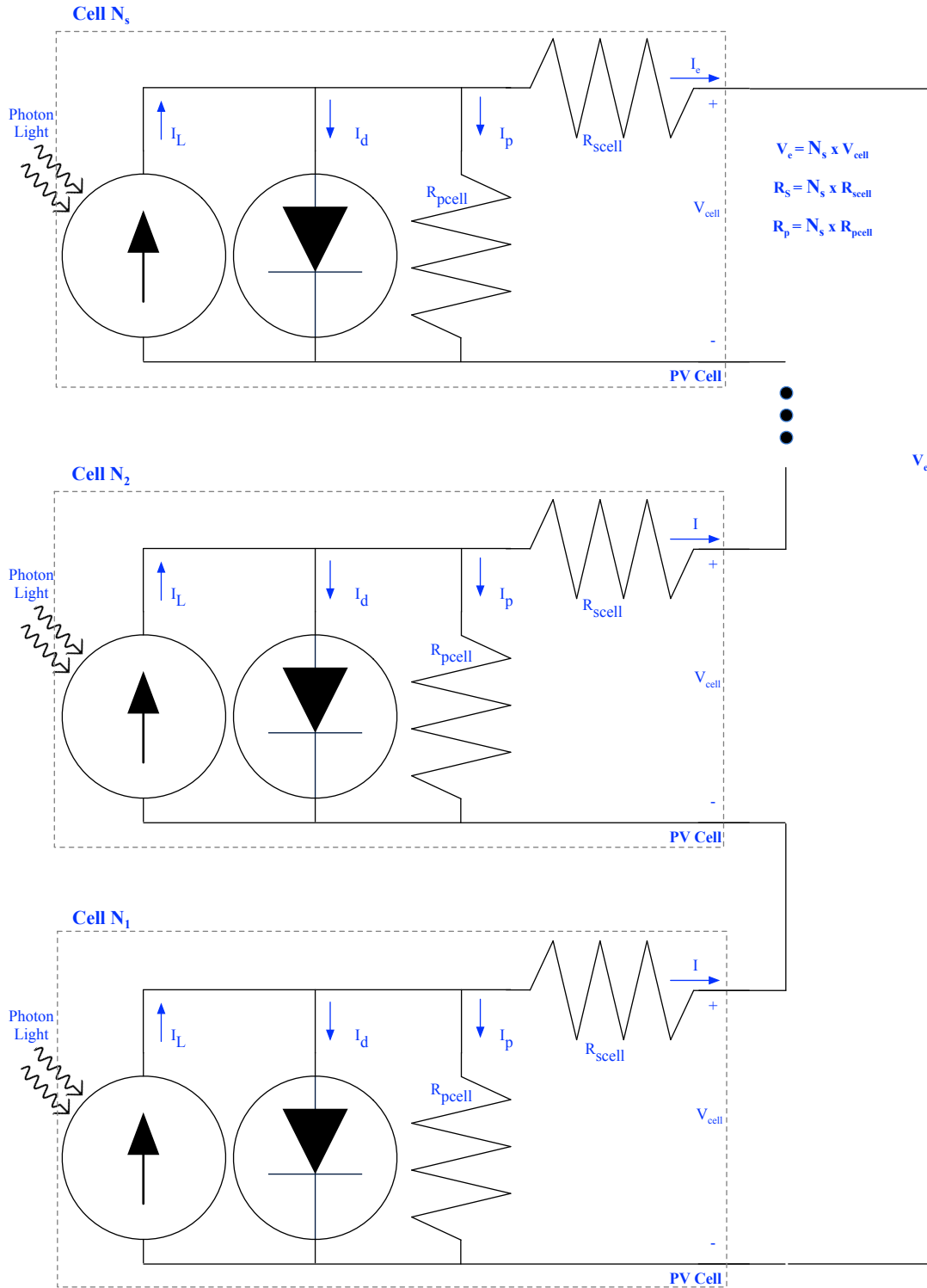


Figure 4.9 PV Module Model with Five Parameter Cells

4.3.3 PV Cell to Module Equations

As shown in Figure 4.9, I_e and I_L are the same for single or multiple series cells. With revised nomenclature, the single PV cell becomes Equation (9).

$$I_e = I_L - I_o \left(e^{\frac{V_{cell} + I_e R_{scell}}{\eta v_t}} - 1 \right) - \frac{V_{cell} + I_e R_{scell}}{R_{pcell}} \quad (9)$$

The new factor N_s was added to account for the number of PV series connected cells. The factor N_s/N_s was included along with a substitution for $V_{cell} = V_e / N_s$, resulting in Equation (10).

$$I_e = I_L - I_o \left(e^{\frac{\left(\frac{V_e}{N_s} + I_e R_{scell}\right) N_s}{\eta v_t} - 1} \right) - \frac{\left(\frac{V_e}{N_s} + I_e R_{scell}\right) N_s}{R_{pcell} N_s} \quad (10)$$

Equation (11) was derived by multiplying the respective cell series and parallel resistances. Note that if $N_s = 1$, Equation (7) was obtained, which means the 5 Parameter Model shown in Figure 4.2 applies to both an individual PV cell and PV modules of any number of series connected cells.

$$I_e = I_L - I_o \left(e^{\frac{(V_e + I_e R_s)}{\eta v_t N_s}} - 1 \right) - \frac{(V_e + I_e R_s)}{R_p} \quad (11)$$

4.4 PV Module Test Conditions and Characteristics

4.4.1 Test Conditions

Testing and labeling standards were developed to ensure consistent reporting of PV module performance. The International Electrotechnical Commission IEC has numerous standards for PV module tests. One of interest was “Photovoltaic devices – Part 1: Measurement of photovoltaic current-voltage characteristics” [31]. This standard and others established consistent methods to measure PV module performance. “Test Method for Photovoltaic Module Ratings” by the Florida Solar Energy Center [32] provided an excellent summary. The Standard Test Conditions STC is

based on 1 sun of solar photon input and other specific conditions. The solar input is in power density in the units of watts per meter squared, where the standard is an irradiance of $1,000 \text{ W/m}^2$ with spectral distribution specified by ASTM E-490 or ISO 9845-1 [33]. A spreadsheet of the spectra is available at [34]. The reference spectra data are AM1.5 for Air Mass, an atmospheric model with a solar zenith angle at 48.2° and other conditions. Figure 4.10 shows the spectral data and the result of the data integration, which is the STC irradiance, rounded to 1000 W/m^2 . In Figure 4.10, the x-axis scale is nanometers nm. and the y-axis scale is spectral irradiance in units of $\text{W}/(\text{m}^2 \cdot \text{nm})$. Integration of the spectral data provides the correct unit of power density in W/m^2 . The last condition is the test temperature set at 25° C or 298.15 K .

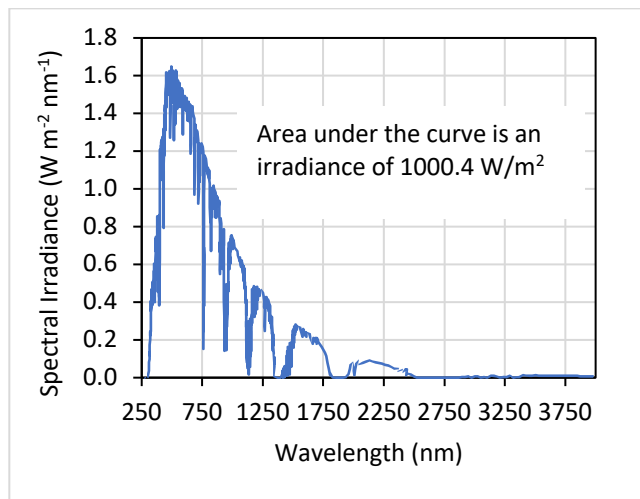


Figure 4.10 AM1.5 Global Solar Irradiance Data.

4.4.2 Test Results

PV modules are tested under STC from short circuit to open circuit. Short circuit is a PV module with a shorted connection with 0 ohms load, open circuit is with an open connection with $\infty \text{ ohms}$ load, and varying resistance between the two extremes. Three primary data points are determined: current at short circuit I_{sc} , with external voltage $V_e = 0$, voltage at open circuit V_{oc} , with external current $I_e = 0$, and the maximum power condition m_p . Maximum power is the STC

power output of the module, with current at I_{mp} and voltage at V_{mp} . A testing system that utilizes STC is shown in Appendix E. Figure 4.11 shows the results of the manufacturer’s STC test, with an example PV module performance label attached to the Newpowa PV modules shown in Figure 4.7.

Model: NPA50-12		
Max Power	Pmax	50W
Operating Voltage	Vmp	17.2V
Operating Current	Imp	2.91A
Open Circuit Voltage	Voc	21.6V
Short Circuit Current	Isc	3.23A

All rating at STC 1000W/m², AM 1.5 spectrum, 25°C

Figure 4.11 Newpowa PV Module Performance Label.

4.4.3 Parameter Data

The PV module I-V curve follows the Five Parameter Model Equation (11). Graphing the curve requires the determination of the five parameters, η , R_s , R_p , I_L , and I_o . Table 4.2 shows all the relevant characteristics and parameter data for the Newpowa NPA50-12 PV module. The characteristics are from the PV module datasheet, with item #1 stated in the datasheet or available by counting the number of series PV cells N_s installed in the PV module. Items #2, #3, #4, and #5 are available from the datasheet or the PV module performance label. Item #6 is STC temperature of 25° C, stated in Kelvin. Items #7 and #8 are Boltzmann’s constant k and the charge of an electron q , respectively. The following three parameters, η , R_s , and R_p , are determined by solving three concurrent transcendental equations, and the final two parameters are determined by calculating the results from two ordinary equations. The method and procedures for determining parameters #9, #10, #11, #12, and #13 are fully described in Chapter 6.

Table 4.2 Newpowa NPA50-12 PV Module Data

#	Symbol	Value	Units	Source	Comment
1	N_s	36	count	datasheet	Number of series PV cells in the module
2	V_{oc}	21.6	Volts	datasheet	Voltage at open circuit
3	V_{mp}	17.2	Volts	datasheet	Voltage at maximum power
4	I_{mp}	2.91	Amps	datasheet	Current at maximum power
5	I_{sc}	3.23	Amps	datasheet	Current at short circuit
6	T	298.15	K	measured	Temperature in Kelvin at STC
7	q	1.6021766E-19	C	constant	Charge of an electron
8	k	1.380649E-23	K/J	constant	Boltzmann's constant
9	η	1.644426	none	solved	Diode ideality factor
10	R_s	.2063455	Ohms	solved	Series resistance
11	R_p	298.8625	Ohms	solved	Parallel resistance
12	I_L	3.232230	Amps	calculated	Current from Photon Irradiance Φ
13	I_o	2.282643 μ A	Amps	calculated	Diode reverse saturation current

4.4.4 Short, Open, and Maximum Power Condition Equations

Figure 4.12 shows the configurations for each primary circuit condition: short circuit with an external load 0Ω , open circuit with an external load $\infty \Omega$, and maximum power with an external load $V_{mp}/I_{mp} \Omega$. Table 4.2 shows the values at each condition and the respective equations derived from Equation (11). Chapter 5 shows how these equations can be simplified.

Table 4.3 Primary Circuit Conditions

Condition	Value of V_e	Value of I_e	Equation
Short Circuit	0	I_{sc}	(12)
Open Circuit	V_{oc}	0	(13)
Maximum Power	V_{mp}	I_{mp}	(14)

$$I_{sc} = I_L - I_o \left(e^{\frac{I_{sc}R_s}{\eta v_t N_s}} - 1 \right) - \frac{(I_{sc}R_s)}{R_p} \quad (12)$$

$$0 = I_L - I_o \left(e^{\frac{V_{oc}}{\eta v_t N_s}} - 1 \right) - \frac{V_{oc}}{R_p} \quad (13)$$

$$I_{mp} = I_L - I_o \left(e^{\frac{(V_{mp} + I_{mp}R_s)}{\eta v_t N_s}} - 1 \right) - \frac{(V_{mp} + I_{mp}R_s)}{R_p} \quad (14)$$

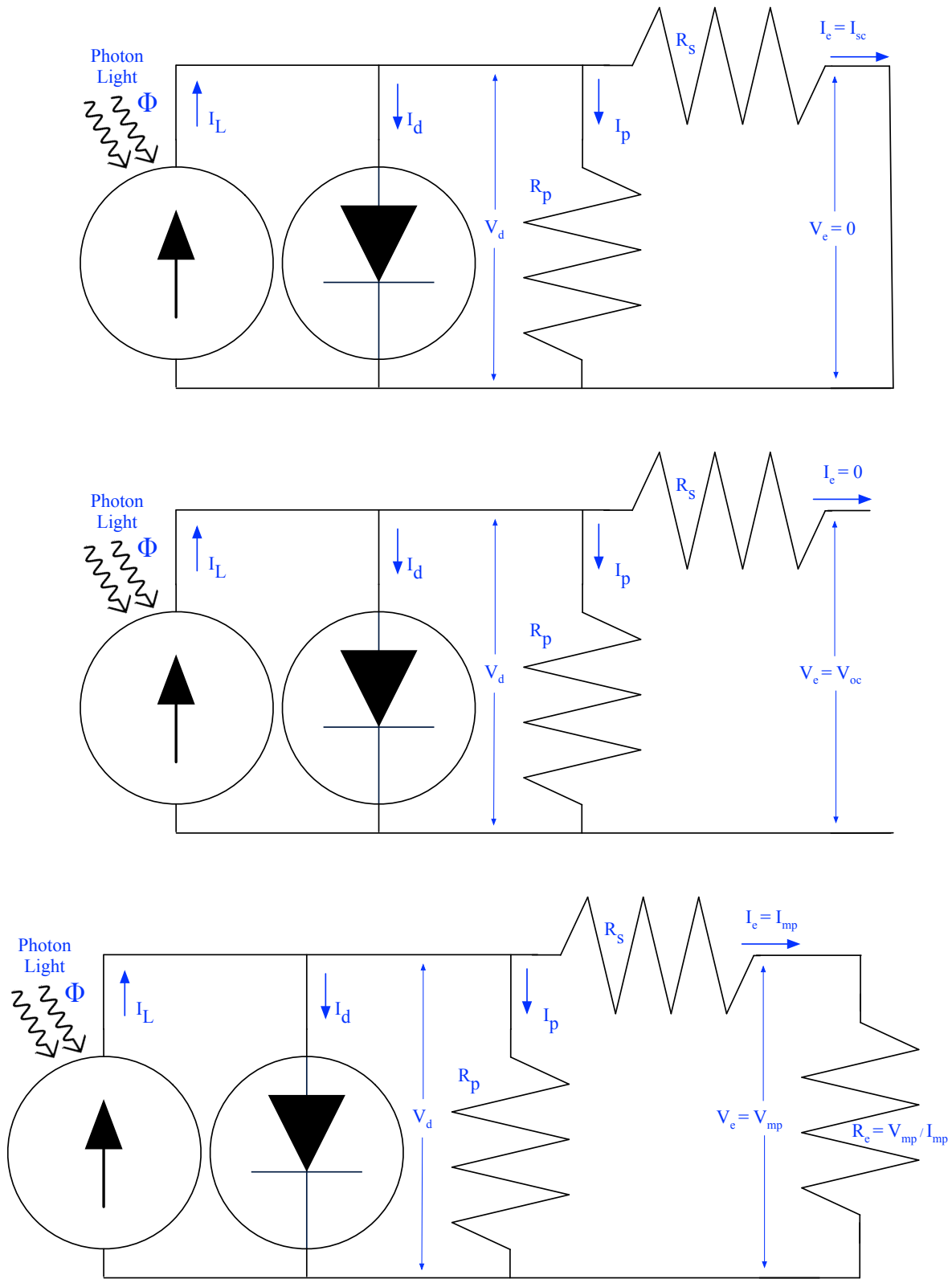


Figure 4.12 Five Parameter Model at Short, Open, and Maximum Power Conditions.

4.4.5 Graphing the I-V and Power Curves

The performance of the PV system was drawn by graphing the Current-Voltage I-V curve with external voltage V_e on the x-axis and external current I_e on the y-axis. With the solved five parameter values, Equation (11) was utilized with voltages ranging from 0 volts at short circuit to V_{oc} volts at open circuit and the matching currents from I_{sc} amps at short circuit to 0 amps at open circuit. Observing Equation (11), the external current I_e is embedded in the right side of the equation, which means the equation is transcendental. Except for the three primary points shown in the datasheet, graphing the other points requires finding a numerical solution for each V_e and I_e point. Figure 4.13 shows the I-V curve graphing solutions using a non-transcendental method described in Chapter 8. With the I-V curve data and applying Equation (8), the power curve was easily calculated and included in the graph. Also identified on the I-V curve are the primary points of short circuit, open circuit, and maximum power.

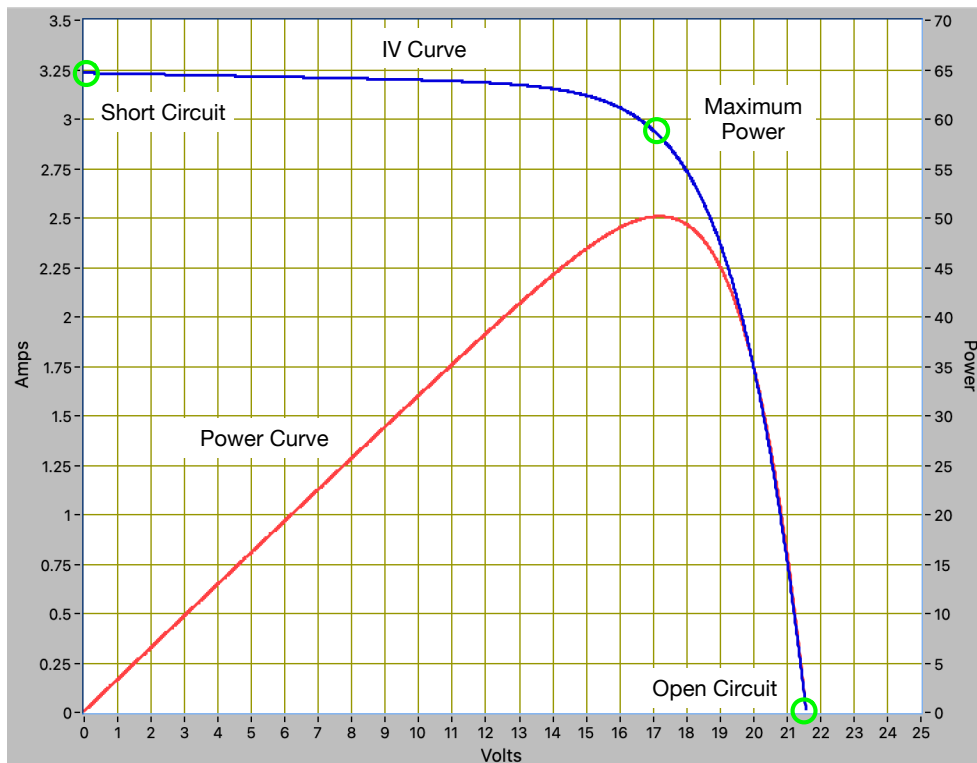


Figure 4.13 I-V and Power Graphs Newpowa PV Module.

4.4.6 Temperature Considerations

All semiconductor devices are sensitive to temperature changes. The effects of increasing temperature on PV systems include loss of power output, a lower voltage, and a moderate increase in current. An increase in temperature T causes a change in the thermal voltage v_t , which, along with the significant increase in the diode reverse saturation current I_o , impacts the overall performance of the PV system. The net result is a loss in the performance of PV systems with temperature increases. A full explanation requires a deep dive into semiconductor physics, which is outside the scope of this dissertation.

The temperature sensitivity is typically documented in a PV module datasheet as a percent change in value per degree C. An example is data from the Mitsubishi PV-UD185MF5 PV module datasheet. The Mitsubishi modules were installed in the FGCU solar field, as shown in Figure 2.2, with temperature data shown in Table 4.4.

Table 4.4 Mitsubishi PV-UD185MF5 Temperature Sensitivity

Parameter	Temperature Coefficient	Value @ 25° C	Value @ 40° C
I_{sc}	+0.054%/C	8.13 Amps	8.19 A
V_{oc}	-0.343%/C	30.6 Volts	29.0 V
P_{max}	-0.425%/C	185 Watts	173 W

The impact of the temperature performance of a PV system depends linearly on the temperature [35]. The linearity means that temperature variation provides no new fundamental information. The linearity only applies to normal operating conditions, where, for example, silicon PV cells' electrical conversion efficiency drops to 0% at 270° C [35]. With no new information provided within normal temperature ranges, only the STC temperature of 25° C, 298.15 K, was utilized in this document.

Chapter 5: Statistical Verification of the Simplification of the PV Equation

5.1 Abstract

Existing literature simplifies the Photovoltaic (PV) Equation by removing terms. For example, under short circuit conditions, the diode current is minimal compared to the short circuit current, and the diode term is removed. Support for these simplifications involves single-case examples, notional values, or the conjecture that $X \ll Y$. This chapter analyzes a statistically relevant sample of 10,413 commercially available silicon based PV modules. Using a modified Newton-Rapson method and subsequent calculations, the series resistance R_s , parallel resistance R_p , diode ideality factor η , photon light current I_L , and diode reverse saturation current I_0 were calculated for each sample. The data were analyzed and compared to measurement uncertainty to verify the PV equation simplifications. This chapter answers the first dissertation research question.

5.2 Introduction

Measuring a PV module's external voltage V_e and current I_e involves irradiating the PV system with a calibrated light source at a set temperature and attaching different load resistances. The resistances vary from infinite for open circuit to zero ohms for short circuit. Open circuit and short circuit are the first two primary measurement conditions. The third primary measurement condition is maximum power, where the PV system generates maximum power output. This chapter compares measurement capability and statistically verifies the simplifications of the PV equation at the primary conditions of short, open, and maximum power. By introducing the PV

module's thermal voltage Y , defined in Equation (15), an update of the fundamental PV Equation (11) produces Equation (16).

$$Y = \eta v_t N_s \quad (15)$$

- Y PV module's thermal voltage, volts
 - η diode ideality factor, no units
 - $v_t = kT/q$ thermal voltage, volts
 - k = Boltzmann's constant, joule per Kelvin
 - T = temperature, Kelvin
 - q = charge of an electron, coulombs
 - N_s number of series PV cells in the PV Module, count

$$I_L = I_o \left(e^{\frac{V_e + I_e R_s}{Y}} - 1 \right) + \frac{V_e + I_e R_s}{R_p} + I_e \quad (16)$$

- I_L photon light generated current, amps
- I_o diode reverse saturation current, amps
- V_e external voltage, volts
- I_e external current, amps
- R_s series resistance, ohms
- R_p parallel resistance, ohms

5.3 Measurement

Measurement of PV characteristics at STC follows methods described in IEC 60904-1 [31] and is limited by availability, cost, and precision of the voltage and current equipment. As in any measurement system, there are uncertainties involved [36]. The IEC source [37] states an uncertainty for short circuit current and open circuit voltage measurement of 0.2% or less. Practical PV module measurement uncertainty is +/- 1.8% [38], and measurement can present challenges [39]. The measurement uncertainty frames the justification for the simplifications. Measurement systems determine the STC data printed on a PV module's performance label; an example is shown in Figure 4.11. Testing systems include, for example, a Sinton FMT-500 [40], described in Appendix E. The Current-Voltage I-V curve measurement includes the 3-point

production: open circuit voltage, short circuit current, and maximum power system measurements. These are the three primary conditions.

5.4 Primary Conditions

PV Equation (11) was derived using the 5 Parameter Model found in Figure 4.2. With the introduction of the module thermal voltage γ , Equation (11) was modified to Equation (16). At the three primary conditions, Equation (16) derives Equations (17), (18), and (19). This analysis verifies the simplification of the three equations at the primary circuit conditions of short, open, and maximum power. Additional analysis shows other reasonable simplifications that should and, in some cases, should not be utilized.

5.5 Circuit Conditions

The two extremes of the I-V curve are open circuit and short circuit. Under short circuit conditions, the external connection of the PV module was shorted. The load under this condition was 0 ohms, the external voltage V_e was 0, and the external current I_e was maximum at I_{sc} , the external current at short circuit. Equation (17) shows the short circuit condition.

$$I_L = I_o \left(e^{\frac{I_{sc}R_s}{\gamma}} - 1 \right) + \frac{I_{sc}R_s}{R_p} + I_{sc} \quad (17)$$

At open circuit, the external connections are left unconnected; therefore, the load was infinite. Under this condition, the external current I_e was 0, and the external voltage V_e was maximum at V_{oc} , the external voltage at open circuit. Equation (18) shows the open circuit condition.

$$I_L = I_o \left(e^{\frac{V_{oc}}{\gamma}} - 1 \right) + \frac{V_{oc}}{R_p} \quad (18)$$

Maximum power output is a primary concern for the practical and economic applications of PV systems. A PV module power is voltage multiplied by current, as shown in Equation (8). Maximum power is where the external load enables the generation of maximum power. The corresponding voltage is V_{mp} , and the current is I_{mp} , where “mp” signifies maximum power. Fig. 4.12 shows the Five Parameter Model for the three primary conditions. Equation (19) shows the maximum power condition.

$$I_L = I_o \left(e^{\frac{V_{mp} + I_{mp} R_s}{\gamma}} - 1 \right) + \frac{V_{mp} + I_{mp} R_s}{R_p} + I_{mp} \quad (19)$$

5.6 Data Sources for Analysis

Two data sources were used in this study. The first was from a BP-MSX120 PV module. The second used data from 385 PV modules chosen to represent all silicon based PV modules with a 95% confidence interval, 0.5 population proportion, and a 5% margin of error.

As of 1 December 2022, the California Solar Equipment database [41] contained 18,049 modules, of which 10,413 were single-sided mono or multi-crystalline silicon. The Excel function “randbetween” was used to select 385 samples. Where duplicate samples were chosen, another selection was made. The samples were imported into a spreadsheet, and calculations were performed to solve for the five unknown PV parameters, η , R_s , R_p , I_L , and I_o . Additional calculations were completed, and the results were used to verify the equation simplifications. Figure 5.1 illustrates the workflow. A spreadsheet of the 385 sample modules, parameter results, and analysis are available [42].

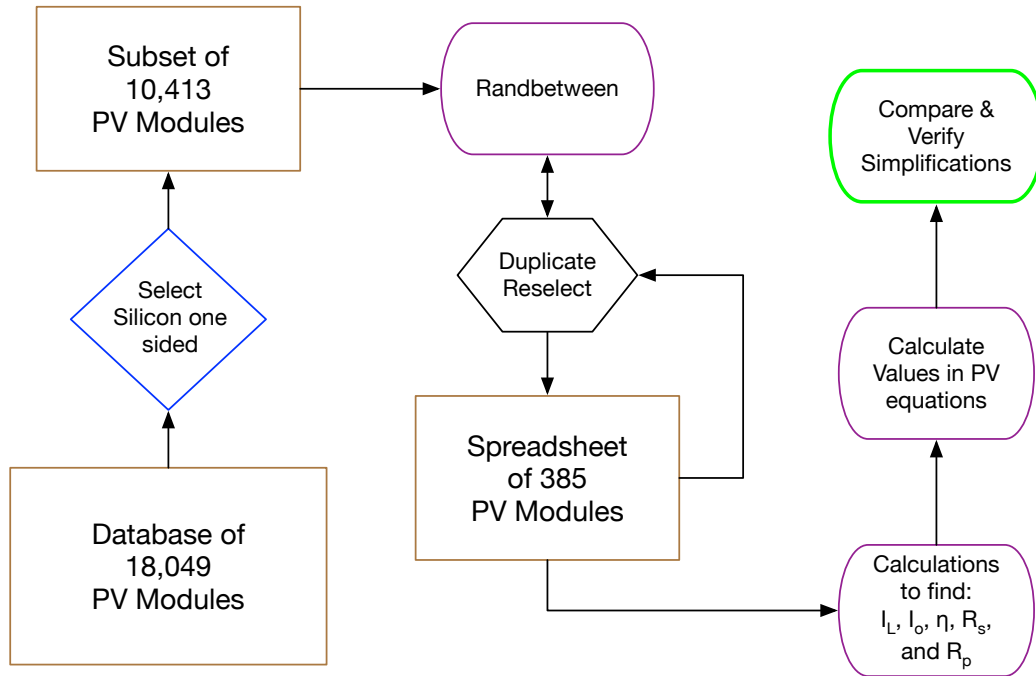


Figure 5.1 Sample Selection Process Flow.

5.7 BP-MSX120 Reference PV Module

The specific example uses a BP-MSX120 PV module with a summary of the parameters in Table 5.1. The five module characteristics, N_s , V_{oc} , V_{mp} , I_{mp} , and I_{sc} are available from datasheets for the BP and all the California solar equipment database modules. The performance parameters were obtained from test results performed under Standard Test Conditions STC of AM1.5 sunlight, 25° C, and an irradiance of 1,000 W/m².

Table 5.1 BP-MSX120 Performance Characteristic Data

Symbol	Parameter	Information from Datasheet
N_s	72	Number of series PV cells in the module
V_{oc}	42.1	Voltage at open circuit
V_{mp}	33.7	Voltage at maximum power
I_{mp}	3.56	Current at maximum power
I_{sc}	3.87	Current at short circuit

With PV equation manipulation following the method fully described in Chapter 6, three concurrent transcendental equations were solved using a modified Newton-Rapson method to provide the parameter values for η , R_s , and R_p . The values of I_L , I_o , and Υ were found from subsequent standard calculations. The results in Table 5.2 closely matched the solutions from other sources and were confirmed by the methods described in Chapter 7.

Table 5.2 Solver Parameter Values for a BP-MSX120 PV Module

Solver/Calculations	Symbol	Comment
0.4728	R_s	PV module series resistance
1,366	R_p	PV module parallel resistance
322.7E-9	I_o	PV module reverse saturation current
3.873	I_L	PV module Photon Light Current
1.391	η	Diode Ideality Factor
2.584	Υ	PV module thermal voltage

5.8 PV Equations at Primary Conditions

By entering the PV parameter values, for example, the BP-MSX120 PV module data found in Table 5.2 and solving Equation (16) for different load conditions, a graph of the external current versus external voltage I-V curve can be plotted. Using Equation (8), the Power Curve was also plotted. Fig. 5.2 shows the I-V and power curves for the BP-MSX120 module. Also identified are the three primary conditions: short circuit, open circuit, and maximum power.

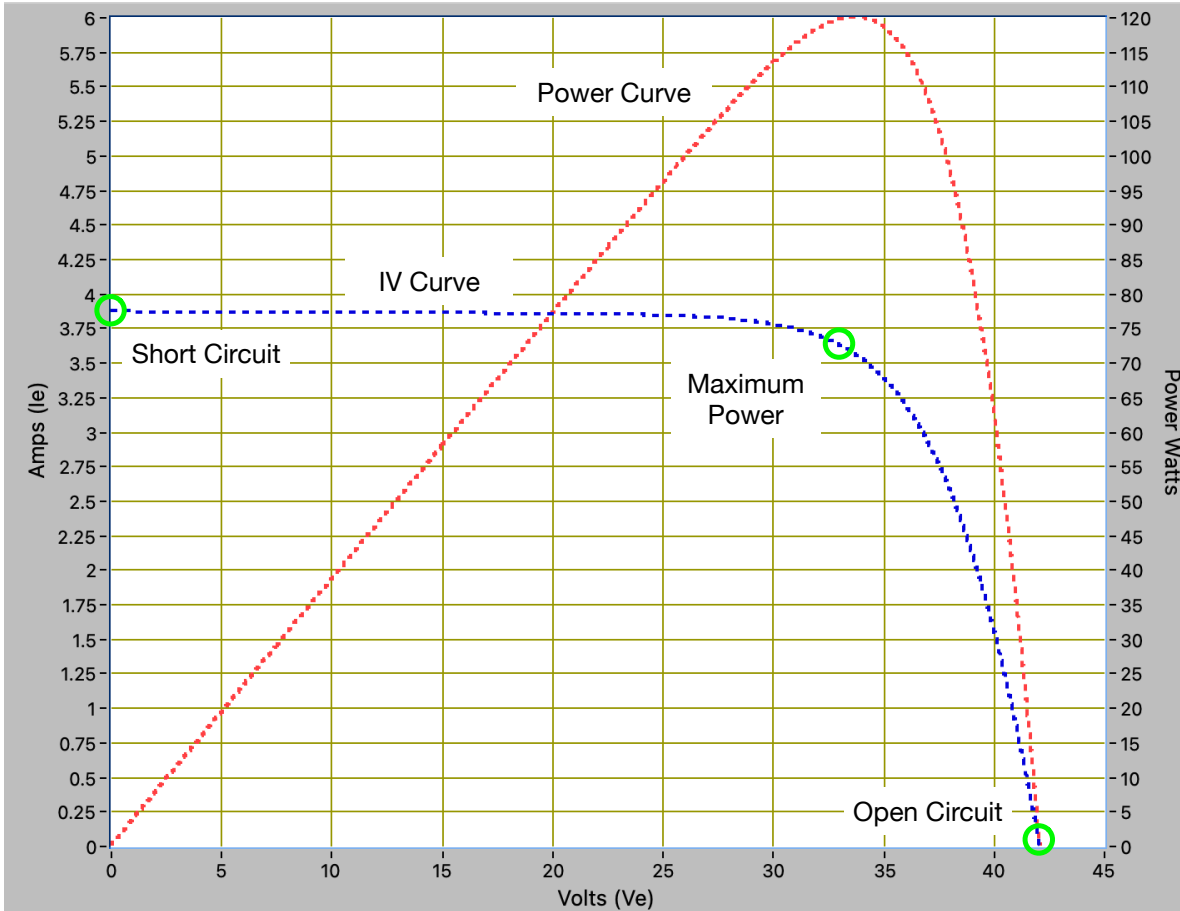


Figure 5.2 PV I-V and Power Graphs for BP-MSX120 Module.

5.9 Simplification Method Data Analysis and Results

5.9.1 Comparison Analysis

This section discusses the methods and calculations used to justify the simplification of Equations (17), (18), and (19). The diode current I_d was calculated by the reverse saturation current I_o multiplied by the exponential term -1 , as shown in Equation (20).

$$I_d = I_o \left(e^{\frac{V_e + I_e R_s}{Y}} - 1 \right) \quad (20)$$

The diode voltage $V_d = V_e + I_e R_s$, shown in Figure 4.2, in the numerator, and the module thermal voltage Y in the denominator controls the exponential. Different external loads establish

the V_e and I_e values of the numerator, while the denominator Y , with terms η , v_t , T , and N_s , remains fixed at STC. The short circuit condition simplification compares the diode current I_d with the short circuit current I_{sc} .

The open circuit and maximum power conditions simplifications compare the exponential part with the -1 factor from the Shockley diode equation. Equation (21) shows the the comparison.

$$e^{\frac{V_e + I_e R_s}{Y}} \text{ compared with } -1. \quad (21)$$

5.9.2 Short Circuit Condition

For the BP-MSX120 module characteristics, from Table 5.1, the short circuit current I_{sc} is 3.87 A. Solving Equation (20), with data from Table 5.1 and Table 5.2, $I_{sc} = 3.87$ A, $R_s = 0.4728$ Ω , $Y = \eta v_t N_s = 2.584$ V, and $I_o = 322.7$ nA, the calculated diode current I_d is 332.4 nA. In this case, the diode current I_d is 0.00000859% of short circuit current I_{sc} . Results are shown in Table 5.3.

Table 5.3 Short Circuit Factors for a BP-MSX120 PV Module

Calculation	Symbol	Comment
1.8297	V_d	Diode Voltage V_d at Short Circuit: $I_{sc} \times R_s$
0.7081	V_d/Y	Exponential Factor
332.4E-9	I_d	Diode current I_d ($I_o \times$ (Exponential Factor -1))
0.00000859%	n/a	Percent I_d versus I_{sc}

Because of its insignificant size, for the BP-MSX120 module, the diode current I_d can be removed without a measurable difference in the result. The summary of the statistical analysis of 385 PV modules is shown in Table 5.4. The calculated worst-case percent of I_d to I_{sc} was 0.0000424%.

Table 5.4 Short Circuit Values for 385 PV Modules

Bound	Percent Ratio of I_d to I_{sc}
High	0.0000424%
Low	0.00000000%
Average	0.00000109%
Standard Deviation	0.00000392%

The results show that, under open circuit conditions, the diode current I_d is insignificant, not normally measurable, and can be removed for silicon based PV modules in general. From Equation (17), the current at short circuit simplifies to Equation (22).

$$I_L = \frac{I_{sc}R_s}{R_p} + I_{sc} \quad (22)$$

5.9.3 Open Circuit Condition

The standard simplification involves the removal of the “-1” from the diode equation. Set in terms of I_L , Equation (18) at open circuit produces the simplified Equation (23).

$$I_L = I_o \left(e^{\frac{V_{oc}}{V}} \right) + \frac{V_{oc}}{R_p} \quad (23)$$

The simplification is supported by comparing the exponential part to “-1”. As shown in Table 5.5, the exponential value for the BP-MS120 module “1” is 0.00000840% of 11.91E6. This means the “-1” can be removed for the BP module. For silicon based PV modules, the worst-case percent showed the exponential term compared to “1” as 0.000106%. Table 5.6 shows the statistical results for open circuit conditions. In general, for silicon based PV modules, Equation (23) holds under open circuit conditions.

Table 5.5 Open Circuit Factors for a BP-MSX120 PV Module

Calculation	Symbol	Comment
42.1	V_d	Diode Voltage V_d at Open Circuit: V_{oc}
16.29	V_d/γ	Exponential Factor
11.91E6	$e^{\frac{V_{oc}}{\gamma}}$	Exponent Value
0.00000840%	n/a	Percent of “1” versus Exponent Value

Table 5.6 Open Circuit Values for 385 PV Modules

Bound	Percent Ratio of “1” versus Exponent Value
High	0.000106%
Low	0.00000000%
Average	0.00000288%
Standard Deviation	0.0000112%

5.9.4 Maximum Power Condition

The standard simplification involves the removal of the “-1” from the diode equation. Set in terms of I_L , Equation (19) at open circuit produces the simplified Equation (24).

$$I_L = I_o \left(e^{\frac{V_{mp} + I_{mp}R_s}{\gamma}} \right) + \frac{V_{mp} + I_{mp}R_s}{R_p} + I_{mp} \quad (24)$$

The BP module data for the maximum-power conditions are summarized in Table 5.7. The “1” term is only 0.00113% on the exponential factor, which is approximately 885.0E3 times larger. So, for the BP module, the “-1” can be removed. For the 385 module samples, at worst, the “1” was calculated as 0.00126% of the exponential value, and thus, in general, Equation (24) holds. Table 5.8 shows the statistical results for maximum power.

Table 5.7 Maximum Power Factors for a BP-MSX120 PV Module

Calculation	Symbol	Comment
35.38	V_d	Diode Voltage V_d at Maximum Power: $V_{mp} + I_{mp} \times R_s$
13.69	$(V_{mp} + I_{mp}R_s)/\gamma$	Exponential Factor
885.0E3	$e^{\frac{V_{mp} + I_{mp}R_s}{\gamma}}$	Exponent Value
0.000113%	n/a	Percent of “1” versus Exponent Value

Table 5.8 Maximum Power Values for 385 PV Modules

Bound	Percent Ratio of “1” versus Exponent Value
High	0.00126%
Low	0.00000000%
Average	0.0000376%
Standard Deviation	0.000138%

5.10 Discussion and Explanation of Results

The simplification involves the removal of an equation term that is small compared to adjacent factors. The basis of the simplification uses the engineering principles of measurement and magnitude. The determination of the PV parameters starts with STC values, which, according to the IEC standards, only require a measurement accuracy of 0.2%, and real-world data shows an accuracy of +/-1.8%. For short circuit conditions, the worst-case simplification removes a term that is 0.0000424% of the short circuit current. For open circuit conditions, for the worst-case, the simplification removes a term that is 0.000106% of the adjacent value. In the worst-case maximum power condition, the removed term is 0.00126% of the adjacent factor. Even with a measurement system of 0.02%, which is 10X better than the IEC standard, the removed factor is practically unmeasurable, and the simplification is justified.

5.11 Conclusion

A statistically significant sample of silicon PV modules was analyzed to determine whether the commonly used simplification of the five-parameter PV Equation holds at short circuit, open circuit, and maximum power conditions. The analysis compared the equations with and without the simplification and statistically verified the simplification. Within measurement and statistical tolerances, Equation (22) for short circuit, Equation (23) for open circuit, and Equation (24) apply to all silicon based PV modules.

5.12 Additional Simplifications

5.12.1 R_s to R_p Ratio

Under short circuit conditions, as stated in Equation (22), the photon light current I_L equals the short circuit current I_{sc} plus the parallel path current I_p , which is I_{sc} multiplied by the series resistance R_s divided by parallel resistance R_p . If the ratio of R_s/R_p is sufficiently small, I_L would equal I_{sc} . From the statistical data criterion, the ratio is generally not small enough to support this simplification. In a specific case where R_s is very small, R_p very large, and the resulting I_p current is tiny, Equation (25) could apply.

$$I_L \approx I_{sc} \quad (25)$$

5.12.2 R_p versus $R_s + R_p$

In manipulating equations, specifically a derivation in Chapter 6, the analysis and the finding of solved parameters are greatly simplified when parallel resistance R_p replaces the terms $R_s + R_p$. Reviewing the statistical sample of 385 modules, only 7 have a difference of 0.04% or higher, with only one at 0.07%, one at 0.06%, four at 0.05%, and one at 0.04%. This means the simplification shown in Equation (26) is supported with verification.

$$R_p \approx R_p + R_s \quad (26)$$

5.12.3 Simplification of V_{oc}

Starting with Equation (23), some sources obtain a simplified equation for the open circuit voltage V_{oc} . The simplification depends on the relatively small size of the parallel path current I_p . With a small parallel path current I_p , the V_{oc}/R_p term is removed, which derives Equation (27).

$$I_L \approx I_o \left(e^{\frac{V_{oc}}{Y}} \right) \quad (27)$$

Expanding Y and solving for V_{oc} derived Equation (28). The advantage of Equation (28) is it enables a simple solution, unlike Equation (23), which requires a numerical solution method

of the transcendental equation. MATLAB code for a numerical solution of Equation (23) is found in Appendix F.

$$V_{oc} \approx \eta v_t N_s \ln \left(\frac{I_L}{I_o} \right) \quad (28)$$

Analysis of this simplification requires comparing the relative size of the diode current I_d with the parallel path current I_p . From the analysis, the average parallel path current can be over 0.5% of the diode current, so this simplification should not be utilized except for a rough approximation.

Chapter 6: Solving for the Parameters in the Five Parameter Model

6.1 Module Characteristics and Parameters

For a specific PV module, the material's characteristics and construction were fixed during the manufacturing process. The five characteristic values provided on the PV panel datasheet include N_s , the number of series connected PV cells, fixed by the design topology, and the last four characteristics, open circuit voltage V_{oc} , maximum power voltage V_{mp} , maximum power current I_{mp} , and short circuit current I_{sc} , obtained by measurement at Standard Rest Condition STC. An example of a PV Module's characteristic values printed on a performance label is shown in Figure 4.11.

With the PV panel characteristics, manipulation of the PV diode equation, the application of some electrical engineering conditions, and the derivation of additional equations, a solution for the parameters contained in the Five Parameter Model can be found. The five parameters are the diode ideality factor η , series resistance R_s , parallel resistance R_p , photon light current I_L , and the diode reverse saturation current I_o .

6.2 Solution Analysis

The analysis shown was based on the fundamental PV Equation (11) modified with the use of γ to Equation (16), operational characteristics, and multiple manuscripts, with examples including [43] and [44]. Finding the five unknown parameters requires five equations. This chapter leverages the simplifications shown in Chapter 5 and corrects errors discovered in some previously presented solutions. Applying systems engineering principles, the simplifications incorporated in this chapter were verified by the methods described in Chapter 7.

This chapter uses the simplified and verified Equations (22) for short circuit, Equation (23) for open circuit, and Equation (24) for maximum power. Solving for the parameter involves a divide and conquer method, where equations to solve for the values for I_L and I_o are stated in terms of the PV module's characteristic values and the parameters of η , R_s , and R_p . The two equations for finding I_L and I_o are ordinary. Equations to solve for η , R_s , and R_p are more complex, requiring the concurrent solutions of three transcendental equations.

6.3 Equations for I_L and I_o

Equation (22), repeated here, shows I_L in terms of only the known characteristic value I_{sc} and the two unknown parameters R_s and R_p .

$$I_L = I_{sc} + \frac{I_{sc}R_s}{R_p} \quad (22)$$

Equation (23) and Equation (24) both calculate the photon light current I_L . At STC, the photon light current I_L is fixed for any load condition and is the same in all equations. Equation (29) was derived by equating the right side of Equation (23) with the right side of Equation (22).

$$I_o \left(e^{\frac{V_{oc}}{Y}} \right) + \frac{V_{oc}}{R_p} = I_{sc} + \frac{I_{sc}R_s}{R_p} \quad (29)$$

The V_{oc}/R_p term was moved to the right side to derive Equation (30).

$$I_o \left(e^{\frac{V_{oc}}{Y}} \right) = I_{sc} + \frac{I_{sc}R_s}{R_p} - \frac{V_{oc}}{R_p} \quad (30)$$

The terms on the right side of the equation were combined using the common denominator R_p to derive Equation (31).

$$I_o \left(e^{\frac{V_{oc}}{Y}} \right) = \frac{I_{sc}(R_p + R_s) - V_{oc}}{R_p} \quad (31)$$

The exponential term was divided into both sides to derive Equation (32), the diode reverse saturation current I_o in terms of only the fixed characteristic values of I_{sc} , V_{oc} , v_t , and N_s and the

three unknown parameters η , R_s , and R_p . Using Equation (15), the term Y was replaced with $\eta v_t N_s$ to show η separately.

$$I_o = \frac{I_{sc}(R_p + R_s) - V_{oc}}{R_p} \left(e^{\frac{-V_{oc}}{\eta v_t N_s}} \right) \quad (32)$$

6.4 Three Additional Equations for η , R_s , and R_p

With the equations for I_L and I_o found, three additional equations were required to solve for the last three unknown parameters.

6.4.1 First Equation

Taking Equation (24) for the maximum power condition of I_{mp} & V_{mp} and replacing I_L with the right side of Equation (22) produces Equation (33).

$$I_{sc} + \frac{I_{sc}R_s}{R_p} = I_{mp} + I_o \left(e^{\frac{(V_{mp} + I_{mp}R_s)}{\eta v_t N_s}} \right) + \frac{V_{mp} + I_{mp}R_s}{R_p} \quad (33)$$

Substituting the right side of Equation (32) for the I_o term produces Equation (34).

$$I_{sc} + \frac{I_{sc}R_s}{R_p} = I_{mp} + \frac{I_{sc}(R_p + R_s) - V_{oc}}{R_p} \left(e^{\frac{-V_{oc}}{\eta v_t N_s}} \right) \left(e^{\frac{(V_{mp} + I_{mp}R_s)}{\eta v_t N_s}} \right) + \frac{V_{mp} + I_{mp}R_s}{R_p} \quad (34)$$

For clarity, Equation (34) was rearranged in terms of I_{mp} to derive Equation (35).

$$I_{mp} = I_{sc} - \frac{I_{sc}R_s}{R_p} - \frac{V_{mp} + I_{mp}R_s}{R_p} - \frac{I_{sc}(R_p + R_s) - V_{oc}}{R_p} \left(e^{\frac{-V_{oc}}{\eta v_t N_s}} \right) \left(e^{\frac{(V_{mp} + I_{mp}R_s)}{\eta v_t N_s}} \right) \quad (35)$$

Combining the terms divided by R_p and the exponential terms produces Equation (36).

$$I_{mp} = I_{sc} - \frac{V_{mp} + R_s(I_{mp} - I_{sc})}{R_p} - \frac{I_{sc}(R_p + R_s) - V_{oc}}{R_p} \left(e^{\frac{(V_{mp} + I_{mp}R_s - V_{oc})}{\eta v_t N_s}} \right) \quad (36)$$

Equation (36) only includes the module's characteristic values and three unknown parameters η , R_s , and R_p . The equation is transcendental since the I_{mp} current in Equation (36) is embedded in both sides and not separable. Solving transcendental equations requires numerical solution methods. Equation (36) includes current and voltage in the form of $I = f(I, V)$. This

equation is the first of three solution equations required to solve for the unknown parameters of η , R_s , and R_p .

6.4.2 Conditions for Additional Equations

Acquiring two more equations requires mathematical manipulation and direct current electrical engineering involving voltage, current, and power. Utilizing characteristics of the I-V curve, graphed by Equation (11), one location of interest was the slope of the curve at the I_{sc} point. A second point utilized the PV power curve for the third equation. On the curve, where $P = IV$, the maximum power P_{mp} occurs at I_{mp} and V_{mp} , and the derivative equals zero. Figure 6.1 shows the location of the short circuit, the slope at I_{sc} , maximum power points P_{mp} , and the slope at P_{mp} .

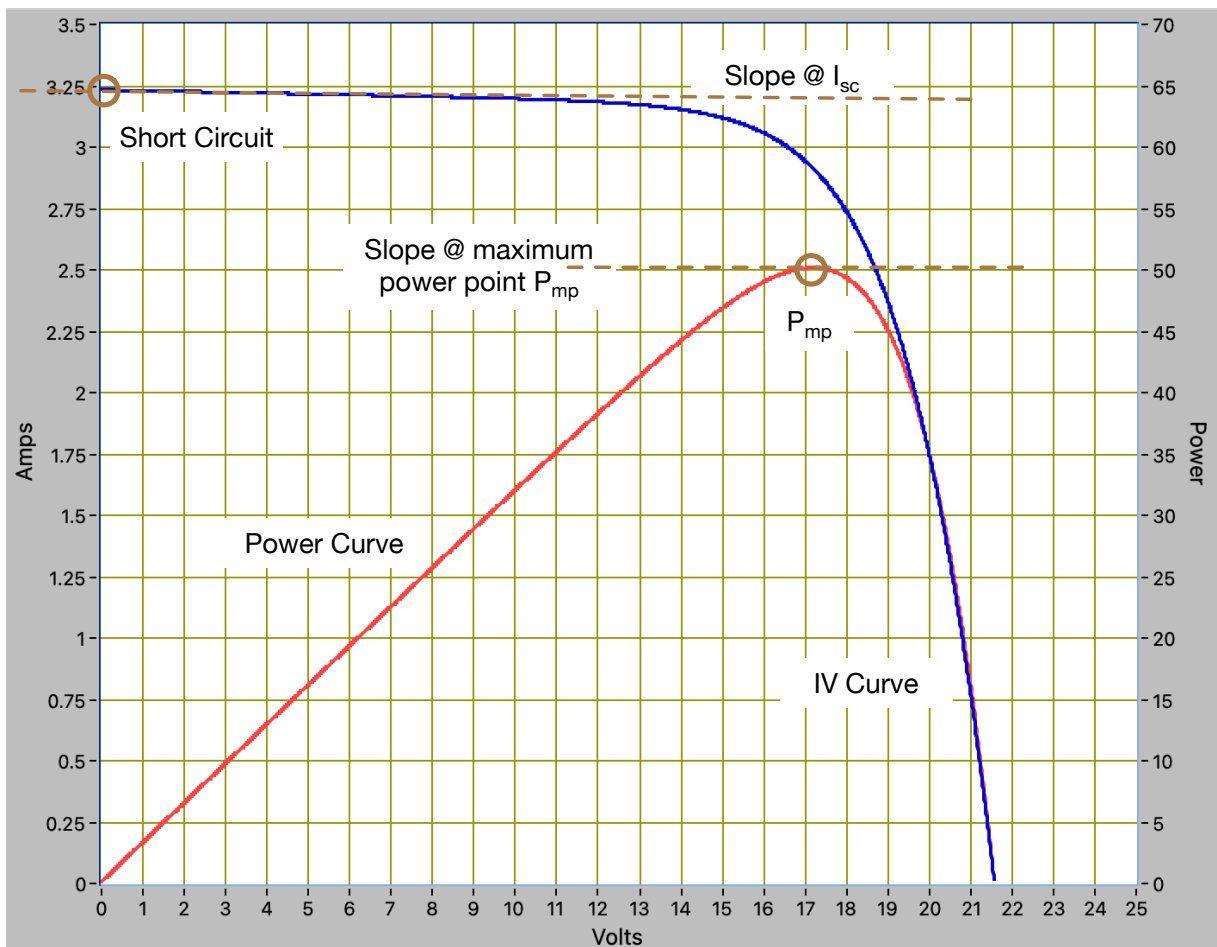


Figure 6.1 Slopes at I_{sc} and P_{mp} .

6.4.3 Second Equation

Starting with Equation (11), duplicated here for convenience, the derivative of current with respect to voltage was found.

$$I_e = I_L - I_o \left(e^{\frac{(V_e + I_e R_s)}{\eta v_t N_s}} - 1 \right) - \frac{(V_e + I_e R_s)}{R_p} \quad (11)$$

Recalling that for an exponential function, if $h(x) = e^{j(x)}$, $h(x)' = j(x)' e^{j(x)}$, where $j(x) = (V_e + I_e R_s) / \eta v_t N_s$, derives Equation (37).

$$\frac{dI_e}{dV_e} = 0 - \frac{I_o}{\eta v_t N_s} \left(1 + \frac{dI_e}{dV_e} R_s \right) e^{\frac{V_e + I_e R_s}{\eta v_t N_s}} - \frac{1}{R_p} \left(1 + \frac{dI_e}{dV_e} R_s \right) \quad (37)$$

Expanding this produced Equation (38).

$$\frac{dI_e}{dV_e} = - \frac{I_o}{\eta v_t N_s} e^{\frac{V_e + I_e R_s}{\eta v_t N_s}} - \frac{dI_e}{dV_e} \frac{I_o R_s}{\eta v_t N_s} e^{\frac{V_e + I_e R_s}{\eta v_t N_s}} - \frac{1}{R_p} - \frac{dI_e}{dV_e} \frac{R_s}{R_p} \quad (38)$$

Collecting the dI_e/dV_e terms on the left side produced Equation (39).

$$\frac{dI_e}{dV_e} \left(1 + \frac{R_s}{R_p} + \frac{I_o R_s}{\eta v_t N_s} e^{\frac{V_e + I_e R_s}{\eta v_t N_s}} \right) = - \frac{I_o}{\eta v_t N_s} e^{\frac{V_e + I_e R_s}{\eta v_t N_s}} - \frac{1}{R_p} \quad (39)$$

Isolating dI_e/dV_e and rearranging some terms, the general Equation (40) was obtained.

$$\frac{dI_e}{dV_e} = - \frac{\left(\frac{1}{R_p} + \frac{I_o}{\eta v_t N_s} e^{\frac{V_e + I_e R_s}{\eta v_t N_s}} \right)}{\left(1 + \frac{R_s}{R_p} + \frac{I_o}{\eta v_t N_s} R_s e^{\frac{V_e + I_e R_s}{\eta v_t N_s}} \right)} \quad (40)$$

At short circuit condition, $I_e = I_{sc}$ and $V_e = 0$. Inserting these conditions into Equation (40) produced Equation (41).

$$\frac{dI_e}{dV_e} = - \frac{\left(\frac{1}{R_p} + \frac{I_o}{\eta v_t N_s} e^{\frac{I_{sc} R_s}{\eta v_t N_s}} \right)}{\left(1 + \frac{R_s}{R_p} + \frac{I_o}{\eta v_t N_s} R_s e^{\frac{I_{sc} R_s}{\eta v_t N_s}} \right)} \quad (41)$$

From Chapter 5, it was shown at short circuit conditions that the exponential term multiplied by the reverse saturation current I_o is tiny compared to other terms. This means Equation (41) simplifies to Equation (42).

$$\frac{dI_e}{dV_e} = - \frac{\left(\frac{1}{R_p} \right)}{\left(1 + \frac{R_s}{R_p} \right)} \quad (42)$$

Equation (42) was further simplified to derive Equation (43).

$$\frac{dI_e}{dV_e} = - \frac{\left(\frac{1}{R_p} \right)}{\left(\frac{R_s + R_p}{R_p} \right)} = - \left(\frac{1}{R_p + R_s} \right) \quad (43)$$

Applying the simplification from Equation (26) in Chapter 5 derives Equation (44). The simplifications were verified in the analysis described in Chapter 7. This equation shows that the slope of the I-V curve at I_{sc} was the negative inverse of the PV module parallel resistance R_p .

$$\frac{dI_e}{dV_e} = - \frac{1}{R_p} \quad (44)$$

Equation (45) was derived from equating the right side of Equation (44) to the right side of Equation (40), where I_o was replaced with the right side of Equation (32).

$$- \frac{1}{R_p} = - \frac{\left(\frac{1}{R_p} + \frac{I_{sc}(R_p + R_s) - V_{oc}}{\eta v_t N_s R_p} e^{\frac{V_e + I_e R_s - V_{oc}}{\eta v_t N_s}} \right)}{\left(1 + \frac{R_s}{R_p} + \frac{I_{sc}(R_p + R_s) - V_{oc}}{\eta v_t N_s R_p} R_s e^{\frac{V_e + I_e R_s - V_{oc}}{\eta v_t N_s}} \right)} \quad (45)$$

Values from short circuit conditions, where $I_e = I_{sc}$ and $V_e = 0$, were applied to Equation (45). The equation was then rearranged to show R_p on the left and the rest of the terms on the right. Equation (46) contains only PV characteristic values and three unknown parameters η , R_s , and R_p . This is the second required equation, which is transcendental and thus requires a numerical solution.

$$R_p = \frac{\left(1 + \frac{R_s}{R_p} + \frac{I_{sc}(R_p + R_s) - V_{oc}}{\eta v_t N_s R_p} R_s e^{\frac{I_{sc} R_s - V_{oc}}{\eta v_t N_s}}\right)}{\left(\frac{1}{R_p} + \frac{I_{sc}(R_p + R_s) - V_{oc}}{\eta v_t N_s R_p} e^{\frac{I_{sc} R_s - V_{oc}}{\eta v_t N_s}}\right)} \quad (46)$$

6.4.4 Third Equation

For the last equation, applying direct current electrical engineering, where the power output of a PV module is current (I) multiplied by voltage (V). This was expressed by Equation (8).

$$P = IV \quad (8)$$

By definitions, Equation (47) is presented, expanded in Equation (48), reordered, and simplified in Equation (49).

$$d(IV) = (I + dI)(V + dV) - IV \quad (47)$$

$$d(IV) = IV + VdI + IdV + dIdV - IV \quad (48)$$

$$d(IV) = IdV + VdI + dIdV \approx IdV + VdI \quad (49)$$

Utilizing Equation (49) and solving for the derivative of power Equation (8) with respect to voltage, Equation (50) was derived.

$$\frac{dP}{dV} = \frac{d(IV)}{dV} = I + V \frac{dI}{dV} \quad (50)$$

At maximum power m_p , the derivative of power with respect to voltage equals 0, and the result generated Equation (51).

$$\frac{dP}{dV_{@mp}} = \frac{d(IV)}{dV} = I + V \frac{dI}{dV} = 0 \quad (51)$$

Including the maximum power values for I_e and V_e and rearranging the two right side parts produced Equation (52).

$$\frac{dI_e}{dV_e} = -\frac{I_{mp}}{V_{mp}} \quad (52)$$

Equation (53) was derived from modifying the general Equation (40) for the maximum power condition where $I_e = I_{mp}$, $V_e = V_{mp}$, and I_o was replaced with the right side of Equation (32).

$$\frac{dI_e}{dV_e} = -\frac{\left(\frac{1}{R_p} + \frac{I_{sc}(R_p + R_s) - V_{oc}}{\eta v_t N_s R_p} e^{\frac{V_{mp} + I_{mp} R_s - V_{oc}}{\eta v_t N_s}}\right)}{\left(1 + \frac{R_s}{R_p} + \frac{I_{sc}(R_p + R_s) - V_{oc}}{\eta v_t N_s R_p} R_s e^{\frac{V_{mp} + I_{mp} R_s - V_{oc}}{\eta v_t N_s}}\right)} \quad (53)$$

Substituting the right side of Equation (52) into the left side of Equation (53) derived Equation (54).

$$-\frac{I_{mp}}{V_{mp}} = -\frac{\left(\frac{1}{R_p} + \frac{I_{sc}(R_p + R_s) - V_{oc}}{\eta v_t N_s R_p} e^{\frac{V_{mp} + I_{mp} R_s - V_{oc}}{\eta v_t N_s}}\right)}{\left(1 + \frac{R_s}{R_p} + \frac{I_{sc}(R_p + R_s) - V_{oc}}{\eta v_t N_s R_p} R_s e^{\frac{V_{mp} + I_{mp} R_s - V_{oc}}{\eta v_t N_s}}\right)} \quad (54)$$

With some manipulation, the results obtain the third required transcendental Equation (55).

The equation only contains PV characteristic values and three unknown parameters: η , R_s , and R_p .

$$0 = I_{mp} - V_{mp} \frac{\left(\frac{1}{R_p} + \frac{I_{sc} R_p - V_{oc}}{R_p \eta v_t} e^{\frac{V_{mp} + I_{sc} R_s - V_{oc}}{\eta N_s v_t}}\right)}{\left(1 + \frac{I_{sc} R_p - V_{oc}}{R_p \eta v_t} R_s e^{\frac{V_{mp} + I_{sc} R_s - V_{oc}}{\eta N_s v_t}}\right)} \quad (55)$$

6.5 Transcendental Numerical Solutions

Solving transcendental equations requires numerical solutions, which are now performed using computer software. The software to find the parameter values applies various mathematical

solution methods such as bisection and Newton-Raphson. Software solutions methods for this class of problems include software languages like Python and custom software programs. The Newton-Raphson method was chosen for this analysis. Alternate methods are available and are discussed in Chapter 7. Market forces have provided many sources to find numerical transcendental solutions. Table 6.1A includes a few examples.

Table 6.1 Sample Sources for Numerical Solutions

Vendor	Solution	Method
MathWorks	MATLAB	Custom or premade M code
MathWorks	Simulink	Custom or premade circuit model solutions
Python	Software	Custom or premade Python code
Wolfram	Alpha	Solution framework
UTC	TK Solver	Framework for custom code

The systems engineering analysis, summarized in Appendix G, determined that the optimal solution was TK Solver [45]. Solutions and analysis in this document utilized a custom-built framework to solve the five parameters for any PV module. The input included fixed constants and characteristics obtained from the PV module datasheet are listed in Table 6.2.

Table 6.2 PV Characteristic Inputs to Solve Five Parameters

Name	Symbol	Value	Units	Source
Temperature	T	298.15	K	Fixed STC conditions
Charge of electron	q	1.602176634E-19	C	Fundamental Unit
Boltzmann's Constant	k	1.380649E-23	K/J	Fundamental Unit
Number of series PV cells	N_s		count	PV Datasheet
Voltage at open circuit	V_{oc}		Volts	PV Datasheet
Voltage at maximum power	V_{mp}		Volts	PV Datasheet
Current at maximum power	I_{mp}		Amps	PV Datasheet
Current at short circuit	I_{sc}		Amps	PV Datasheet

6.6 Equations to Solve

The solutions to solve the primary unknown parameters, η , R_s , and R_p , include Equation (36), Equation (46), and Equation (55). The three equations, shown here for clarity, must be solved concurrently.

$$I_{mp} = I_{sc} - \frac{V_{mp} + R_s(I_{mp} - I_{sc})}{R_p} - \frac{I_{sc}(R_p + R_s) - V_{oc}}{R_p} \left(e^{\frac{(V_{mp} + I_{mp}R_s - V_{oc})}{\eta v_t N_s}} \right) \quad (36)$$

$$R_p = \frac{\left(1 + \frac{R_s}{R_p} + \frac{I_{sc}(R_p + R_s) - V_{oc}}{\eta v_t N_s R_p} R_s e^{\frac{I_{sc}R_s - V_{oc}}{\eta v_t N_s}} \right)}{\left(\frac{1}{R_p} + \frac{I_{sc}(R_p + R_s) - V_{oc}}{\eta v_t N_s R_p} e^{\frac{I_{sc}R_s - V_{oc}}{\eta v_t N_s}} \right)} \quad (46)$$

$$0 = I_{mp} - V_{mp} \frac{\left(\frac{1}{R_p} + \frac{I_{sc}R_p - V_{oc}}{R_p \eta v_t v_t} e^{\frac{V_{mp} + I_{sc}R_s - V_{oc}}{\eta N_s v_t}} \right)}{\left(1 + \frac{I_{sc}R_p - V_{oc}}{R_p \eta v_t v_t} R_s e^{\frac{V_{mp} + I_{sc}R_s - V_{oc}}{\eta N_s v_t}} \right)} \quad (55)$$

Once η , R_s , and R_p were found, Equation (22) solves for I_L . I_o was found from Equation (32).

$$I_L = I_{sc} + \frac{I_{sc}R_s}{R_p} \quad (22)$$

$$I_o = \frac{I_{sc}(R_p + R_s) - V_{oc}}{R_p} \left(e^{\frac{-V_{oc}}{\eta v_t N_s}} \right) \quad (32)$$

6.7 Transcendental Equation Solution Process Flow

Solutions to transcendental equations require applying a numerical method to move toward a solution via a series of refinements. The Newton-Raphson method starts with solution estimates or seed values; in TK Solver, a seed value is called a ‘guess.’ The Newton-Raphson method uses a seed value, the equation’s tangent, and the derivative to successively refine the calculation of the function roots. The value calculated by the derivative of the original equation was used to improve

the solved solution estimate. This new estimation was used for the iteration, with a subsequent tangent utilized to arrive at a solution. The process was repeated until the derived solutions provide an answer within a specified error tolerance. An example of MATLAB M code, utilizing the Newton-Raphson method to solve Equation (23), is contained in Appendix F. The process flow to solve solutions of Equations (36), (46), (55), (22), and (32) are shown in Figure 6.2.

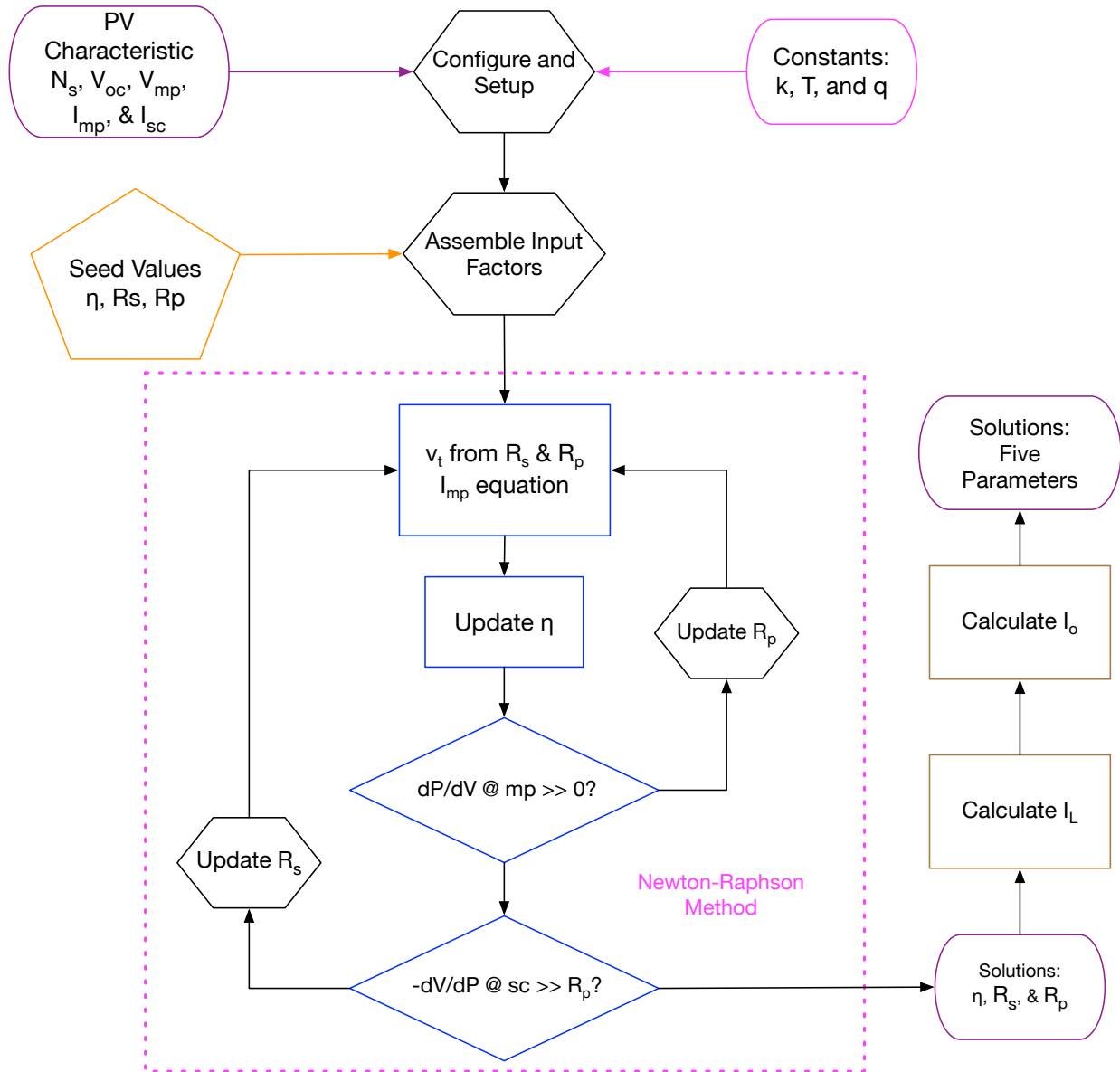


Figure 6.2 Equation Solution Process Flow.

6.8 TK Solver Equation Solutions

6.8.1 Equation Set Up

Observation of Equations (36), (46), and (55) shows similarities in some of the component parts. The similarities were exploited to lessen the possibility of errors in entering equations into TK Solver and to aid in the configuration and troubleshooting of any issues. The software supplier recommended these groupings of similar equation subparts.

For an ideal diode, the thermal voltage, v_t , was expressed in Equation (2). The voltage only applies to an ideal diode with an ideality factor of 1. The diode ideality factor of η was introduced to account for an actual diode. Also included was the number of series cell N_s to account for the construction of the PV module. As shown in Equation (15), repeated here, a PV module's thermal voltage Y can replace the three terms η , v_t , and N_s . This substitution supports the grouping method utilized in this analysis. In a PV system, the PV module thermal voltage is contained in the exponential term in Equations (36), (46), (55), and (36).

$$Y = \eta v_t N_s \quad (15)$$

Additional changes include the creation of a grouped exponential term for Equations (36), Equation (46), and another for Equation (55). The groupings are shown in Equation (56) and Equation (57).

$$e^{\frac{I_{sc}R_s - V_{oc}}{Y}} = E_2 \quad (56)$$

$$e^{\frac{V_{mp} + I_{sc}R_s - V_{oc}}{Y}} = E_{13} \quad (57)$$

A final grouping involves the combination shown in Equation (58).

$$L = (I_{sc}(R_p + R_s) - V_{oc})/(RpY) \quad (58)$$

Applying the groupings to Equations (36), (46), and (55) derived the updated Equations (59), (60), and (61).

$$I_{mp} = I_{sc} - \frac{V_{mp} + R_s(I_{mp} - I_{sc})}{R_p} - \frac{I_{sc}(R_p + R_s) - V_{oc}}{R_p} E_{13} \quad (59)$$

$$R_p = \frac{\left(1 + \frac{R_s}{R_p} + LR_s E_2\right)}{\left(\frac{1}{R_p} + LE_2\right)} \quad (60)$$

$$0 = I_{mp} - V_{mp} \frac{\left(\frac{1}{R_p} + E_{13}\right)}{\left(1 + \frac{R_s}{R_p} + LR_s E_{13}\right)} \quad (61)$$

6.8.2 TK Solver Inputs

Setting up TK Solver involves inputting the desired equations into a framework, which then solves for the required unknowns. The framework setup included Equation (2) for v_t , Equation (8) for power, Equation (15) for module thermal voltage Υ , grouping Equations (56), (57), (58), and solution Equations (59), (60), and (61) to solve for unknown η , R_s , and R_p . In addition, Equation (22) and Equation (32) were required to solve I_L and I_o .

TK Solver uses FORTRAN software like syntax for equation entry. In addition, TK Solver has a MathLook feature that crudely shows the entered equation. The MathLook feature, along with the grouping, enables syntax check and code debugging. Figure 6.3 shows a TK solver screen image of ten equations entered for the calculations and the MathLook formula for the PV module thermal voltage Υ , represented by U_p , which included diode ideality factor η , represented by A.

Satisfied	$U_p = (N_s \cdot A \cdot k \cdot T) / q$
Satisfied	$P_{mp} = I_{mp} \cdot V_{mp}$
Satisfied	$E_{13} = \exp((V_{mp} + I_{mp} \cdot R_s - V_{oc}) / (U_p))$
Satisfied	$E_2 = \exp((I_{sc} \cdot R_s - V_{oc}) / (U_p))$
Satisfied	$L = (I_{sc} \cdot (R_p + R_s) - V_{oc}) / (R_p \cdot U_p)$
Satisfied	$I_{mp} = I_{sc} - ((V_{mp} + R_s \cdot (I_{mp} - I_{sc})) / R_p) - ((I_{sc} \cdot (R_p + R_s) - V_{oc}) / R_p) \cdot E_{13}$
Satisfied	$R_p = (1 + R_s / R_p + (L \cdot R_s \cdot E_2)) / (1 / R_p + (L \cdot E_2))$
Satisfied	$0 = I_{mp} - V_{mp} \cdot (1 / R_p + (L \cdot E_{13})) / (1 + R_s / R_p + (L \cdot R_s \cdot E_{13}))$
Satisfied	$I_L = I_{sc} + I_{sc} \cdot (R_s / R_p)$
Satisfied	$I_o = (I_L - V_{oc} / R_p) / (\exp(V_{oc} / (U_p)))$

Output

$$U_p = \frac{N_s \cdot A \cdot k \cdot T}{q}$$

Figure 6.3 TK Solver Equations and Formula for $Y (U_p)$.

Figure 6.4 shows a compilation of nine MathLook equations utilized in the TK Solver solution. The equations were entered in the TK Solver Rules tab.

$$P_{mp} = I_{mp} \cdot V_{mp} \quad \text{EQ (8)}$$

$$E_2 = e^{\left[\frac{I_{sc} \cdot R_s - V_{oc}}{U_p} \right]} \quad \text{EQ (56)} \quad \quad \quad I_L = I_{sc} + I_{sc} \cdot \left[\frac{R_s}{R_p} \right] \quad \text{EQ (22)}$$

$$E_{13} = e^{\left[\frac{V_{mp} + I_{mp} \cdot R_s - V_{oc}}{U_p} \right]} \quad \text{EQ (57)} \quad \quad \quad I_o = \frac{I_L - \frac{V_{oc}}{R_p}}{e^{\left[\frac{V_{oc}}{U_p} \right]}} \quad \text{EQ (32)}$$

$$L = \frac{I_{sc} \cdot (R_p + R_s) - V_{oc}}{R_p \cdot U_p} \quad \text{EQ (58)}$$

$$I_{mp} = I_{sc} - \left[\frac{V_{mp} + R_s \cdot (I_{mp} - I_{sc})}{R_p} \right] - \left[\frac{I_{sc} \cdot (R_p + R_s) - V_{oc}}{R_p} \right] \cdot E_{13} \quad \text{EQ (59)}$$

$$R_p = \frac{1 + \frac{R_s}{R_p} + (L \cdot R_s \cdot E_2)}{\frac{1}{R_p} + (L \cdot E_2)} \quad \text{EQ (60)} \quad \quad \quad 0 = I_{mp} - \frac{V_{mp} \cdot \left[\frac{1}{R_p} + (L \cdot E_{13}) \right]}{1 + \frac{R_s}{R_p} + (L \cdot R_s \cdot E_{13})} \quad \text{EQ (61)}$$

Figure 6.4 TK Solver Formula Equations.

Once the equations were entered, following the flow chart shown in Figure 6.2, the constants and PV module characteristics were entered into the Variables tab. The constants were fixed, and the characteristics are from the PV module. Once the input data, shown in Figure 6.5, was entered, the next step was to input seed values for the three primary parameters of η (A), R_s , and R_p .

Status	Input	Name	Output	Unit	Comment
	1.380649E-23	k			Boltmann's Constant
	298.15	T			Temperature in Kelvin
	1.60217663E-19	q			Charge of an electron
	17.2	Vmp			Maximum Power Voltage
	21.6	Voc			Open circuit voltage
	2.91	Imp			Maximum Power Current
	3.23	Isc			Short circuit Current
	36	Ns			Number of Series Cells

Figure 6.5 Constants and PV Module Characteristic Data Inputs.

6.8.3 Seed Value Inputs and Convergence

With any numerical solution, quality inputs are required to enable the finding of solutions. Inputs that differ significantly from the correct values can prevent convergence on the solutions set. Problematic seed inputs can prevent or thwart convergence within a reasonable number of iterations. For example, in Appendix F, the number of iterations is limited to 5,000. With an excellent seed input, the solution for Equation (23) was found in five iterations.

The selection of reasonable seed values was discovered while configuring and testing TK Solver. With convergence experimentation of over 1,000 solver runs, the following criteria were found suitable for choosing the TK Solver 'guess' input seed values.

An ideal diode has an ideality factor of 1, with higher numbers reflecting a lower quality diode and values under 1 not physically reasonable. A good starting seed is 1.2.

Observing Equation (11) and the Five Parameter Model in Figure 4.2 shows that the higher the value of series resistance R_s , the lower the external voltage. Better performing PV systems have R_s resistance approaching 0Ω as a lower bound. The upper bound is the slope of a line from the maximum power point to the V_{oc} point. The resistance of this line is shown in Equation (62), where the equation was adjusted to enable correct units and a positive value. Experimentation with TK Solver shows a value lower than the found solutions generally enables convergence. One-tenth of the R_s value calculated by Equation (62) was found to be a good starting seed value.

$$R_{s \text{ (max)}} = \frac{V_{oc} - V_{mp}}{I_{sc}} \quad (62)$$

The negative inverse of the slope of the I-V curve at I_{sc} is the value of the parallel resistance R_p . From Equation (11) and Figure 4.2, it is seen that high values of the parallel resistance, with an ideal number of $\infty \Omega$, provide less leakage current and thus more available external current I_e . The lower resistance bound is the slope from the short circuit point at I_{sc} to the point at maximum power. Equation (63) shows the minimum value of the parallel resistance R_p . This value is lower than the final solution and was found to be a reasonable starting seed value.

$$R_{p \text{ (min)}} = \frac{V_{mp}}{I_{sc} - I_{mp}} \quad (63)$$

Figure 6.6 shows the maximum and minimum range for R_s and R_p . Note that, from Ohm's law, resistance is voltage divided by current. The slope of the parallel resistance, from Equation (46), is the negative inverse of the tangent line at the I_{sc} point. Figure 6.6 shows notional ranges to provide bounds to determine seed values for the unknown parameters R_s and R_p . The transition from ideal conditions, $R_p = \infty \Omega$ and $R_s = 0 \Omega$, to the actual value shows how the change in these values influences the shape of the I-V curve.

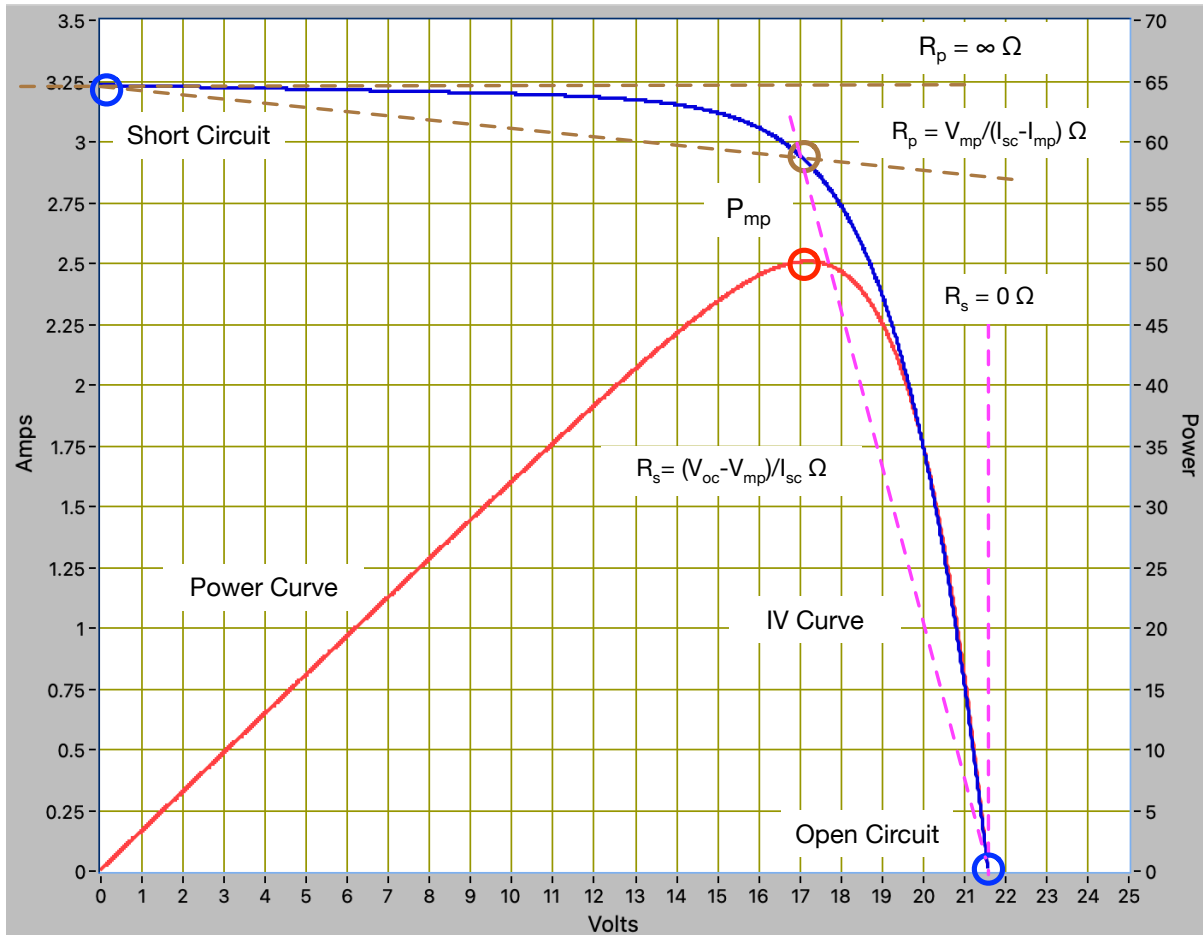


Figure 6.6 Notional Ranges of R_s and R_p .

6.8.4 TK Solver Example

With TK Solver configured, the constants were input, and a template framework configuration was saved. With a PV module selected, the five parameters can be determined. A template TK Solver framework was launched, and the PV characteristic values from the datasheet were entered. For this example, data from the Newpowa 50W PV module, with an image shown in Figure 4.7 and the label shown in Figure 4.11, was used. The outline rectangle shown in Figure 6.7 shows where the PV module, V_{mp} , V_{oc} , I_{mp} , I_{sc} , and N_s , characteristic values were entered.

Input	Name	Output	Unit	Comment
1.380649E-19	k		K/J	Boltmann's Constant
298.15	T		K	Temperature in Kelvin
1.6021E-19	q		C	Charge of an electron
	vt		Volts	Thermal Voltage
17.2	Vmp		Volts	Maximum Power Voltage
21.6	Voc		Volts	Open circuit voltage
2.91	Imp		Amps	Maximum Power Current
3.23	Isc		Amps	Short circuit Current
36	Ns		Count	Number of Series Cells

Figure 6.7 Inputs of PV Characteristic Data.

The next step is the calculation of the input seed guess values. The diode ideality factor η , shown as A in TK Solver, is guessed as 1.2. The guess for R_s is 1/10 of the value calculated by Equation (62), which is 0.136 Ω . The guess for R_p is calculated by Equation (63), which is 53.7 Ω . The inputs are shown in Figure 6.8.

Guess	1.2	A	none	Diode Ideality Factor: To Find
Guess	.136	R_s	ohms	Series Resistance: To Find
Guess	53.7	R_p	ohms	Parallel Resistance: To Find

Figure 6.8 Input of Seed Values.

Once all the data was input, the “Direct Solve” icon was clicked to run the solver. With reasonable inputs, the solutions, along with other calculation results, were displayed. Figure 6.9 shows the results. Figure 6.10 shows the Five Parameter Model, with the solved parameters for the Newpowa 50W PV Module included.

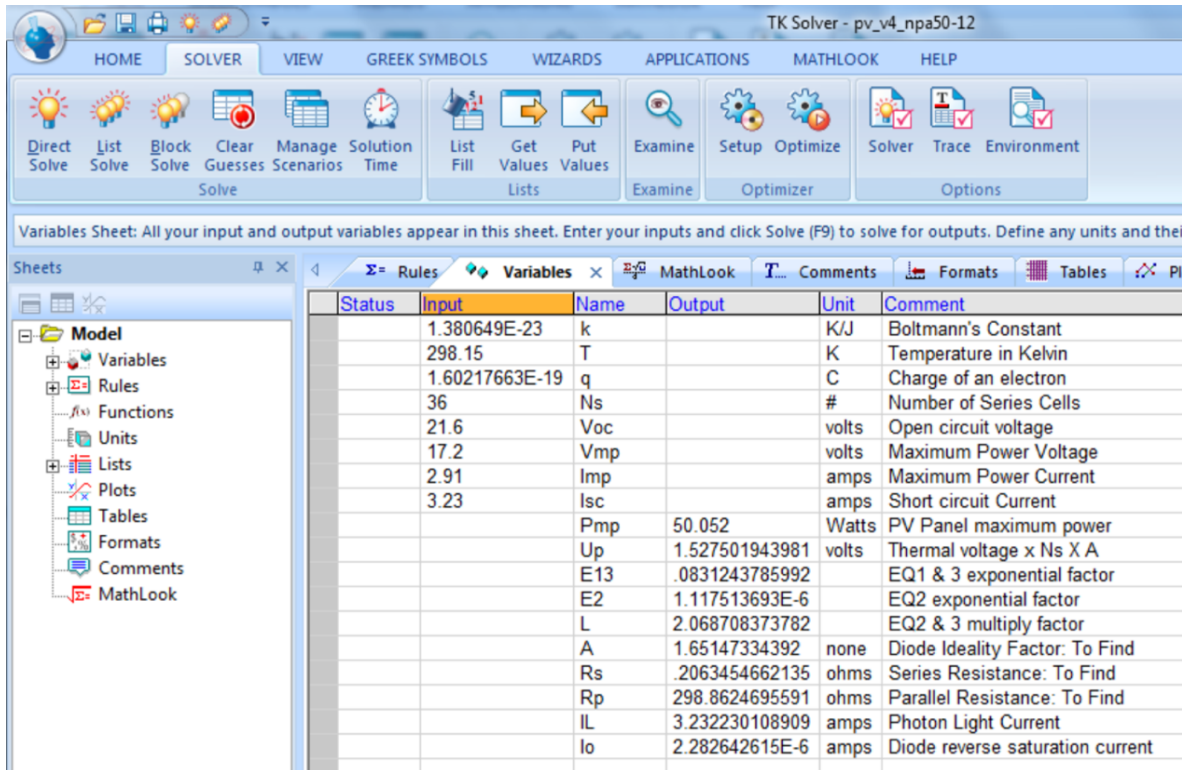


Figure 6.9 Solutions for Newpowa 50W PV Module.

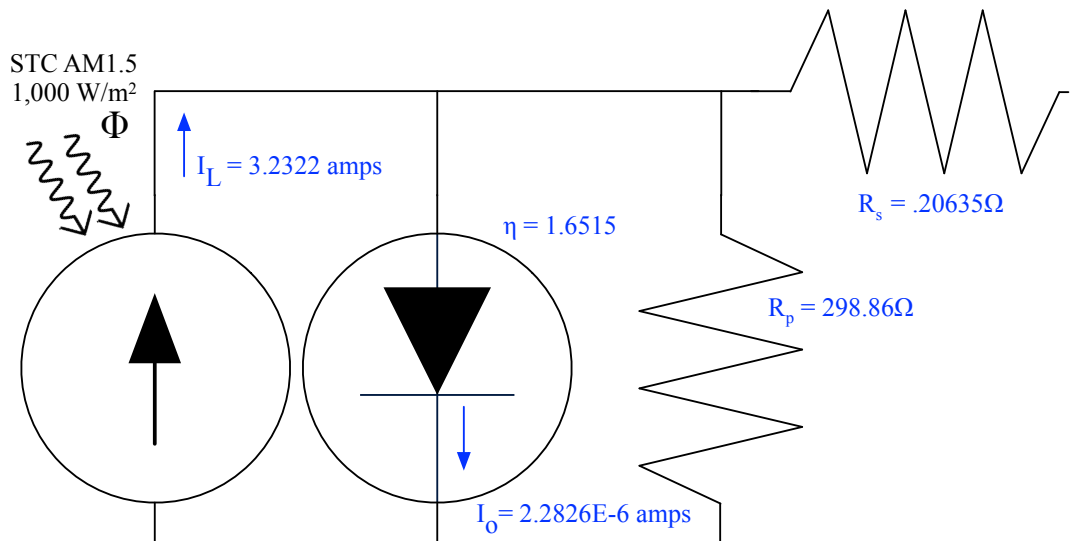


Figure 6.10 Newpowa 50W PV Module Five Parameter Model.

Sometimes, convergence is not achieved, and a solution is not found. An example is shown in Figure 6.11. Poor input values will generate an error, and troubleshooting is required. Typical

examples of errors include the input of incorrect values of the PV characteristics, errors in seed calculations, or errors in the input of seed values. Once correctly updated, a solution is typically found.

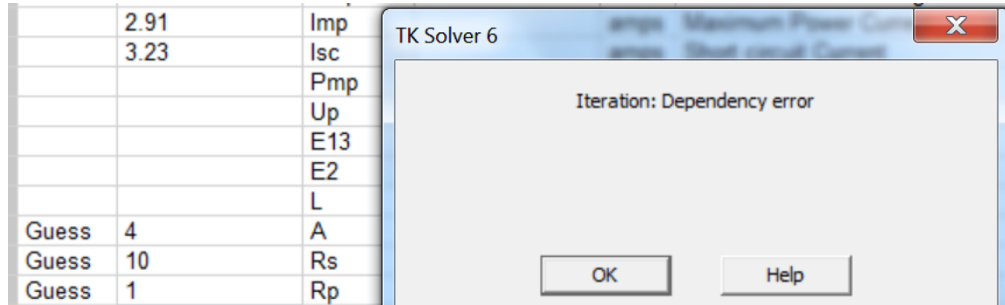


Figure 6.11 Solution Error Example.

Once a solution set for η , R_s , R_p , I_L , and I_o is found, a systems engineering verification check should be performed. The check verifies the found solutions correctly fit the model and the simplifications determined in Chapter 5 are supported. After an extensive search, no verification method was found, so Chapter 7 presents a novel method to verify the results.

Chapter 7: Systems Engineering Methodology for Verification of PV Module Parameter

Solutions ¹

7.1 Background

This chapter incorporates an updated version of a published manuscript [46]. Updates include minor edits, revision of equation numbers, new figures assignments, and reference number changes. The manuscript provides a systems engineering methodology to verify the simplification of equations and five parameter solutions found by various numerical solver methods. This chapter answers the second dissertation research question.

7.2 Abstract

Numerous sources provide methods to extract Photovoltaic parameters from PV module datasheet values. The inputs were the number of series cells N_s , open circuit voltage V_{oc} , maximum power voltage V_{mp} , maximum power current I_{mp} , and short circuit current I_{sc} . The Five Parameter Model solutions outputs were diode ideality factor η , series resistance R_s , parallel resistance R_p , photon light current I_L , and diode reverse saturation current I_o . The parameter solution requires solving three concurrent transcendental equations for η , R_s , and R_p and additional calculations for I_L and I_o . One of the primary tenets of Systems Engineering, verification, was applied to parameter solution results to check for physical and model fitness. This chapter provides methods to verify parameter results and applies them to available solutions.

¹ This is a modified version of “Systems Engineering Methodology for Verification of PV Module Parameter Solutions” by P. Michael, D. Johnston, and W. Moreno, 2023-07815, IEEE Access on 28 April 2023. Reprinted under CC-BY 4.0 license with permission shown in Appendix A.

7.3 Introduction

Typically, the analysis of a PV system uses the Five Parameter Model. A notional diagram is shown in Figure 7.1, which is a duplicate of Figure 4.2.

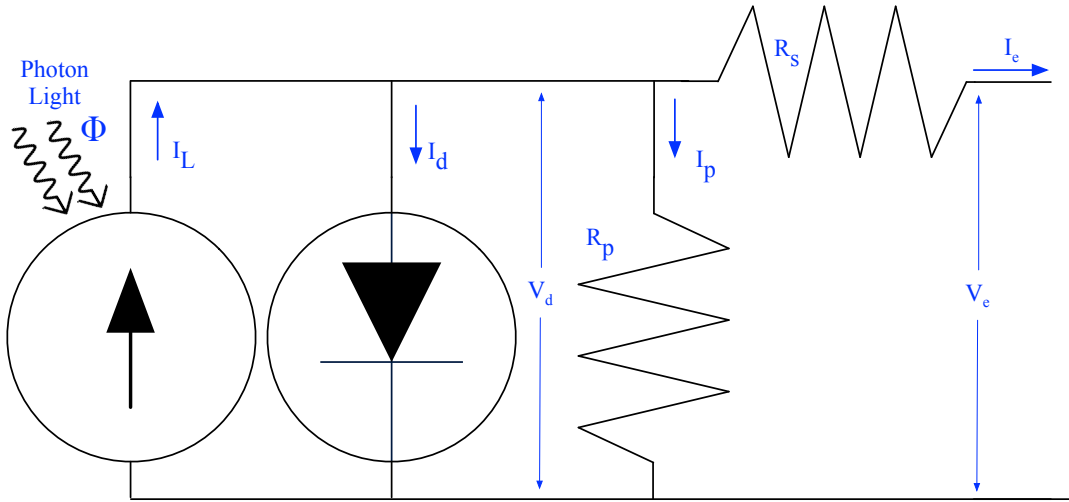


Figure 7.1 Five Parameter PV Model.

Photon light input Φ generates the light current I_L . The generated light current conducts through the diode as I_d , the parallel resistance as I_p , and the external load as I_e . Equation (5) duplicated here was derived using Kirchoff's Current Law.

$$I_L = I_d + I_p + I_e \quad (5)$$

Equation (5) is modified to a format with the external current on the left, the diode current I_d , replaced with the Shockley diode equation, and the parallel current I_p shown in terms of the circuit parameters. This yields a PV module primary Five Parameter Equation (16) utilizing the module's thermal voltage format from Equation (15).

$$I_e = I_L - I_o \left(e^{\frac{V_e + I_e R_s}{Y}} - 1 \right) - \frac{V_e + I_e R_s}{R_p} \quad (16)$$

- I_e external current, amps
- I_L photon light current, amps
- I_o diode reverse saturation current, amps
- V_e external voltage, volts

- R_s series resistance, ohms
- R_p parallel resistance, ohms
- γ PV module's thermal voltage ($\gamma = N_s \eta v_t$), volts
 - N_s number of series PV cells, count
 - η diode ideality factor, no units
 - v_t thermal voltage, volts

7.4 PV Module Conditions

PV module datasheets provide five characteristics: N_s , the number of series PV cells in the module, the open circuit voltage V_{oc} , the voltage at maximum power V_{mp} , the current at maximum power I_{mp} , and the current at short circuit I_{sc} . The last four parameters were obtained from testing under Standard Test Conditions STC of AM1.5 sunlight, 25° C, with an irradiance of 1,000 W/m². Figure 7.2, which graphs Equation (16) for a Kyocera KC200GT PV module, shows the locations of the open circuit, short circuit, and maximum power point conditions on the PV I-V, I_e - V_e Current-Voltage curve. In addition, the power curve, using Equation (8) $P=I_e V_e$, was graphed.

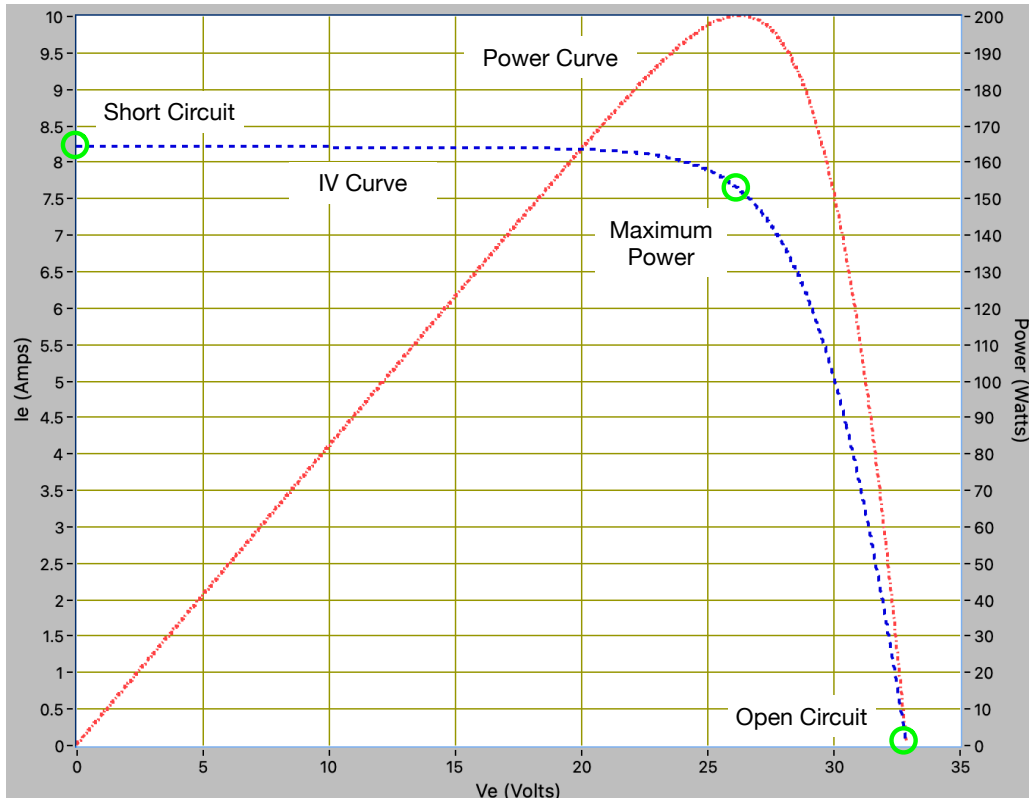


Figure 7.2 PV I-V and Power Graphs for KG200GT PV Module.

Manipulation of the PV equation under open circuit, short circuit, and maximum power conditions results in the following equations in terms of the photon current I_L . Following the procedure described in Chapter 5, Equation (22) for I_L at short circuit, Equation (23) for I_L at open circuit, and Equation (24) for maximum power were derived.

$$I_L = I_{sc} + \frac{I_{sc}R_s}{R_p} \quad (22)$$

$$I_L = I_o \left(e^{\frac{V_{oc}}{Y}} \right) + \frac{V_{oc}}{R_p} \quad (23)$$

$$I_L = I_{mp} + I_o \left(e^{\frac{(V_{mp} + I_{mp}R_s)}{Y}} \right) + \frac{V_{mp} + I_{mp}R_s}{R_p} \quad (24)$$

7.5 Solution Equations for Five PV Parameters

The Five Parameter Model contains five unknowns, η , R_s , R_p , I_L , and I_o . Note that finding Y and applying Equation (15) enables a solution for η . Equation (32), utilizing equations (22) and (23), derives a solution for I_o in terms of datasheet characteristics and unknown parameters R_s , R_p , and Y .

$$I_o = \frac{I_{sc}(R_p + R_s) - V_{oc}}{R_p} \left(e^{\frac{-V_{oc}}{Y}} \right) \quad (32)$$

With Equation (22) to find I_L and Equation (32) solving for I_o , the three remaining unknowns, R_s , R_p , and Y , require three additional equations. Following the method described in Chapter 6 and combining Equations (22), (23), and (24), a solution for I_{mp} shown in Equation (36) was derived. The transcendental equation is in terms of unknowns R_s , R_p , and Y and known datasheet characteristic values of N_s , V_{oc} , V_{mp} , I_{mp} , and I_{sc} .

$$I_{mp} = I_{sc} - \frac{V_{mp} + R_s(I_{mp} - I_{sc})}{R_p} - \frac{I_{sc}(R_p + R_s) - V_{oc}}{R_p} \left(e^{\frac{(V_{mp} + I_{mp}R_s - V_{oc})}{Y}} \right) \quad (36)$$

Two more equations were derived by using the characteristics of the PV I-V and Power curves. The two locations chosen were at the short circuit and the maximum power points, identified in Figure 7.2.

Another transcendental was derived by taking the derivative of the PV equation at short circuit, manipulating, simplifying, and generating the second Equation (46).

$$R_p = \frac{\left(1 + \frac{R_s}{R_p} + \frac{I_{sc}(R_p + R_s) - V_{oc}}{\gamma R_p} R_s e^{\frac{I_{sc}R_s - V_{oc}}{\gamma}}\right)}{\left(\frac{1}{R_p} + \frac{I_{sc}(R_p + R_s) - V_{oc}}{\gamma R_p} e^{\frac{I_{sc}R_s - V_{oc}}{\gamma}}\right)} \quad (46)$$

The third equation uses the power curve, where the derivative is zero at maximum power. Equation (55), also transcendental, provides the required third for the solutions.

$$0 = I_{mp} - V_{mp} \frac{\left(\frac{1}{R_p} + \frac{I_{sc}R_p - V_{oc}}{\gamma R_p} e^{\frac{V_{mp} + I_{sc}R_s - V_{oc}}{\gamma}}\right)}{\left(1 + \frac{I_{sc}R_p - V_{oc}}{\gamma R_p} R_s e^{\frac{V_{mp} + I_{sc}R_s - V_{oc}}{\gamma}}\right)} \quad (55)$$

By solving the three concurrent transcendental Equations (36), (46), and (55), parameter solutions for the values of R_s , R_p , and γ were found. The diode ideality factor η was found using γ and Equation (64). Equation (2) finds the value of v_t .

$$\eta = \frac{\gamma}{N_s v_t} \left(v_t = \frac{kT}{q} \right) \quad (64)$$

Equation (22) found the solutions for I_L , and I_o was found by applying Equation (32).

7.6 Solving for Five PV Parameters

7.6.1 Datasheet Values

Various sources utilized different methods to solve these three concurrent transcendental equations. The Kyocera KC200GT PV module data was utilized to demonstrate this error analysis.

Table 7.1 provides datasheet characteristics for the KC200GT PV module.

Table 7.1 KG200GT Datasheet Characteristics

Parameter	Term	Information from Datasheet
54	N_s	Number of series PV cells
32.9	V_{oc}	Open circuit voltage
26.3	V_{mp}	Maximum power voltage
7.61	I_{mp}	Maximum power current
8.21	I_{sc}	Short circuit current

7.6.2 Solution Methods and Sources

Table 7.2 summarizes the solution set, the methods used to solve for the five parameters, and the source of the solutions. The authors analyzed the first two, and the following were from a collection of thirteen different sources. A total of twenty parameter solution sets were analyzed.

Table 7.2 Solution Set Methods and Sources

Set#	Method	Source
1	TK Solver modified Newton-Raphson	Configured by Authors [46]
2	MATLAB “PV Array.slx” version 1.4	MATLAB R2022b [47]
3	Laplacian Nelder-Mead spherical	Weng X., et all, [48]
4	De Soto	Lun, S., et all, [49]
5	Pade’ approximants	“
6	Basic Taylor model	Lun, S., et all, [50]
7	Five Parameter model	“
8	MATLAB S-function	Yildiran, N, Tacer E. [51]
9	Novel iterative method	Wang, G, et al. 1 [52]
10	Villalva’s method	“
11	Adaptive Harris hawks optimization	Song, S. et all [53]
12	Simple iterative	Chaibi, Y., et all [54]
13	New explicit mathematical	Pindado, S, Cubas, J., [55]
14	Whippy Harris Hawks	Naeijian, M., [56]
15	Analytical-numerical approach	Hejri, M., et all [57]
16	Approximate Analytical Solution	“
17	Lambert W function	Tayyan, A., [58]
18	Easy and Accurate	Villalva, J., et all, [59]
19	Conjugate Gradients	Tayyan, A., [60]
20	New Simplified Method	Muhammadsharif, F., [61]

7.6.3 Solution Parameter Sets

Using the PV data from the KC200GT PV module listed in Table 7.1 and the solutions provided by the sources listed in Table 7.2, sets of the five parameter solution values were copied into Table 7.3. The table lists the solutions of the five parameters η , R_s , R_p , I_L , and I_o . The parameter digits listed were those provided from each source solution method and subsequently used in the error calculations.

Table 7.3 Parameter Solutions

Set #	η	$R_s \Omega$	$R_p \Omega$	I_o Amps	I_L Amps
1	1.341061130	0.2171524429	951.9318193	1.710643752E-7	8.211872846
2	0.60957	0.49485	80.0174	9.9924E-17	8.2608
3	1.076405798	0.34381505	763.5403341	2.24175E-9	8.216891354
4	1.391	0.3355	160.1	4.255571E-10	8.22721
5	1.391	0.3405	155.7	4.254766E-10	8.22795
6	1.391	0.3596	153.2	4.254686E-10	8.22927
7	1.391	0.3355	160.1	4.255571E-10	8.22721
8	1.3	0.222	462	9.8252E-8	8.21
9	1.3	0.226	508.99	9.83E-8	8.2136
10	1.3	0.229	593.24	9.83E-8	8.2132
11	1.0748	0.40909	775.03	1.5524E-9	8.2174
12	1.22	0.2555	358	3.26E-8	8.215859 *
13	1	0.336	159	4.03E-10	8.123
14	1.05528589	0.24093983	774.212315	1.43601E-9	8.21860582
15	1.34	0.217	951.932	1.71E-7	8.212
16	1.41	0.194	640.771	4.1E-7	8.21
17	1.277	0.239	490.218	6.9127E-9	8.214
18	1.3	0.221	415.405	9.825E-8	8.214
19	1.235	0.247	414.89	4.812E-8	8.215
20	1.192	0.212	388.6	1.675E-8	8.184

* I_L was not provided. A calculated solution using Equation (22) was inserted.

7.6.4 Reported Solution Errors

Many of the sources reported solution error results. Table 7.4 summarizes the source Set #, error calculation methods, and the reported errors. For consistency, all errors were, when required, converted and presented in percent. RMS is Root Mean Square, and RMSE is Root Mean

Square Error. When “Graph” was listed, the error referenced a graph in the source, which reported different error values depending on conditions.

Table 7.4 Solution Set Error Reporting

Set #	Error Determination Method	Reported Error
1	RMS 5 Error method from this manuscript	0.00%
2	RMS 5 Error method from this manuscript	5.64%
3	Table A7: RMSE calculated model to its experimental value	0.15390%
4	Fig 6: I-V Graph Model value versus De Soto measured	Graph
5	Fig 6: I-V Graph Model value versus proposed measured	Graph
6	Table 2: RMSE Explicit Method for Basic Taylor model	2.90%
7	Table 2: RMSE Explicit Method for Five Parameter model	1.56%
8	No error calculation included	Not reported
9	Appendix B: Relative RMSE calculated versus experimental	1.6212%
10	Villalva’s method	Not reported
11	Table A.9: RSME simulated versus measured	0.12294%
12	Table 3: Datasheet versus proposed method	1.73%
13	Table 4: RMSE Normalized at set points	1.62% & 1.21%
14	Table 13: RMSE Datasheet versus proposed	1.822%
15	Table 4: Normalized RSME measured versus approach	4.65%
16	Approximate Analytical Solution	Not reported
17	Figure 8: RSME Calculated versus experimental	Graph
18	No error calculation included	Not Reported
19	No error calculation included	Not Reported
20	Table 3: maximum relative error	1.87%

The Five Parameter Model contains five unknowns, η , R_s , R_p , I_L , and I_o . Concurrently solving Equations (36), (46), and (55) solves for R_s , R_p , and Y . Using Equation (64) finds η from Y . I_L is found from Equation (22) and then I_o from Equation (32).

7.7 Solution Verification

Two general methods are recommended for systems engineering solution verification.

- Physical Parameter
- RMS 5 Error Equation

7.7.1 Physical Parameter Verifications

This check involves physical parameter verification. Even if an equation provides a valid mathematical solution, the solved values may not provide a physically reasonable answer. An example is optimizing a fence length problem, where the mathematically correct negative root solutions are ignored. The checks verify parameters determined by transcendental equation solutions for η , R_s , and R_p . All the parameter solutions listed in Table 7.2, except for the value of diode ideality factor η solved by method #2, passed these physical parameter checks.

7.7.1.1 Diode Ideality Factor

An ideal diode has a value of 1.0, and for silicon devices, a reasonable number is 1.2 to 1.3 [61]. The diode factor limit was set from 1.0 to 1.8, which supports a wider range of solutions. For example, in set #2, the MATLAB “PV_Array.slx” provided a relatively low error solution, but the solved diode ideality factor of 0.60957 is not physically reasonable.

7.7.1.2 Series Resistance

The series resistance R_s is the contributions of the PV cell material, contact between the PV cell to metal, and the metal contact path resistances. Values for R_s are bound by the ideal, but not physically possible 0Ω on the low end, and the slope of the I-V curve from V_{oc} to the maximum power point on the high end. For the KC200GT, from Equation (62), the slope from V_{oc} to the maximum power point $(V_{oc}-V_{mp})/I_{sc}$ establishes the maximum series resistance of 0.867Ω for R_s . Typical PV modules have external 2.6 mm, #10 AWG copper cables with a resistance of about 0.006Ω per meter. One meter of the connecting cable has a resistance of 0.006Ω . Other resistance, such as the PV cell material, interfaces, and conductive traces, increase this resistance. The calculated lower limit was set to 1/50 of the R_s maximum or an R_s minimum of 0.016Ω .

7.7.1.3 Parallel Resistance

The parallel resistance R_p sources include manufacturing defects and leakage paths around the PV cells. From Fig 7.2, the minimum resistance R_p is the inverse slope of the IV curve at short circuit. From Equation (63), for the KC200GT, the slope from the I_{sc} to the maximum power point at V_{mp} and I_{mp} is calculated as $V_{mp}/(I_{sc}-I_{mp})$ or 43.8Ω . This calculation set the lower bound for R_p . Parallel resistance paths control the upper limit. Using the ratio determined for R_s , the R_p upper limit was set at 50 times for an R_p maximum of $2,190 \Omega$.

7.7.2 RMS 5 Error Equation Verification

The verification checks the model fit by calculating errors on the three primary points of the I-V curve defined by Equation (16) at short circuit, open circuit, and maximum power conditions. The equation checks involve taking the solved solution parameters, plugging them into the set of five check equations, and calculating each error. The error is the absolute difference in the provided solution versus the value calculated from the check equations. For comparison, the absolute error is converted to percent.

The merit of the solved parameters was judged by the RMS of the five calculated errors. The PV module datasheet contains the N_s , V_{oc} , V_{mp} , I_{mp} , and I_{sc} factors. The values of η , embedded in the module thermal voltage Υ , R_s , R_p , I_L , and I_o were from the solved parameter solutions. Equation (65) checks the current at short circuit, Equation (66) the current at open circuit, and Equation (67) the current at maximum power. These three equations check the fit of I_L solved versus the currents I_d , I_p , and I_c under short circuit, open circuit, and maximum power conditions. Equations (68) compares the datasheet V_{oc} with solved V_{ocs} using I_L , I_o , R_p , and Υ . Equations (69) compares the datasheet V_{mp} with a solved V_{mps} using the datasheet I_{mp} and solved parameters I_L , I_o , R_s , R_p , and Υ . Finding V_{ocs} and V_{mps} requires finding solutions for transcendental Equation

(68_s) and Equation (69_s), which were found using a MATLAB solver. Appendix F includes an example.

$$error_{sc} = I_L - \frac{I_{sc}R_s}{R_p} - I_{sc} \quad (65)$$

$$error_{oc} = I_L - I_o \left(e^{\frac{V_{oc}}{Y}} \right) - \frac{V_{oc}}{R_p} \quad (66)$$

$$error_{mp} = I_L - I_o \left(e^{\frac{V_{mp} + I_{mp}R_s}{Y}} \right) - \frac{V_{mp} + I_{mp}R_s}{R_p} - I_{mp} \quad (67)$$

$$I_L = I_o \left(e^{\frac{V_{ocs}}{Y}} \right) + \frac{V_{ocs}}{R_p} \quad (68_s)$$

$$error_{V_{oc}} = V_{oc} - V_{ocs} \quad (68)$$

$$I_L = I_o \left(e^{\frac{V_{mps} + I_{mp}R_s}{Y}} \right) + \frac{V_{mps} + I_{mp}R_s}{R_p} + I_{mp} \quad (69_s)$$

$$error_{V_{mp}} = V_{mp} - V_{mps} \quad (69)$$

The overall merit of the solution set was judged by the RMS error of the results of the five error equations. The ‘RMS 5 Error’ calculation treated all five error results with equal weights, as shown in Equation (70). Table 7.5 shows the Set # method from Table 7.2, the five absolute error calculations in percent for Equations (65), (66), (67), (68), and (69), and the overall absolute RMS 5 Error in percent from Equation (70). The spreadsheet contains the values and calculations [62].

$$RMS_5 \text{ error} = \sqrt{\frac{[(error_{sc})^2 + (error_{oc})^2 + (error_{mp})^2 + ((error_{V_{oc}})^2 + (error_{V_{mp}})^2]}{5}} \quad (70)$$

Table 7.5 RMS 5 Error Analysis Results

Set #	Error _{sc}	Error _{oc}	Error _{mp}	Error _{V_{oc}}	Error _{V_{mp}}	RMS _{5 error}
1	0.00%	0.00%	0.00%	0.00%	0.00%	0.00%
2	0.00%	-0.54%	-11.9%	-0.07%	-0.03%	5.33%
3	-0.32%	10.9%	-9.15%	1.99%	1.73%	6.48%
4	0.00%	-801%	43.4%	-1,274%	-1,087%	830%
5	0.00%	-801%	43.0%	-1,274%	-1080%	828%

Table 7.5 (Continued)

6	0.00%	-800%	42.7%	-1,274%	-1064%	824%
7	0.00%	-801%	43.4%	-1,274%	-1087%	830%
8	0.39%	-806%	53.3%	-829%	-824%	635%
9	0.00%	6.52%	-4.34%	1.44%	0.01%	3.56%
10	0.00%	5.64%	-4.42%	1.24%	-0.02%	3.25%
11	-0.31%	-225%	-10.5%	-47.9%	0.65%	103%
12	0.00%	88.6%	-10.4%	17.5%	14.8%	41.2%
13	-0.27%	-0.78%	-6.56%	-0.14%	-1.14%	3.00%
14	-0.61%	6.97%	22.1%	1.24%	-85.8%	39.7%
15	-0.01%	11.2%	-4.83%	2.53%	1.98%	5.64%
16	0.25%	9.73%	-8.20%	2.32%	15.1%	8.89%
17	0.00%	-734%	48.8%	405%	403%	417%
18	0.04%	7.52%	-4.18%	1.66%	0.17%	3.92%
19	-0.01%	237%	-19.2%	43.7%	37.1%	109%
20	3.05%	-79.2%	11.5%	-14.5%	-34.4%	39.5%

7.8 Discussion of Errors

7.8.1 Current Check at Short Circuit

The first check compares the solved I_L parameter versus the I_L calculated with Equation (65). This is an easy check, and generally, the errors were low since the controlling factor is the ratio of R_s to R_p . Any reasonable solution should have a very low error for this verification. Except for parameter Set #20, with an error of 3.05%, all errors were under 1%, with an average of 0.11% and several 0.00%.

7.8.2 Current Check at Open Circuit

The check for current at open circuit uses Equation (66), which includes an exponential function. Because of the exponential, any error in the solution for η will significantly impact the results. The exponential result is then multiplied by the diode reverse saturation current I_o to determine the diode current I_d . This means a low error solution must include accurate values of both η and I_o . These calculations showed that several solution sets contained significant errors for

this verification test. For Set #17, the diode factor η of 1.277 is a reasonable value but, combined with an I_o of 6.9127 nA, produces an unreasonable diode current I_d of only 802 mA.

7.8.3 Current Check at Maximum Power

The third check utilized Equation (67), which also includes an exponential factor. In the case of maximum power, the diode current I_d , calculated with the exponential function and I_o , was a smaller part of the overall current compared to the open circuit case. This was reflected, for example, in Set #8, where the current error at maximum power was 53.3% versus -806% for the open circuit current error.

7.8.4 Voltage Check at Open Circuit

The influence of the exponent, diode ideality factor η , and reverse saturation current I_o is also important in this error verification. In the worst cases, Sets #4, #5, #6, and #7 contain errors of almost -1,300%.

7.8.5 Voltage Check at Maximum Power

The fifth check includes the influence of the exponent but with a lower effect than in the open circuit check. The worst cases were again in Sets #4, #5, #6, and #7, with errors of almost -1,100%.

7.8.6 Overall RMS 5 Error

Set #1 shows the lowest error, which to 3 decimals was 0.00%. The worst cases were Sets #4 and #7, with an error of 830%. Table 7.5 shows that solutions with a high error have solved for an inferior value for the diode current I_d , found from the diode ideality factor η and the diode reverse saturation current I_o .

7.9 Analysis of Error Sensitivity

Solution Sets #1 and #15 parameters were similar, with the difference in the number of digits provided by each solution set. The rounding of results of Set #1 matches Set #15, η , R_s , and I_o to 3 digits, R_p to 6 digits, and I_L to 4 digits. Table 7.6 explores the effect of the number of digits and the errors calculated by this method. The table presents parameters from solution Set #1 rounded to fewer digits, the calculated errors for each of the five verifications, and the overall RMS 5 Errors.

Table 7.6 Error Analysis with Fewer Digits

	η	R_s	R_p	I_o	I_L	{digits}
	Error_{sc}	Error_{oc}	Error_{mp}	Error_{voc}	Error_{vmp}	RMS 5 Error
factor	1.341061130	0.2171524429	951.9318193	1.710643752E-7	8.211872846	{10}
errors	0.000%	0.000%	0.000%	0.000%	0.000%	0.000%
factor	1.341061	0.2171524	951.9318	1.710644E-7	8.211873	{7}
errors	0.000%	0.002%	0.000%	0.000%	0.000%	.001%
factor	1.34106	0.217152	951.932	1.71064E-7	8.21187	{6}
errors	0.000%	0.011%	-0.001%	0.000%	0.000%	0.005%
factor	1.3411	0.21715	951.93	1.7106E-7	8.2119	{5}
errors	-0.003%	-0.443%	0.030%	0.000%	0.000%	0.198%
factor	1.341	0.2172	951.9	1.711E-7	8.212	{4}
errors	-0.013%	0.817%	-0.026%	0.000%	0.000%	0.731%
factor	1.34	0.217	952	1.71E-7	8.21	{3}
errors	0.187%	11.41%	-0.814%	0.00%	0.000%	5.11%
factor	1.3	0.22	950	1.7E-7	8.2	{2}
errors	1.19%	604%	-36.5%	-110%	-70.0%	277%

For Set #1, an analysis of Table 7.6 data shows little difference between 10 and 6 digits. Five digits provide a high precision result of under 0.2%. Note that the IEC [31] test standard for

PV modules specifies 0.2% measurement accuracy. Four digits provide a reasonable solution with an error of under 1%.

7.10 Recommendations

It is recommended that any solution in calculating values for the Five Parameter Model, η , R_s , R_p , I_L , and I_o , should include verification checks. A solution that results in unreasonable physical values or high RMS 5 Error should be re-evaluated. Any solution with less than 4 digits can provide unreliable results and should not be used.

Since the solution to the RMS 5 Error method requires solving the transcendental Equations (68_s) and (69_s) to find the voltage errors at open circuit and maximum power point, an alternative RMS 3 Error method can be used. This method only checks the RMS errors from Equations (65), (66), and (67), with the error calculation shown in Equation (71). Table 7.7 summarizes the results of the sources, reported errors, RMS 3 Errors, and RMS 5 Errors.

$$RMS_{3\ error} = \sqrt{\frac{[(error_{sc})^2 + ((error_{oc})^2 + ((error_{mp})^2)]}{3}} \quad (71)$$

Table 7.7 Source, RMS 3 Error, and RMS 5 Error

Set #	Source	RMS 3	RMS 5
1	0.00%	0.00%	0.00%
2	5.33%	6.89%	5.33%
3	0.154%	8.22%	6.48%
4	Graph	463%	830%
5	Graph	463%	828%
6	2.90%	463%	824%
7	1.56%	463%	830%
8	Not reported	466%	635%
9	1.6212%	4.52%	3.56%
10	Not reported	4.14%	3.25%
11	0.12294%	130%	103%
12	1.73%	51.5%	41.2%
13	1.62% & 1.21%	3.82%	3.00%
14	1.822%	13.4%	39.7%
15	4.65%	7.05%	5.64%

Table 7.7 (Continued)

16	Not reported	7.35%	8.89%
17	Graph	425%	417%
18	Not Reported	5.00%	3.92%
19	Not Reported	137%	109%
20	1.87%	46.2%	39.5%

7.11 Conclusion

A new method was presented to verify the solved values for the Five Parameter PV model solution of η , R_s , R_p , I_o , and I_L . This chapter showed all but one solved parameter, the method utilized in the document, passed the Physical Parameter Verification test. When checked at the primary conditions of short circuit, open circuit, and maximum power, most published parameter solutions have a significantly high calculated error found via the RMS 5 Error and RMS 3 Error methods.

Chapter 8: Six Parameter PV Model and I-V Graphing

8.1 Introduction

With the solved five parameter values, graphing the PV I-V curve requires finding the transcendental Equation (11) solution for each data point. A new Six Parameter Model and accompanying equations are introduced to enable graphing the I-V curve without finding multiple solutions to the transcendental Equation (11). This chapter answers the third dissertation research question.

8.2 Existing PV Equation

The existing five parameter Equation (11) provides the PV I-V curve graphing formula. The five parameters were found utilizing the method described in Chapter 6 and verified by methods described in Chapter 7. Equation (72) shows the PV I-V curve graphing equation for a Kyocera KC200GT PV module with the solution parameters to six digits.

$$I_e = 8.21188 - \left(e^{\frac{(V_e + 0.217152I_e)}{1.86062}} - 1 \right) - \frac{(V_e + 0.217515I_e)}{951.932} \quad (72)$$

For the KC200GT, values for short circuit, open circuit, and maximum power were found from either solving Equation (72) or from the PV module characteristic values listed on the label or the datasheet. As described in Chapter 7, verification should be performed to ensure the parameter values are reasonable. The primary data points are provided on the PV module data label or datasheet; since I_e is on both sides of the equation, any other point requires a numerical solution method to solve Equation (72). A new procedure that utilizes a six parameter model is presented in this chapter.

8.3 Six Parameter Model

A new Six Parameter Model includes an additional parameter R_e , the external load resistance. The addition of a sixth parameter requires another equation for solutions. Equation (73), a simple application of Ohm's law, presents minimal calculation difficulty.

$$R_e = \frac{V_e}{I_e} \quad (73)$$

Figure 8.1 shows the Six Parameter Model, which includes I_L , the terms η and I_o , which are embedded in I_d , R_p , R_s , and the new parameter R_e .

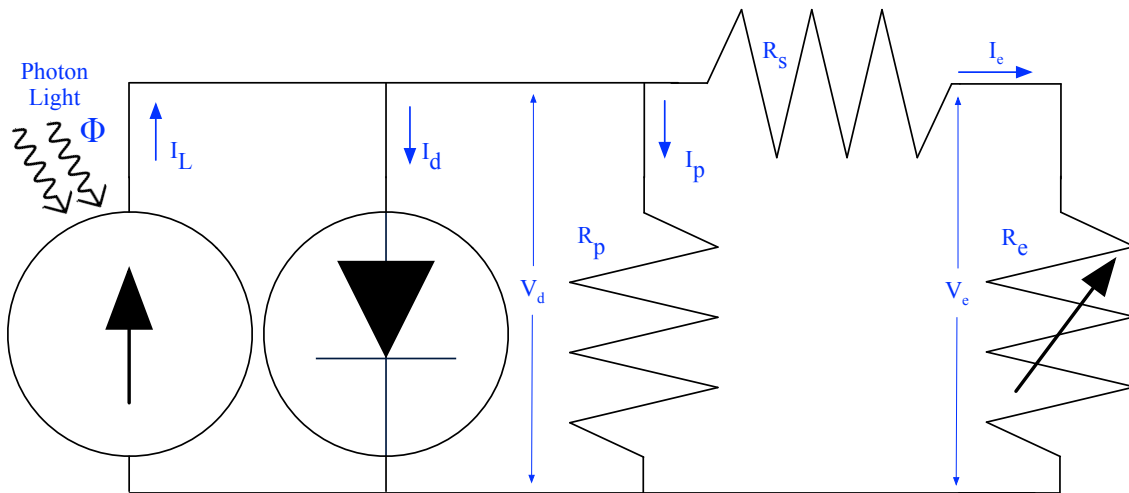


Figure 8.1 Six Parameter PV Model.

The model terms include the following:

- Photon Light input: Φ , photons
- Light generated current: I_L , amps
- Diode current: I_d , amps, which includes
 - Diode Ideality Factor: η , no units
 - Diode reverse saturation current: I_o , amps
- Diode voltage: V_d , volts
- Parallel resistance current: I_p , amps
- Parallel resistance: R_p , ohms
- Series resistance: R_s , ohms
- External current: I_e , amps
- External voltage: V_e , volts
- External resistance: R_e , ohms

8.4 Six Parameter Equations

From Figure 8.1 and Kirchhoff's Current Law, Equation (6), duplicated here, shows the model's current in terms of the external current I_e .

$$I_e = I_L - I_d - I_p + \quad (6)$$

Observing the Six Parameter Model in Figure 8.1, Equation (74) derived the diode voltage V_d .

$$V_d = V_e + I_e R_s \quad (74)$$

Utilizing the module thermal voltage Υ from Equation (15), the diode voltage V_d from Equation (74), and inserting into Equation (11), duplicated here, Equation (75) was derived.

$$I_e = I_L - I_o \left(e^{\frac{(V_e + I_e R_s)}{\eta v_t N_s}} - 1 \right) - \frac{(V_e + I_e R_s)}{R_p} \quad (11)$$

$$I_e = I_L - I_o \left(e^{\frac{V_d}{\Upsilon}} - 1 \right) - \frac{V_d}{R_p} \quad (75)$$

Equation (75) is an ordinary equation and thus easy to solve, but only contains I_e and not the V_e required to graph the I-V curve of external current versus external voltage. Using the Six Parameter Model and manipulating Equation (75) enables the derivation of V_e without solving the transcendental equation. The model, however, has limits that can be addressed by applying proper bounds. Limiting the ranges of external voltage and current values to those established by the PV module characteristics prevents mathematical issues with division by 0 and dealing with open circuit ∞ resistance.

8.5 Voltage and Current Bounds

In a PV module, for fixed STC irradiance and temperature, the external voltage and current are bounded by characteristic values found on the PV module datasheet. External voltage is limited to 0 volts at short circuit and V_{oc} at open circuit. The external current bounds are 0 amps at open

circuit and I_{sc} at short circuit. The new parameter R_e has the value of 0Ω at short circuit, $\infty \Omega$ at open circuit, and intermediate resistance values for various load conditions such as maximum power point. Table 8.1 shows the range of parameters for the model.

Table 8.1 Range of Parameters

Parameter	Low Limit	State		High Limit	State
V_d diode voltage	$I_{sc} \times R_s$	Short circuit		V_{oc}	Open circuit
I_e external current	0	Open circuit		I_{sc}	Short circuit
V_e external voltage	0	Short circuit		V_{oc}	Open circuit
R_e external resistance	0	Short circuit		∞	Open circuit

8.6 Calculation of V_e for the Six Parameter Model

The calculation of V_e from V_d requires utilizing a series of equations. Equation (76) calculates the parallel resistance current I_p . Equation (77) calculates the diode current I_d .

$$I_p = \frac{V_d}{R_p} \quad (76)$$

$$I_d = I_o \left(e^{\frac{V_d}{Y}} - 1 \right) \quad (77)$$

The value of I_o was found by using Equation (32), updated to Equation (78) by the inclusion of Y from Equation (15).

$$I_o = \frac{I_{sc}(R_p + R_s) - V_{oc}}{R_p} \left(e^{\frac{-V_{oc}}{Y}} \right) \quad (78)$$

Using I_{sc} , R_s , and R_p , I_L was found by Equation (22).

$$I_L = I_{sc} + \frac{I_{sc}R_s}{R_p} \quad (22)$$

With the calculated results for I_L from Equation (22), I_p from Equation (76), and I_d from Equation (77), the value for the external current I_e was found from Equation (6). Referencing

Figure 8.1 and with solved parameter R_s , the diode voltage V_d , and the calculated external current I_e , the external resistance R_e was found from Equation (79).

$$R_e = \frac{V_d}{I_e} - R_s \quad (79)$$

With the values of R_e and I_e determined, the external voltage V_e was found by Equation (80).

$$V_e = I_e R_e \quad (80)$$

This process, shown in Figure 8.2, describes the method to find the I_e and V_e data pairs to enable the graphing of the I-V and Power curves. Using fixed constants at STC, N_s , v_t , and the solved value η , the module thermal voltage Y was calculated. Multiplying $R_s \times I_{sc}$ calculates the starting V_d voltage. Other inputs include V_{oc} , R_p , and the V_d increment. The V_d voltage was used to sequentially calculate I_p , I_d , I_e , R_e , and finally, V_e . After a calculation, V_d is increased by the step voltage increment, and the calculations were repeated until V_d reaches V_{oc} . The V_d increment was chosen to enable enough resolution to correctly identify V_{mp} and I_{mp} values at maximum power P_{mp} , which were compared with the datasheet values to help verify the solution method.

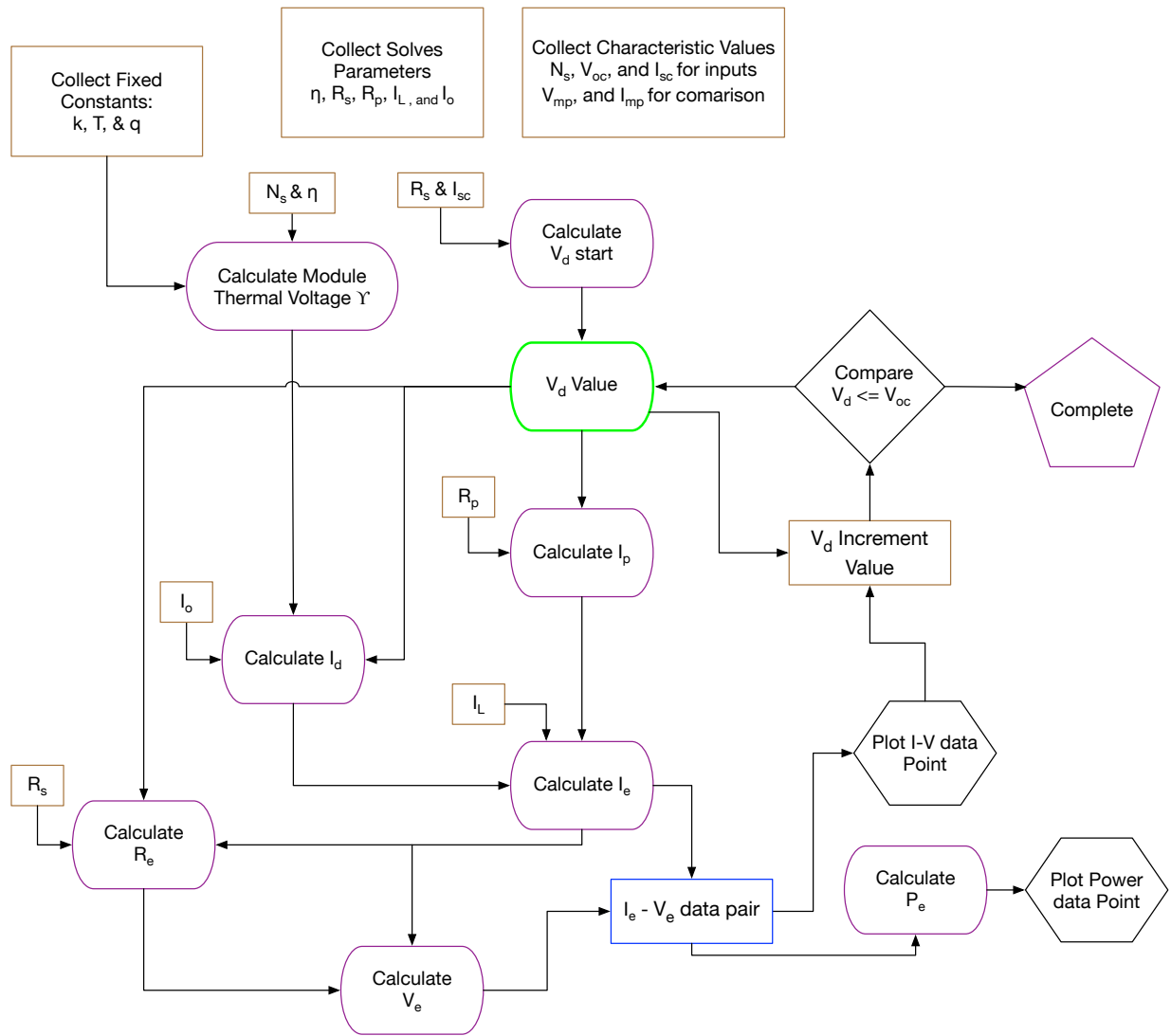


Figure 8.2 Six Parameter I-V Data Process Flow.

8.7 Spreadsheet Implementation

The process flow shown in Figure 8.2 was implemented in a spreadsheet. A captured image of the spreadsheet for the Kyocera KC200GT PV module is shown in Figure 8.3. Once the input data was collected, trials were performed to determine that an increment of 75 mV provided adequate resolution. The resolution check was performed using the spreadsheet to find the maximum power and the contributory I_e and V_e values. A verification compared the calculated maximum power and the contribution current and voltage values of the P_{mp} , I_{mp} , and V_{mp} to the

datasheet values. The spreadsheet shows the starting diode voltages V_d and the equations used in the calculation for each column for I_p , I_d , I_e , R_e , V_e , and Power. The maximum power was found by applying the “MAX” function to the power column. The contributing current and voltages were found via the “INDEX” function on the I_e and V_e spreadsheet columns.

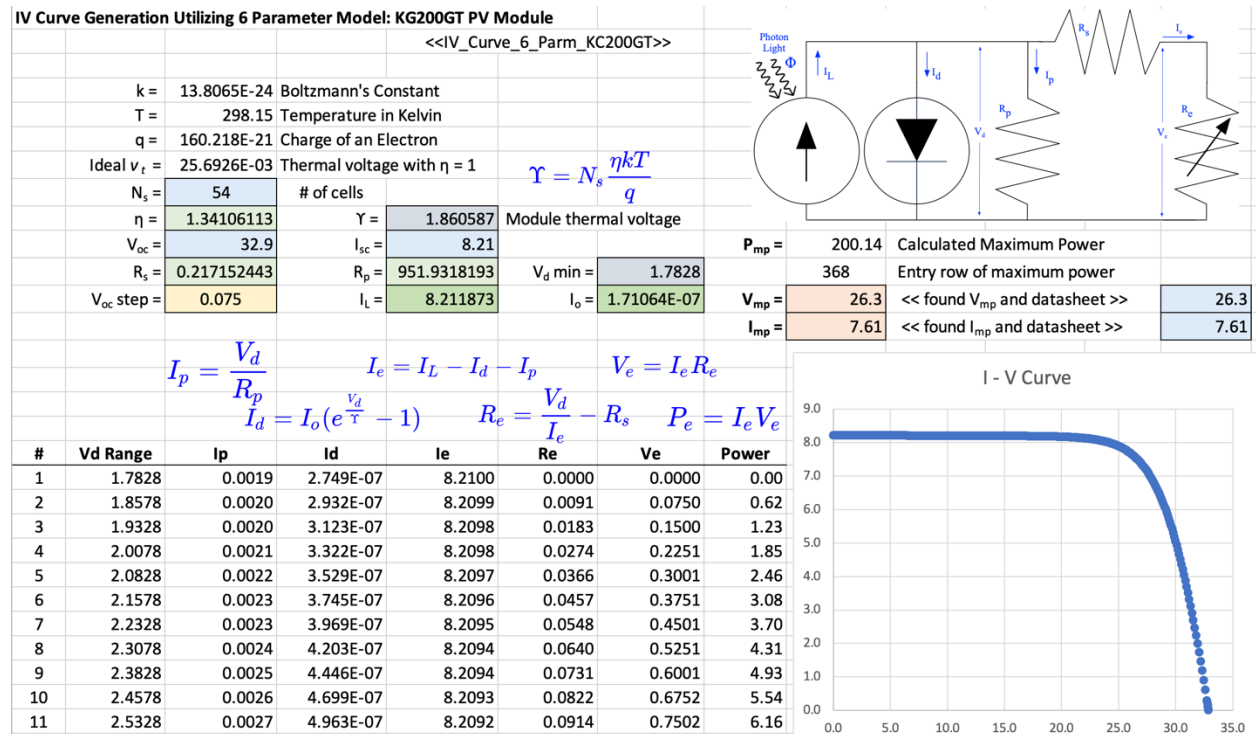


Figure 8.3 Spreadsheet Implementation of KC200GT PV Module.

8.8 LabVIEW Configuration

An alternate and more capable method of graphing the I-V was constructed utilizing LabVIEW software. According to the LabVIEW Web page, “LabVIEW is a graphical programming environment engineers use to develop automated research, validation, and production test systems” [63]. A virtual instrumentation system was created to graph the I-V curves using the six parameter model. The application enables the wiring of virtual instruments and the implementation of mathematical functions. Figure 8.4 shows a calculation block diagram that solves Equation (22) for finding the photon light current I_L and Equation (32) to find the diode

reverse saturation current I_o . Inputs were the three fixed constants, Boltzmann's constant k , temperature T , and charge of an electron q , three PV module characteristic values, number of PV series cells N_s , short circuit current I_{sc} , and open circuit voltage V_{oc} , and three solved PV parameters, diode ideality factor η , series resistance R_s , and parallel resistance R_p .

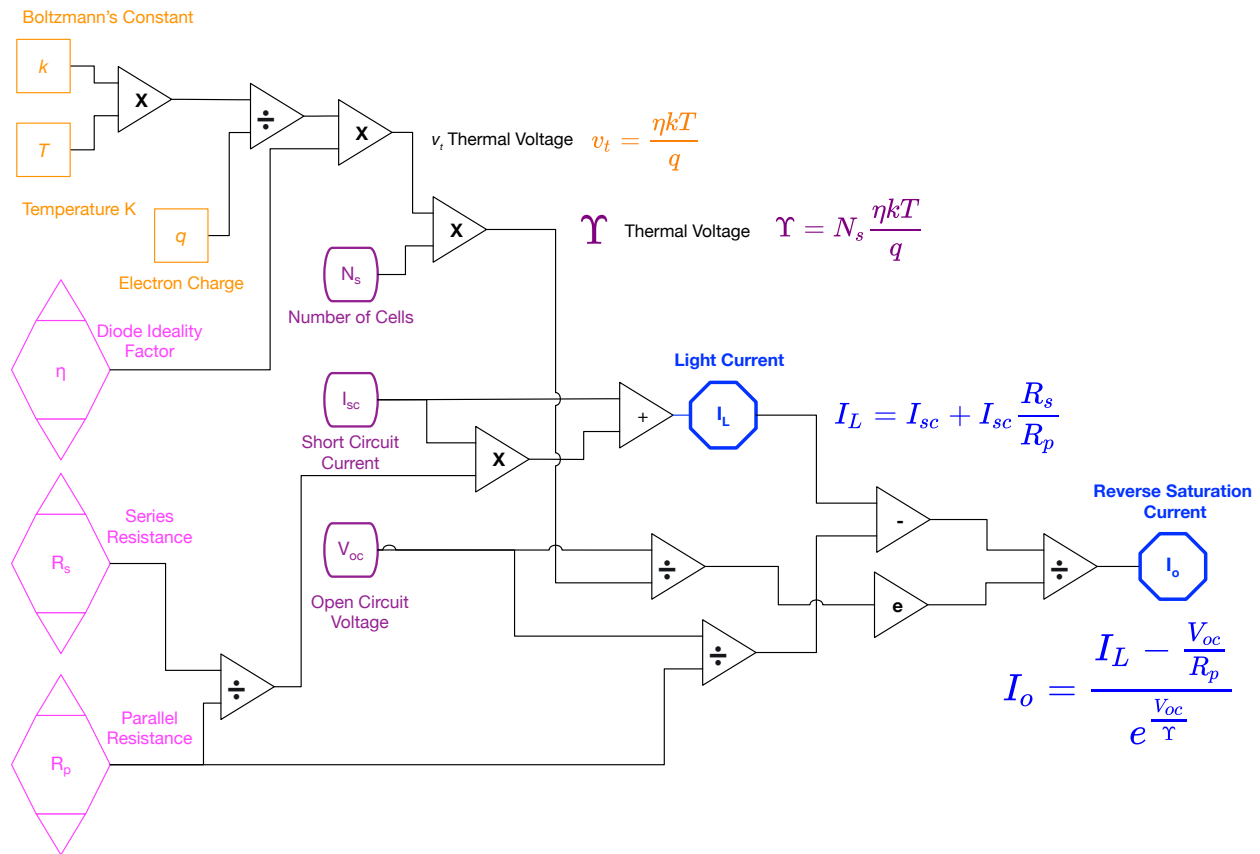


Figure 8.4 I_L and I_o Calculation Block Diagram.

LabVIEW consists of two views: the front panel, which shows the display interface, and the block diagram, which shows the functions and connections of the instrument. The block diagrams mimic the calculation block diagram shown in Figure 8.4, with the LabVIEW block diagram implementation of the I_L and I_o calculations shown in Figure 8.5. LabVIEW calls the combination of the front panel and block diagram a virtual instrument or VI.

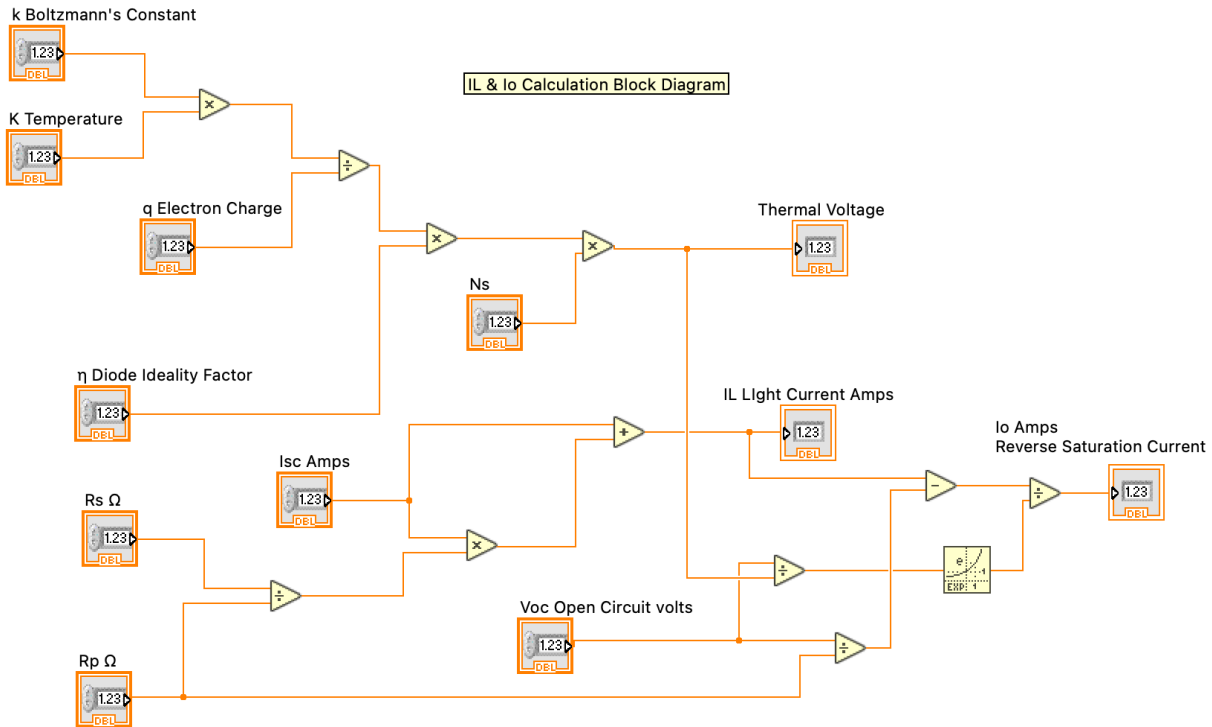


Figure 8.5 LabVIEW I_L and I_o Calculation Block Diagram.

In the front panel, the fixed constants, k , T , and q , PV module characteristics, N_s , V_{oc} , and I_{sc} , and the solved parameters, η , R_s , and R_p , were entered, and the VI was run. The LabVIEW front panel displays the result of the I_L and I_o calculations and is shown in Figure 8.6. The results were verified by matching the calculated values found via the TK Solver solution from Chapter 6.

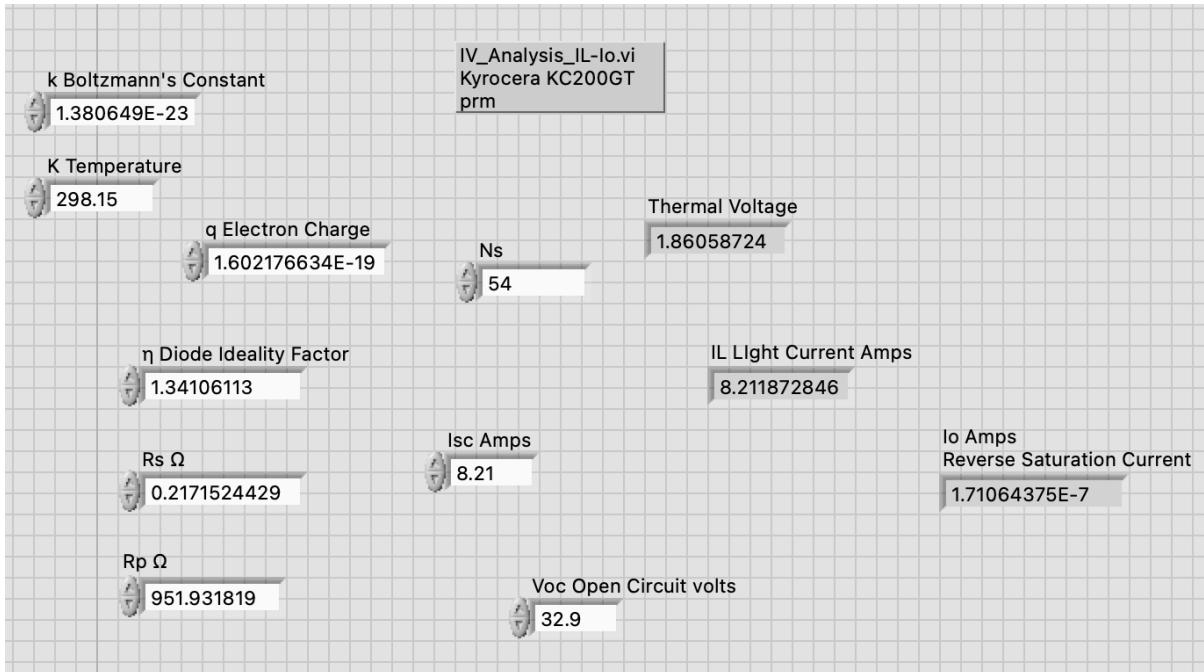


Figure 8.6 LabVIEW I_L and I_o Calculation Front Panel.

8.9 Implementation in LabVIEW

Table 8.2 shows the inputs and verification values required to run the instrument. The V_{mp} and I_{mp} values were used for a verification check. The process flow shown in Figure 8.2 was implemented with LabVIEW to create the functional diagram shown in Figure 8.7.

Table 8.2 I-V Graph Input Data for KC200GT

Description	Type	Symbols	Value	Units
Botlzmann's Constant	Constant	k	1.380649E-23	J/K
Thermal Temperature	Constant	T	298.15	K
Charge of an Electron	Constant	q	1.602176634E-19	C
Number of Series Cells	Characteristic	N_s	54	Count
Open Circuit Voltage	Characteristic	V_{oc}	32.9	V
Short Circuit Current	Characteristic	I_{sc}	8.21	A
Diode ideality factor	Parameter	η	1.34106113	No units
Series resistance	Parameter	R_s	0.2171524429	Ω
Parallel resistance	Parameter	R_p	951.931819	Ω
Maximum power volts	Verification	V_{mp}	26.3	V
Maximum power amps	Verification	I_{mp}	7.61	A

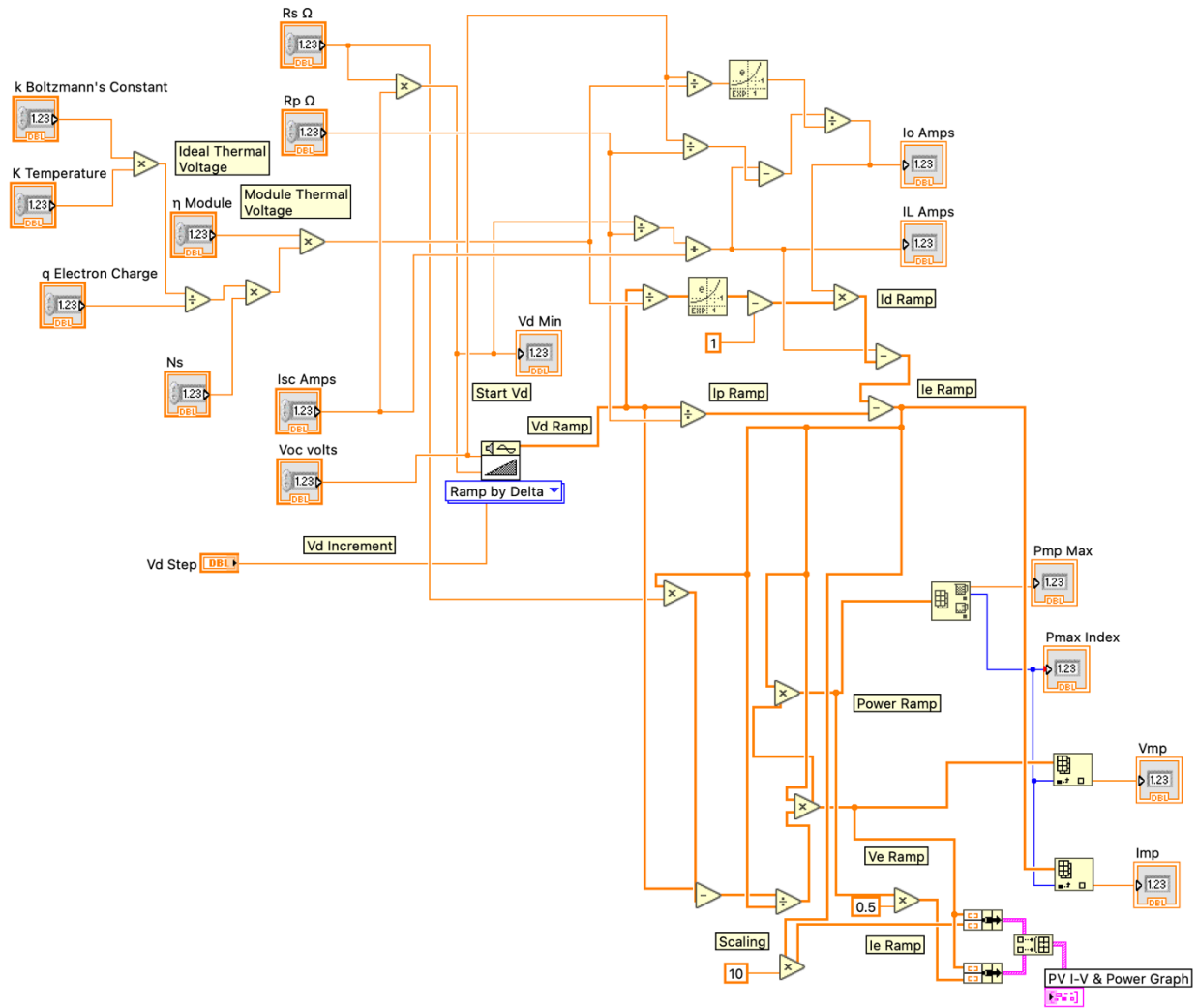


Figure 8.7 LabVIEW I-V and Power Graph Block Diagram.

Figure 8.8 shows the front panel of the I-V and Power Graphing instrument for the KC200GT PV module. To operate the instrument, the constants, characteristics, parameter values, and the V_d step value were input, and the VI run. With proper input, the result graphs the I-V and the power curves and displays the maximum power value, the maximum array term, and the contributing values of V_{mp} and I_{mp} . If the values mismatch, all the entered input values should be checked, and potentially, a smaller V_d step increment should be utilized. A version of this VI was used to create all the PV I-V and Power curves contained in this document.

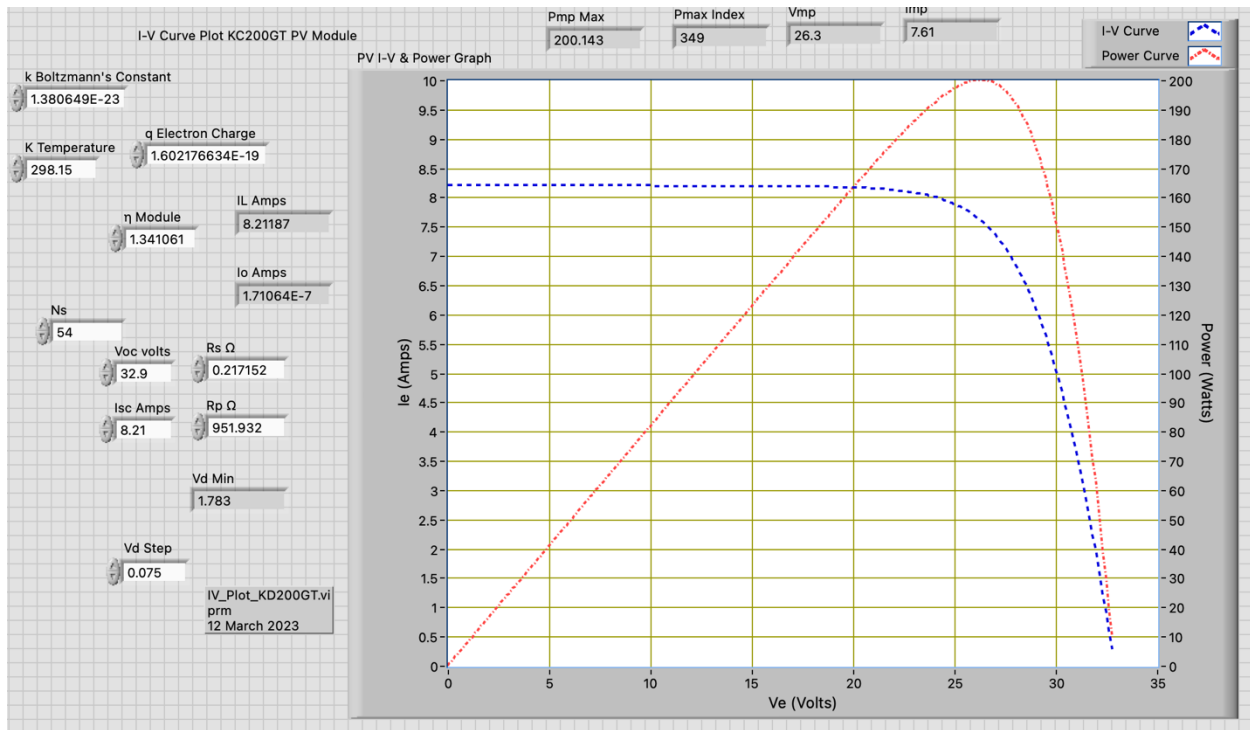


Figure 8.8 LabVIEW I-V and Power Graph Front Panel.

8.10 LabVIEW Virtual Instrument

The LabVIEW Six Parameter I-V Curve Graphing Instrument implementation of the system is available [64]. The three constants k , T , and q were saved in the instrument. Graphing the I-V and Power curves requires the input of three of the PV module characteristics, N_s , V_{oc} , and I_{sc} , and three solved parameters, η , R_s , and R_p . Once run, outputs include the PV I-V and Power curves, the PV module characteristics values of V_{mp} , I_{mp} , and P_{mp} , and the I_L and I_0 parameters. The LabVIEW output numbers should be verified against values provided on the datasheet, V_{mp} , I_{mp} , and P_{mp} , and solved parameters, I_L and I_0 . The six parameter model, the instrument, and its application provide an answer to the third dissertation question.

Chapter 9: Conclusion

Photovoltaic system applications and installations continue to expand in both number and size. Methods for simplification, verification, and graphing contribute to the understanding and analysis of PV systems.

The practical application of engineering principles enables the simplification of mathematical equations. The simplification of equations enables easier manipulation and solutions. It was shown by using statistical analysis that the PV equations at open circuit, short circuit, and maximum power conditions can be simplified for silicon based systems in general. In addition, it was shown that, under verified conditions, additional simplifications could be applied.

Application of the systems engineering verification principle showed that the values solved by many existing PV parameter solutions generated high errors. A new method was presented to verify the solved values for the Five Parameter PV model solution of η , R_s , R_p , I_o , and I_L . The physical parameter verification, RMS 5 Error, and RMS 3 Error methods provide a consistent process to verify PV parameter solutions.

Applying the six parameter model enables the simplified graphing of the PV I-V curves and provides insight into understanding and verifying PV systems. A new six parameter model with implementations in both spreadsheets and LabVIEW virtual instrument enables the plotting of PV I-V curves without solving a transcendental equation for each data point.

References

- [1] Pearl Street Station, https://en.wikipedia.org/wiki/Pearl_Street_Station and Public Domain photograph of the Pearl Street Station, <https://commons.wikimedia.org/wiki/File:PearlStreetStation.jpg> last accessed 2 February 2023.
- [2] International Energy Agency IEA <https://www.iea.org/data-and-statistics/charts/evolution-of-solar-pv-module-cost-by-data-source-1970-2020> last accessed 29 January 2023.
- [3] Office of Energy Efficiency & Renewable Energy, United States Department of Energy <https://www.energy.gov/eere/solar/photovoltaics> last accessed 30 January 2023.
- [4] National Renewable Energy Lab NREL Systems Advisor Model SAM techno-economic software <https://sam.nrel.gov> last accessed 30 January 2023.
- [5] PV Magazine, US residential PV trends in 2021 <https://www.pv-magazine.com/2021/12/15/us-residential-pv-trends-in-2021/> last accessed 31 January 2023
- [6] Office of Energy Efficiency & Renewable Energy, United States Department of Energy <https://www.energy.gov/eere/solar/solar-energy-united-states>.
- [7] International Energy Agency, World Energy Outlook 2020, figure 4.8
- [8] List Solar, Largest PV power plants, <https://list.solar/plants/largest-plants/largest-pv-plants/> last accessed 30 January 2023
- [9] Florida Power and Light, FPL Solar Energy Centers, <https://www.fpl.com/energy-my-way/solar/energy-centers.html> last accessed 30 January 2023
- [10] A. E. Becquerel, Memoire sur les effects d'electricques produits sous l'influence des rayons solaires, Annalen der Physick und Chemie, vol. 54, 1841.
- [11] W. Smith, Effect of Light on Selenium During the Passage of an Electric Current, Nature 20 February 1873.
- [12] W. Adams and R. Day, On the Action of Light on Selenium, Proceedings of the Royal Society of London, 1876.

- [13] C. Fritts, On a New Form of Selenium Cell, and some Electrical Discoveries made for its use, American Journal of Science, third series, Vol. XXVI, No. 156 December 1883
- [14] E. Chu and D. Tarazano, A Brief History of Solar Panels, Smithsonian Magazine, <https://www.smithsonianmag.com/sponsored/brief-history-solar-panels-180972006/> last access 9 February 2023
- [15] Heinrich Hertz, National Magnetic Lab, <https://nationalmaglab.org/magnet-academy/history-of-electricity-magnetism/pioneers/heinrich-hertz/> last access 2 February 2023
- [16] M. A. Stoletow, On a kind of electrical current produced by ultra-violet rays, Philosophical Magazine Serie 5 (1876-1900), 16:160
- [17] F. R. Richtmyer and E. H. Kennard, Introduction to Modern Physics, 4th edition, New York, McGraw-Hill Book Company, Inc. 1947
- [18] A. Einstein, Über einen die Erzeugung und Verwandlung des Lichtes betreffenden heuristischen Gesichtspunkt, Annalen der Physik 322, Issue 6, January 1905
- [19] A. Einstein, Nobel Prize in Physics 1921, <https://www.nobelprize.org/prizes/physics/1921/summary/> last accessed 2 February 2023.
- [20] Robert A. Millikan Nobel Prize in Physics 1923, <https://www.nobelprize.org/prizes/physics/1923/millikan/facts> last accessed 1 February 2023.
- [21] A. Lamb, Photoelectric Device, United States Patent 2,000,642 July 1932.
- [22] R. Ohl, Light-Sensitive Electric Device, United States Patent 2,402,662 May 1941.
- [23] D. Chapin, C. Fuller, and G. Pearson, Solar Energy Converting Apparatus, United States Patent 2,780,765 May 1954.
- [24] International Energy Agency <https://www.iea.org/reports/solar-pv> 14 February 2023.
- [25] W. Shockley, The Theory of p-n Junctions in Semiconductors and p-n Junction Transistors, The Bell System Technical Journal 28, July 1949
- [26] U. Gianola, Photovoltaic Noise in Silicon Broad Area p-n junctions, Applied Physics volume 27 1956
- [27] W. De Sota, et all, Improvement and validation of a model for photovoltaic array performance, Solar Energy, vol 80 2006

- [28] L. Arhcila, et al. 1, Implicit modeling of series-parallel photovoltaic arrays using double-diode model and its solution, Solar Energy vol 214, 2021
- [29] C. Tofoli, et all, Assessment of the ideal factor on the performance of photovoltaic modules, Energy Conversion and Management vol 167 2018
- [30] National Fire Protection Association, National Electric Code Handbook 2017, Article 690.7
- [31] International Electrotechnical Commission International Standard, IEC 60904-1 Photovoltaic devices – Part 1: Measurement of photovoltaic current-voltage characteristics, September 2020
- [32] K. Lynn, Test Method for Photovoltaic Module Ratings, Florida Solar Energy Center, FSEC-GP-68-01, May 2001
- [33] Standard Solar Spectra, ASTM G-173-03,
<https://www.pveducation.org/pvcdrom/appendices/standard-solar-spectra> last access 9 February 2023
- [34] NREL ASTM G-173 spreadsheet "astm173.xls" containing solar AM1.5 irradiance data,
<https://www.nrel.gov/grid/solar-resource/spectra-am1.5.html> last access 11 September 2023
- [35] S. Dubey, et. all, Temperature Dependent Photovoltaic (PV) Efficiency and Its Effect on PV Production in the World A Review, Energy Procedia 33 2013
- [36] C. Sainsbury, H. Wilterdink, R. Sinton., Measurement Uncertainty in Production Solar Cell and Module Power, IEEE Xplore 6 October 2020
- [37] International Electrotechnical Commission IEC International Standard, IEC 60904-1 Photovoltaic devices – Part 1: Measurement of photovoltaic current-voltage characteristics, September 2020, section 5 d
- [38] Fraunhofer ISE, STC measurement, available online <https://www.ise.fraunhofer.de/en/rd-infrastructure/accredited-labs/callab/callab-pv-modules/stc-messungen.html>, last accessed 4 September 2023
- [39] R. Sinton, et all, Challenges and Opportunities in Cell and Module I-V Testing, IEEE Xplore, 29 November 2018
- [40] Sinton FMT-500 Light I-V Testing for Modules, available online
<https://www.sintoninstruments.com/products/fmt-500/>, accessed 4 September 2023
- [41] California Energy Commission PV Modules,
<https://solarequipment.energy.ca.gov/Home/PVModuleList>, accessed 1 December 2022

- [42] <https://iee-dataport.org/documents/statistical-analysis-silicon-pv-module-solution-parameters> last accessed 26 October 2023
- [43] Sera, D., Teodorescu, R., Rodriquez, P., 2007. PV panel model based on datasheet values, IEEE International Symposium on Industrial Electronics 2007
- [44] D. Chan et. all, A comparative study of extraction methods for solar cell model parameters, Solid-state electronics, Vol. 29 (3), p. 329-337, 1986
- [45] TK Solver Software, <https://www.uts.com/Products/Tksolver> last accessed 14 February 2023
- [46] P. Michael, D. Johnston, W. Moreno, Systems Engineering Methodology for Verification of PV Module Parameter Solutions, IEEE Access 2023-07815, 28 April 2023
- [47] <https://www.mathworks.com/products/matlab.html> last accessed 27 January 2023
- [48] Weng X, et all, 2021. Laplacian Nelder-Mead spherical evolution for parameter estimation of photovoltaic models, Energy Conversion and Management 243 (2021) 114223
- [49] Lun, S., et all, An explicit approximate I–V characteristic model of a solar cell based on pade' approximants, Solar Energy, 92 (2013) 147-159
- [50] Lun, S., et all, A new explicit I–V model of a solar cell based on Taylor's series expansion, Solar Energy 94 (2013) 221-232
- [51] Yldiran, N, Tacer, E., Identification of photovoltaic cell single diode discrete model parameters based on datasheet values, Solar Energy 127 (2016) 175-183
- [53] Wang, G., et all, An iterative approach for modeling photovoltaic modules without implicit equations, Applied Energy 202 (217) 189-198
- [53] Song, S., et all, Adaptive Harris hawks optimization with persistent trigonometric differences for photovoltaic model parameter extraction, Engineering Applications of Artificial Intelligence, 109 (2022) 104608
- [54] Chaibi, Y., et all, A simple iterative method to determine the electrical parameters of photovoltaic cell, Journal of Cleaner Production, 269 (2020) 122363
- [55] Pindado, S., Cubas, J., Simple mathematical approach to solar cell/panel behavior based on datasheet information, Renewable Energy, 103 (2017) 729-738
- [56] Naeijian, M., et all, Parameter estimation of PV solar cells and modules using Whippy Harris Hawks Optimization Algorithm, Energy Reports, 7 (2021) 4047-4063

- [57] Hejri, M., et al, An analytical-numerical approach for parameter determination of a five-parameter single-diode model of photovoltaic cells and modules, *International Journal of Sustainable Energy*, vol. 35, No. 4, 396-410, 2016
- [58] Tayyan, A., An approach to extract the parameters of solar cells from their illuminated I – V curves using the Lambert W function, *Turkish Journal of Physics*, (2015) 339: 1-15
- [59] Villalva, M., et al, MODELING AND CIRCUIT-BASED SIMULATION OF PHOTOVOLTAIC ARRAYS, *Brazilian Journal of Power Electronics*, 2009 vol. 14, no. 1, pp 35-45
- [60] Tayyan, A., PV system behavior based on datasheet, *Journal of Electronic Devices*, Vol. 9, 2011, pp. 335-341
- [61] Muhammadsharif, F., A New Simplified Method for Efficient Extraction of Solar Cells and Modules Parameters from Datasheet Information, *Silicon* (2022), 14:3059-3067
- [62] <https://iee-dataport.org/documents/error-checking-methodology-verify-pv-module-parameter-solutions> last accessed 26 October 2023
- [63] <https://www.ni.com/en-us/shop/labview.html> last accessed 13 March 2023
- [64] <https://iee-dataport.org/documents/labview-virtual-instrument-6-parameter-pv-model-graph> last accessed 26 October 2023
- [C1] Boltzmann’s constant, <https://physics.nist.gov/cgi-bin/cuu/Value?k> last accessed 22 February 2023
- [C2] Charge of an electron, <https://physics.nist.gov/cgi-bin/cuu/Value?e> last accessed 22 February 2023
- [C3] S. Sharma and P. Ahluwalia, Can virtual labs become a new normal? A case study of Millikan’s oil drop experiment, *European Journal of Physics*, 39 2018
- [C4] P. Mohr, et al, CODATA Recommended Values of the Fundamental Physical Constants: 2014, National Institute of Standards and Technology, 25 June 2015

Appendix A: Copyright Permissions

This Appendix lists copyright clearances and permissions for all figures and the edited manuscript included in Chapter 7 of this dissertation. The figures are listed in order, including all copyright clearances and permissions. The manuscript was published by the author and two members of the dissertation committee. The majority of the document was written by the author, Dr. Johnston, provided mathematical checks, and Dr. Moreno provided supervision and review.

{1} Figure 1.1 is a Public Domain image.

<https://commons.wikimedia.org/wiki/File:PearlStreetStation.jpg> last accessed 30 July 2023



{2} Figure 3.1 is a Public Domain image.

https://en.wikipedia.org/wiki/File:Alexandre_Edmond_Becquerel,_by_Pierre_Petit.jpg last accessed 30 July 2023



{3} Figure 3.2 has No Copyright: Mr. Cove and His Sun Electric Generator,

<https://archive.org/details/popularelectrici02chi/page/804/mode/1up> last accessed 30 July 2023, from Popular Electricity in plain English, Volume 2, nr. 12, April 1910 pp. 804

<https://library.si.edu/digital-library/book/popularelectrici02chi> last accessed 30 July 2023, No copyright.

 **Published:** 1908

 **Subject(s):** [History and Culture](#); [Natural and Physical Sciences](#); [Electricity](#)

 [No Copyright - United States](#) ©

 **Cite This:** [View Citations](#)

 **Find In:** [Catalog](#) | [Internet Archive](#) | [Local Library](#)

{4} Figures 3.5 and 3.6 are US Patent images not subject to copyright restrictions

Screen captures from LabVIEW, Figures 4.13, 5.2, 6.1, 6.6, 7.2, 8.5, 8.6, 8.7, 8.8, TK Solver, Figures 6.3, 6.4, 6.5, 6.7, 6.9, 6.11, Excel, Figure 8.3, and Sinton MultiFlash software, Figures D.8, D.9, D.10 programs were used under the fair use exception to the Copyright Act 1976, section 107, and judicial decisions. The fair use worksheet is included below.

Peter R. Michael 28 Feb 2023
 Name: _____ Date: _____
 USF Ph.D. Dissertations
 Class or Project: _____
 TK Solver, LabVIEW, and Sinton MultiFlash software screenshots
 Title of Copyrighted Work: _____

PURPOSE AND CHARACTER OF THE USE

Likely Supports Fair Use	Likely Does Not Support Fair Use
<input type="checkbox"/> Educational <input type="checkbox"/> Teaching (including multiple copies for classroom use) <input checked="" type="checkbox"/> Research or Scholarship <input type="checkbox"/> Criticism, Parody, News Reporting or Comment <input checked="" type="checkbox"/> Transformative Use (your new work relies on and adds new expression, meaning, or message to the original work) <input type="checkbox"/> Restricted Access (to students or other appropriate group) <input type="checkbox"/> Nonprofit	<input type="checkbox"/> Commercial <input type="checkbox"/> Entertainment <input type="checkbox"/> Bad-faith behavior <input type="checkbox"/> Denying credit to original author <input type="checkbox"/> Non-transformative or exact copy <input checked="" type="checkbox"/> Made accessible on Web or to public <input type="checkbox"/> Profit-generating use

Overall, the purpose and character of your use supports fair use or does not support fair use.

NATURE OF THE COPYRIGHTED MATERIAL

Likely Supports Fair Use	Likely Does Not Support Fair Use
<input type="checkbox"/> Factual or nonfiction <input checked="" type="checkbox"/> Important to favored educational objectives <input type="checkbox"/> Published work	<input type="checkbox"/> Creative or fiction <input type="checkbox"/> Consumable (workbooks, tests) <input type="checkbox"/> Unpublished

Overall, the nature of the copyrighted material supports fair use or does not support fair use.

AMOUNT AND SUBSTANTIALITY OF MATERIAL USED IN RELATION TO WHOLE

Likely Supports Fair Use	Likely Does Not Support Fair Use
<input checked="" type="checkbox"/> Small amount (using only the amount necessary to accomplish the purpose) <input type="checkbox"/> Amount is important to favored socially beneficial objective (i.e. educational objectives) <input checked="" type="checkbox"/> Lower quality from original (ex. Lower resolution or bitrate photos, video, and audio)	<input type="checkbox"/> Large portion or whole work <input type="checkbox"/> Portion used is qualitatively substantial (i.e. it is the 'heart of the work') <input type="checkbox"/> Similar or exact quality of original work

EFFECT ON THE MARKET FOR ORIGINAL

Likely Supports Fair Use	Likely Does Not Support Fair Use
<input checked="" type="checkbox"/> No significant effect on the market or potential market for the original <input type="checkbox"/> No similar product marketed by the copyright holder <input type="checkbox"/> You own a lawfully acquired copy of the material <input type="checkbox"/> The copyright holder is unidentifiable <input type="checkbox"/> Lack of licensing mechanism for the material	<input type="checkbox"/> Replaces sale of copyrighted work <input type="checkbox"/> Significantly impairs market or potential market for the work <input type="checkbox"/> Numerous copies or repeated, long-term use <input checked="" type="checkbox"/> Made accessible on Web or to public <input type="checkbox"/> Affordable and reasonably available permissions or licensing

Overall, the effect on the market for the original supports fair use or does not support fair use.

CONCLUSION

The combined purpose and character of the use, nature of the copyrighted material, amount and substantiality of material used in relation to the whole and the effect on the market for the original likely supports fair use or likely does not support fair use.

Chapter 7 includes an updated version of a published manuscript by the author and two members of the candidate's Ph.D. committee. The manuscript is published via open access under the Creative Commons Attribution 4.0 International CC BY 4.0.

Systems Engineering Methodology for Verification of PV Module Parameter Solutions

Publisher: IEEE

Cite This

PDF

Peter R. Michael  ; Danvers E. Johnston  ; Wilfrido A. Moreno  [All Authors](#)

53

Full

Text Views

R



Open Access



Comment(s)

Under a Creative Commons License



Attribution 4.0 International (CC BY 4.0)

This is a human-readable summary of (and not a substitute for) the [license](#). [Disclaimer](#).

You are free to:

- Share** — copy and redistribute the material in any medium or format
- Adapt** — remix, transform, and build upon the material for any purpose, even commercially.

The licensor cannot revoke these freedoms as long as you follow the license terms.



Under the following terms:

-  **Attribution** — You must give [appropriate credit](#), provide a link to the license, and [indicate if changes were made](#). You may do so in any reasonable manner, but not in any way that suggests the licensor endorses you or your use.
- No additional restrictions** — You may not apply legal terms or [technological measures](#) that legally restrict others from doing anything the license permits.

Appendix B: 5.94 kW PV System

The following one-line diagram shows the 5.94 kW PV System engineered and built by the author. The system, installed on the author's home, is shown in Figure 2.1.

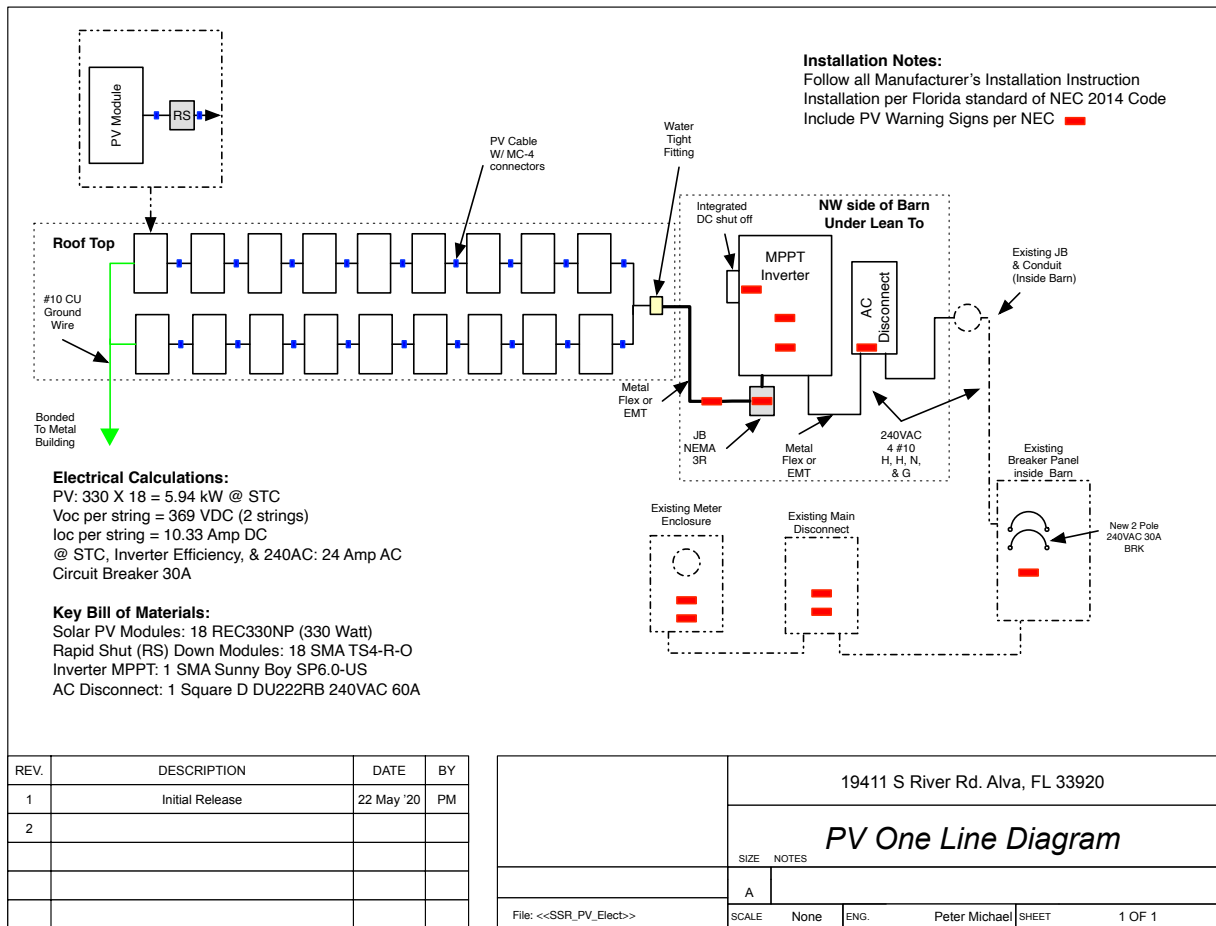


Figure B.1 5.94 kW PV System One Line Diagram.

Appendix C: Thermal Voltage

The thermal voltage is defined by Equation (2), where the thermal voltage v_t is defined as Boltzmann's constant multiplied by the temperature divided by the charge of an electron.

$$v_t = \frac{kT}{q} \quad (2)$$

For this dissertation, the temperature is set to a constant 25° C as defined in STC. The temperature in centigrade was converted to Kelvin by adding 298.15. This is shown in Equation (C1).

$$K = ^\circ C + 273.15 \quad (C1)$$

The other constants were established by international standards and available from the United States National Institute of Standards and Technology NIST. Boltzmann's constant is a fundamental physical constant defined as exactly 1.380649E-23 joule per Kelvin [C1] and shown in Equation (C2). The charge of an electron, shown in Equation (C3), is defined as exactly 1.602176634E-19 coulombs [C2]. The values were established in 2018 by the Committee on Data for Science and Technology CODATA.

Note that the value of Boltzmann's constant, k , and the charge of an electron, q , has changed over time. CODATA 2014 has a value of 1.38064851E-23 for Boltzmann's constant [C3]. Millikan's 1913 oil drop experiment established 1.5924E-19 as the value of q [C4]. CODATA 2014 states q as 1.6021766208E-19.

$$k = 1.380649E - 23 \quad (C2)$$

$$q = 1.602176634E - 19 \quad (C3)$$

Depending on the publication date, the changes in k and q contribute to the different values stated for the thermal voltage and subsequent calculations in various manuscripts. The inconsistency can lead to confusion in interpreting and verifying results and calculations. When attending the University of Colorado in the 1970s, the standard value used for the 25° thermal voltage was 25.8 mV. Using the currently defined values for k and q , the thermal voltage at 25° is calculated to three digits, as 25.7 mV, a difference of almost 0.4%.

Appendix D: PV Terminology Selection Criteria

Section 4.2.1 establishes the PV Model shown in Figure 4.2 and the terminologies utilized.

The following selection criteria chose the terms used in the models and equations.

- Unique
- A single letter subscripts
- Avoid similar and potentially confusing letters

Applying the criteria on the left side of the model, the photon light current is represented in documents as either I_L light current, I_{ph} photon current, or I_{pv} photovoltaic current. Using the selection criteria, I_L was chosen. The selection of I_L conflicts with some documents that utilize I_l or simply I for the external load current. With I_L already chosen for the photon light current, the confusion presented by I_l and the lack of a subscript for I led to assigning I_e to the external load current. The diode current is uniformly chosen at I_d , while V_d represents the diode voltage. Some documents show V_j for the diode junction voltage, but V_d is used to match I_d . The diode ideality factor is set to η versus the term A utilized in some documents. The terms I_s , and I_o are both used for diode reverse saturation current, with I_o used in this document. The parallel path current, which flows through the parallel resistance, leads to I_p and R_p . Both satisfy the selection criteria, which is not met by the commonly use term of I_{sh} for shunt current and R_{sh} for shunt resistance. The external load voltage V_e is referred to as V or V_l in some documents. To match the external current I_e and meet the selection criteria, V_e was used.

Appendix E: Sinton FMT-500 PV Testing and the Two Diode Model

E.1 Summary

The relative diode current in the Seven Parameter versus Five Parameter Model was investigated to test the conjecture that the single diode model provides enough precisions. The investigation measured the I-V characteristic of some sample PV modules and compared the two diode currents. The testing was performed on a Sinton FMT500 PV Flash Tester and MultiFlash software setup in the FGCU Emergent Technology Institute Energy Lab. This Appendix includes the setup, testing, and analysis of results.

E.2 Support Documentation and Equipment

The following manuals and equipment are required for PV module Testing on the Sinton tester. The system is designed to measure the I-V characteristic of a PV system under test, typically a PV module, and determine the PV parameters from measurement.

- FMT-500 Dark Room Dimension Guide
- Sinton Multiflash Software Manual
- This guide
- Sinton Test Cart with:
 - Monitor, Keyboard, & Mouse
 - Dell server with installed NI data acquisition card
 - Sinton FMT-500 electronic load system
 - Sinton flash power supply
 - Connection cables
 - UPS uninterruptible power supply
 - Thermistor yellow cable
- Sinton PV Terminal Box
- Sinton Light Source
- Blackout structural stand, cross braces, and connection hardware
- Blackout cloth and clips
- PV Test Stand with C-clamps for module attachment

E.3 Safety

- Follow safety guidelines in the documentation
- Ensure the PV system is mounted and adequately connected before starting the test
- Only operate the light source when the darkroom is closed, and never look at the light

E.4 PV Module Stand Setup and Test Cart Connections

The test cart should be configured and ready to go. Note the system runs on Windows 7. Do not update software to Windows 10 or 11. The dedicated test system uses Windows 7 software as part of the complex system of hardware, software, and firmware. External connections are a large green cable to the Terminal Box, a large black cable to the Light Source, AC power for UPS, a yellow cable for the thermistor, and a coax cable for the reference cell light sensor. Plug in the UPS, start the system and ensure the computer boots OK. The Sinton electric load should be on and the flash power supply off. Do not turn on the flash power supply until one is ready to test a PV module. Figure E.1 shows the Sinton computer, control box, light power supply, and UPS.



Figure E.1 Sinton Test System.

Place the PV module test stand at the wide end of the test area next to the test cart. UPS power is provided to the computer system. The light power supply is connected to filtered and not UPS power. Attach the large green, thick black, and small black coax cables to the Sinton Terminal Box, attached to the PV stand, the reference cell, and connect the light source at the back of the darkroom tunnel to the power box. The reference cell cable must be routed from inside the darkroom to the “REF Cell” BNC connector on the back of the electronic load. The temperature sensor is placed against the PV module, and the yellow cable connects to the thermistor input on the control box. Figure E.2 shows the green power and control cable at the bottom left, the yellow spiral cable to the temperature sensor, and the two black cables from the PV module under test.

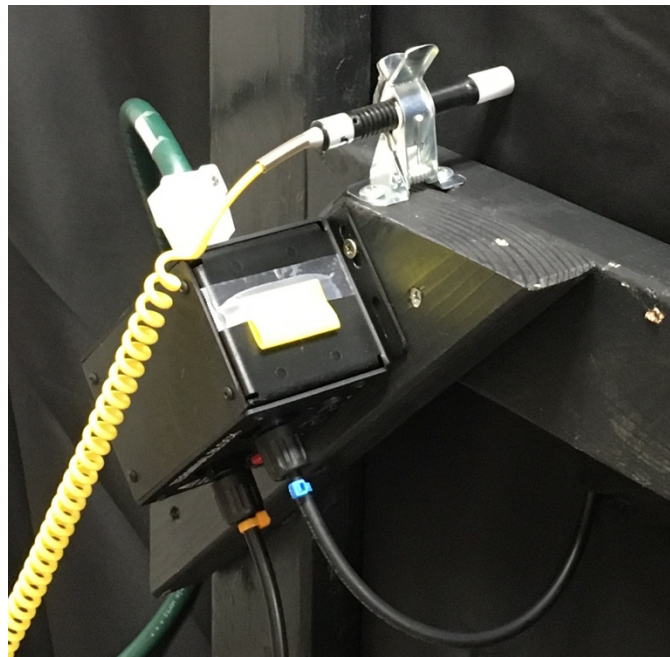


Figure E.2 Test Box Connections.

E.5 Dark Room Setup

Instead of the configuration shown in the FMT-500 Dark Room manual, a trapezoidal dark room is set up with sloping sides. The sloping sides are used in place of the rectangular cutouts from the Sinton layout. The room consists of a frame with eight tripod stands and metal cross

braces, all covered by a black cloth. The braces are attached with clips and hose clamps to provide positive connections. The two stands next to the light source are secured with 2 black bungee cords on top and one green on the bottom. The size of the PV module controls the blackout dimensions. The maximum length of 6 meters is for a 2-meter-wide PV module. Figure E.3 shows a PV module, stand, and part of the dark room framing during assembly. Figure E.4 shows the stands, clamping, and light source.



Figure E.3 PV Module and Stand.



Figure E.4 Clamps and Light Source.

Once the frame is configured and clamped, the black cloth is wrapped around the entire trapezoid, including the top, sides, and bottom. Because of the layout of the braces, some ingenuity is required to cover the area to block out external light and maintain a clear view from the light source to the PV module. Ensure the black cloth doesn't block the light to the PV module transmission. Leave an access area near the PV stand to allow the opening of the darkroom and the movement and connection of PV modules. Figure E.5 shows the assembled system.



Figure E.5 Completed Test Dark Room.

E.6 PV Module Mounting

Testing can proceed once the dark room is assembled, the test system configured, and the PV module mounted. Ensure to follow all these steps for proper PV mounting.

- Adjust the cloth on the PV stand to prevent cloth pinch
- Align the access holes to the PV electrical connection
- Place the module on the PV stand
- Attach two C-Clamps from outside in while holding the module against the stand.
- Make sure the clamps do not block any PV cells.
- When tightening the C-Clamps, do not over tighten
- Clip the light sensor to the front top of the PV module
- Connect the PV + and – cables to the Terminal Box.
- As an alternative, connect the PV connectors to the jumper cable to the terminal box.
- This method eases connection and lowers wear on the Terminal box connectors.
- Push the thermistor into the back of the PV module
- Close the access to the dark room with a clip
- The PV module is ready for testing

Figure D.6 shows the mounted PV module at one end and the light source at the other end of the dark room tunnel. Figure E.7 shows a PV module mounting by hidden c-clamps and the calibration silicon light sensor.

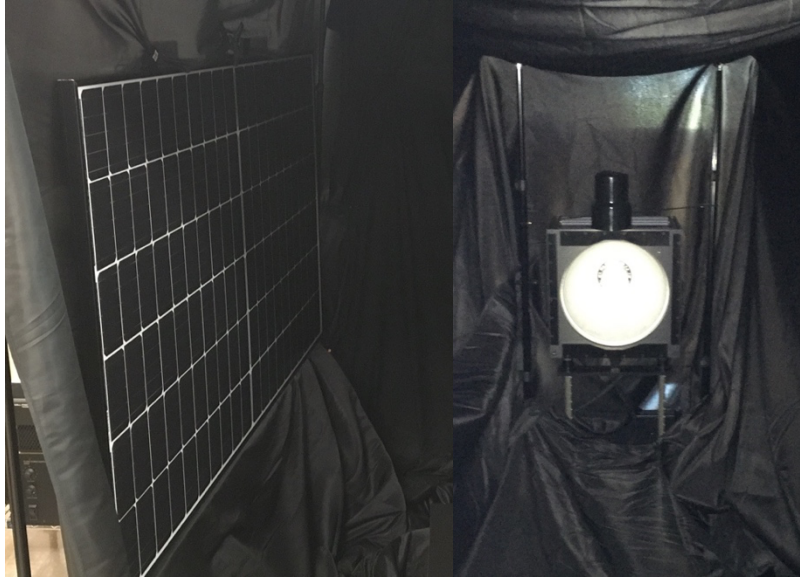


Figure E.6 PV Module and Light Source.

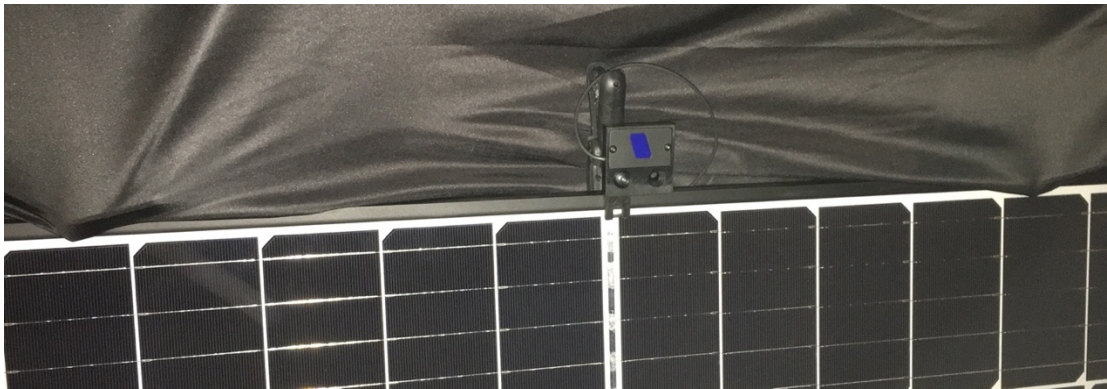


Figure E.7 Hidden C-Clamps and Light Sensor.

E.7 PV Module Testing

Reference the Sinton Software manual for complete details. The basic testing procedure is described in the following bullet points. An image of a sample test result is shown in Figure E.8. The red I-V curve is the ideal characteristic, while the blue curve shows measured data. The right

side shows calculated parameters derived from the measurement. The diode currents for a two diode model, shown with the purple dotted box on the right, are expanded in Figure E.9.

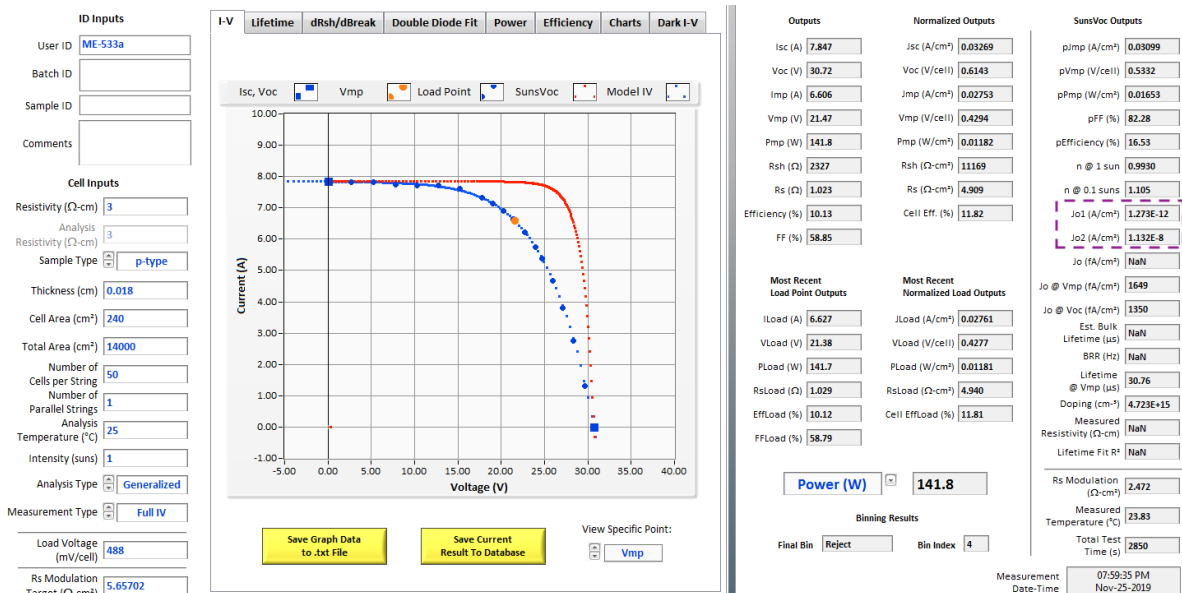


Figure E.8 Example Test Results.

- Turn on all systems, including the light power supply
- Sinton Test software takes a long time to start
- If there is a PV module configuration file load, the file
 - Click “Admin Access”
 - Enter the password “IVTest.”
 - Click “Load” Recipe File and install
- Without a reference Calibration PV module, calibration is via an entered.
 - Click ‘Advanced Settings
 - The type is the voltage for 1 sun for the reference cell
 - The existing calibration value is loaded from the configuration file
- Click initialize to start up
 - The reverse bias may be low, as shown in the image below
 - Adjust with a small flat blade screwdriver the potentiometer in the electronic load
 - Fig D.9 shows a calibration and bias error message
- Once the initialization is OK, click “Measure.”
- Be sure to enter ID input data to identify PV Characteristics
 - These values can be updated from a previous Result File
 - This means you do not need to know all the values for testing
- Save the results in the “Result File” “Save.”
- A Result File can be loaded back into the software, and parameters modified
- A new analysis can be performed without conducting another test

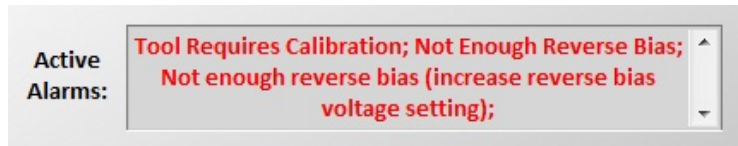


Figure E.9 Error Message.

E.8 Comparison of Two Diode Currents

This section summarizes an analysis of PV modules measured with the Sinton FMT-500 tester. The results were notional because the sample was not random, nor did it include enough samples, which was performed for the discussion in Chapter 5, Statistical Verification of PV Equation Simplification.

The Sinton test results include diode current density for the two diode model. Current can be found by multiplying the PV area in cm^2 by the current density in A/cm^2 . A sample of the results is outlined in the purple dash box in Figure E.8. Figure E.10 shows the current density of a test module's secondary current density, which is only 0.0037% of the primary.

J_{o1} (A/cm^2)	1.273E-12
J_{o2} (A/cm^2)	1.132E-8

Figure E.10 Diode Current Densities.

The results of a sample of 34 tested modules were assembled in a spreadsheet, and the average percent size of the smaller diode current to the larger was 0.00416% and the worst case 0.0112%. A data summary is presented in Table E.1, where Diode 1 is the larger current density. The results and technical references support the conjecture that the single diode Five Parameter Model is sufficient.

Table E.1 Comparison of Diode 1 to Diode 2

#	File Name	Diode 1 Amp/cm ²	Diode 2 Amp/cm ²	% Ratio Difference =1-(D ₁ -D ₂)/D ₁
1	10W1c	4.493E-08	7.930E-13	0.00176%
2	10W2c	2.151E-08	5.854E-13	0.00272%
3	ME-333a	3.861E-08	1.421E-12	0.00368%
4	10W3c	6.310E-08	5.391E-13	0.00085%
5	10W4c	2.681E-08	5.783E-13	0.00216%
6	330 W	4.322E-09	9.843E-14	0.00228%
7	CS-308c	1.632E-08	1.230E-12	0.00754%
8	CS-573c	8.537E-09	7.127E-13	0.00835%
9	CS-599c	1.048E-08	8.234E-13	0.00786%
10	ME-522c	1.716E-08	1.344E-12	0.00783%
11	ME-533ac	1.132E-08	1.273E-12	0.01125%
12	ME-828c	1.224E-08	1.282E-12	0.01047%
13	REC-015c	4.151E-09	1.041E-13	0.00251%
14	REC-042	4.129E-09	1.026E-13	0.00248%
15	REC-109c	4.333E-09	1.023E-13	0.00236%
16	REC-112c	4.322E-09	9.843E-14	0.00228%
17	REC-118xc	3.910E-09	9.958E-14	0.00255%
18	REC-268c	3.825E-09	9.995E-14	0.00261%
19	REC-357c	3.223E-09	9.764E-14	0.00303%
20	REC-395c	4.308E-09	1.047E-13	0.00243%
21	REC-437ac	3.508E-09	1.035E-13	0.00295%
22	REC-482c	3.696E-09	1.044E-13	0.00282%
23	REC-540c	3.843E-09	9.728E-14	0.00253%
24	REC-693ac	3.400E-09	9.682E-14	0.00285%
25	REC-841c	3.938E-09	1.045E-13	0.00265%
26	REC-874c	3.926E-09	1.039E-13	0.00265%
27	REC-912c	3.973E-09	9.952E-14	0.00250%
28	REC-920c	3.612E-09	9.944E-14	0.00275%
29	REC-998c	4.492E-09	1.032E-13	0.00230%
30	Sample	1.676E-08	2.521E-13	0.00150%
31	ME8533	1.224E-08	1.284E-12	0.01049%
32	ME9552	3.759E-08	1.298E-12	0.00345%
33	ME9828	3.861E-08	1.421E-1	0.00368%
34	Example	1.132E-08	1.273E-12	0.0113%
			Minimum =	0.000854%
			Maximum =	0.0114%
			Average =	0.00416%

Appendix F: MATLAB Code to Solve Equation (23)

The following list of the MATLAB computer code used to solve Equation (23). The code utilizes the Newton-Raphson method for finding a solution. The comments identified by the lead

% symbol provide explanations.

```
% Program to calculate Voc from PV Parameters
% Peter R. Michael 2023
%
% The parameters were obtained by PV equation solution
% IL = Photon Light Current
% Io = diode reverse saturation current
% Up (Upsilon) = module thermal voltage ( $\eta N_s v_t$ )
% Rp = Parallel Resistance
%
% Example uses Equation (19)
% Formula Voc:  $f(Voc) = I_o \exp(Voc/Up) + Voc/R_p - I_L$ 
% For Newton Raphson method, the derivative is required
%  $f'(Voc) = I_o/Up \exp(Voc/Up) + 1/R_p$ 
%
% Parameter values from solved PV equation
% From Kyocera KC200GT PV module
IL = 8.21187284584895;
Io = 1.71064375158476E-07;
Up = 1.86058724;
Rp = 951.931819318286;
%
% Initial Conditions
% From datasheet Voc & Ns
Ns = 54; % Number of series PV cell
Voc0 = Ns*0.6; % Ns X 0.6 VDC per cell for starting value
Iter = 5000; % number of iterations of loop
tol = 1e-6; % error tolerance
%
% Computations for Voc
x = Voc0; % shorten to x for loop, Voc0 is initial 'guess'
xold = Voc0; % previous value of x
% Loop to solve for the solution
for i = 1:Iter; % Iter is number of loops
    % Equation
    f = Io*exp(x/Up)+x/Rp-IL;
    % Derivative of the equation
    df = (Io/Up)*exp(x/Up)+1/Rp;
    % Difference
    x = x - f/df;
```

```

% Error in solution
errx = abs(x-xold);
xold = x;
Loops=i+1; % count the number of loops
% If the error is small enough, end loop
if (errx<tol);
    break;
end
end
%
% Plug x back into Voc
Voc = x;
% Data to print answers
V = 'The calculated value of';
disp(V)
% Calculated value of open circuit voltage
format long
Voc
% Number of loops to find the solution
Loops

```

The datasheet value from the KC200GT PV module is $V_{oc} = 32.9$. The output of this code, which required 5 iteration loops, calculates a value that is practically the same.

The calculated value of $V_{oc} = 32.900000064969610$

Loops = 5

Appendix G: Systems Engineering Selection of Solver

The selection of a software tool to solve the concurrent transcendental Equation (32), Equation (46), and Equation (55) followed a systems engineering selection methodology. The method involved the determination of required features, functions, cost, and support. Once determined, a weight factor was applied to each factor from 1, low importance, to 5, high importance. A search for available software tools was performed, and information was collected. Each tool was investigated, and each factor was assigned an evaluation value from 0, no capability, to 5, high capability. The evaluation factors were multiplied by the weight to create a merit figure and then summed for each proposed tool. The system with the highest overall score was selected. Table F.1 shows the evaluation matrix results, including the vendors, weight factors, and evaluation results for each. The high score solution, TK Solver, was chosen and utilized to solve the transcendental equations.

Table G.1 Solver Evaluation Matrix

Vendor		MATLAB	Simulink	Python	Wolfram	TK Solver
	Weight					
Suitability	5	3	3	3	3	5
Premade	3	3	5	4	2	0
Flexibility	4	4	3	5	4	5
Robustness	3	3	3	3	3	3
Self Support	3	3	3	3	2	2
Live Support	5	0	0	0	0	5
Ease of Use	3	4	3	1	2	3
Cost	2	5	4	5	2	4
	Score	83	82	82	64	102

About the Author

Peter Richardson Michael received a bachelor's degree in Electrical Engineering from the University of Colorado, Boulder, in 1979 and a master's degree in Systems Engineering from Arizona State University, Tempe, in 2014.

Peter worked as an electrical engineer, project manager, systems engineer, and instructor for over 40 years. Projects included Hawaiian Electric Company planning, systems operations, energy management systems, SAIC with worldwide travel, design, and deployment of sensors and security systems for Honolulu Airport, US Government facilities, nine Greek Seaports, the Houston Texas Ship Channel, and the implementation of numerous small-scale photovoltaic power systems. In addition, he worked as a high school physics teacher and an instructor at Florida Gulf Coast University. He is a US Naval Reserve veteran, a member of Eta Kappa Nu, Tau Beta Pi, Order of the Engineer, a senior member of the Institute of Electrical and Electronic Engineers, a Project Management Professional, a Physical Security Professional, and a registered professional engineer in Hawaii, Florida, and Texas.